**Sara Sofia Adriano Murilhas**
Degree in Biochemistry

# Saccharification of hemicellulose and cellulose with immobilized enzymes

Dissertation for obtaining the master's degree in Biotechnology

Advisor: Prof. Susana Filipe Barreiros, DQ – FCT/UNL

Co-advisor: Dr. Paula Isabel Pereira Soares, DCM – FCT/UNL

**Jury**

President: Prof. Carlos Alberto Gomes Salgueiro

Arguer: Prof. José Ricardo Ramos Franco Tavares

Additional members of the board: Prof. Susana Filipe Barreiros
Dr. Paula Isabel Pereira Soares

February 2021

FACULDADE DE CIÊNCIAS E TECNOLOGIA
UNIVERSIDADE NOVA DE LISBOA

Departamento de Química (DQ) e Departamento de Ciência dos Materiais (DCM)

Dissertation in Biotechnology
Under advisement of Prof. Susana Filipe Barreiros
And co-advisement of Dr. Paula Isabel Pereira Soares

# Saccharification of hemicellulose and cellulose with immobilized enzymes.

Sara Murilhas
Student number 47965
MSc in Biotechnology

# Copyright

**Saccharification of hemicellulose and cellulose with immobilized enzymes.**

# Acknowledgments

O primeiro agradecimento deve, sem falta, ser dirigido à professora Susana Barreiros, que não só me acolheu de braços abertos como, por mais ocupada que estivesse, sempre arranjou um tempinho para fazer o check-in de como estava tudo a correr, e prontamente "apagou todos os fogos" sempre que precisei de ajuda, quer teórica quer no arranjar de diverso material para poder tornar a realização do trabalho prático possível.

Agradeço também ao professor João Paulo Borges que, apesar de não se ter mantido como meu co-orientador, garantiu que eu estava "em boas mãos". Nomeadamente, à professora Paula Soares, um grande obrigada por me acolher como sua aluna e por toda a sua disponíbilidade em ajudar, mesmo até durante a sua licença de maternidade.

Um obrigada também à professora Isabel Sá Nogueira e à Lia Godinho pelas imensas vezes que me cederam o uso da incubadora, bem como pela solução de azida de sódio e, principalmente, pela enorme disponibilidade em ajudar em tudo o que podessem.

Obrigada também a todos no 427, que me acolheram como família e se mostraram sempre dispostos a ajudar. Um obrigada especial ao Alexandre por ser o "chefe" mais fixe do mundo, às crianças do 427 por serem minhas companheiras tanto dentro como fora do laboratório, e ao meu babysitter Bruno, por me ensinar que "não sou teimosa, sou persistente!" e me dar a enorme honra de lhe arrumar a sua bancada e lavar a sua loiça suja.

Um grande obrigada também á Catarina e Adriana, as minhas salvadoras no DCM, por me ajudarem com tudo o que precisava e que, ao longo de um ano inteiro, sempre tiveram a paciência de me relembrar mensalmente onde estava arrumada toda a loiça em ambos os laboratórios, sem me fazerem cara feia.

Devo ainda um grande, gigante, obrigada ao meu idiota favorito, João Pedro Lavadinho. Pela boa disposição inabalável, a companhia no laboratório e toda a assistência técnica com Mendeley, Origin e todos os demais dramas computacionais de que me socorreste. Mas, acima de tudo, obrigada por seres uma criança que me acompanhou tantas tardes ao frio a apanhar Pokémons, e tantas noites a ver filmes da Disney ou a comer sushi acampados no meio do chão. Quase que compensou seres o pior babysitter do mundo, me rebentares as minhas pobres membranas de diálise, e o trauma de procurar o abrigo mais próximo ao ouvir a frase "confia em mim, sou engenheiro!", que de certo me acompanhará para a vida.

Quero ainda acrescentar um hiper mega gigantesco obrigada a todos os meus demais amiguinhos. Lamento não terem agradecimentos personalizados, mas visto que todos sabem o quanto vos super adoro não acho necessário vos estar a enumerar em estilo lista de compras. Obrigada por todas as Game Nights, tanto presenciais quanto virtuais, os Secret Santas, as idas ao cinema e à praia. Por todos os almoços na Teresa e todas as tardes passadas a tentar estudar em monte na única mesa disponível no DQ, com Wi-fi semi decente, 3 das tomadas avariadas e um barulho descomunal. Obrigada a todos vós, que ajudaram a manter-me sã durante a quarentena, e com os quais sem sombra de dúvida criei as melhores memórias ao longos destes últimos 5 anos que passámos todos juntos. Vocês sim, são o melhor que a FCT me deu.

Finalmente, como não poderia deixar de ser, a autora é extremamente grata ao seu papá, não só pelo seu investimento financeiro mas também por todo o incentivo, todas as sugestões de "inglês mais inglês", e a constante preocupação com o nível de apetite das minhas enzimas.

E, para os demais não se queixarem que sou menina do papá, um obrigada também a todo o resto da minha familia, que é chata até dizer chega mas eu não a trocava por mais nenhuma.

## Abstract

Wine is a very appreciated beverage worldwide, and, in Portugal, the winemaking sector is of major socio-economic significance, substantially contributing to the national economy. However, it results in a lot of residual material called pomace, which is rich in cellulose, hemicellulose, and lignin.

Cellulose and hemicellulose represent a significant portion of vegetal biomass, usually discarded as feed. However, both sugar polymers can be hydrolyzed into C5 and C6 monomers by a saccharification process and then fermented into multiple added-value products, like bioethanol.

The greener and more specific option for saccharification is through enzymes. However, after the reaction is over, the enzymes are inactivated and remain in the final product, as there is no way to retrieve them from the solution. Nonetheless, these enzymes are expensive and still functional after a single use. So, this work's goal is to develop immobilization protocols for cellulases and hemicellulases. That will allow for their reuse, making the process economically more viable.

The immobilization protocols consisted of covalent attachment of cellulase to magnetic nanoparticles (mNPs), specifically superparamagnetic iron oxide nanoparticles (SPIONs), and of hemicellulase to chitosan microparticles (CMPs). SPIONs were used with multiple coatings – dimercaptosuccinic acid (DMSA), (3-aminopropyl)triethoxysilane (APTES), and chitosan. With this approach, the enzymes attached to the supports can be recovered by magnetic separation (for mNPs) or by filtration (for CMPs).

This work aims at the saccharification of subcritical water (SBW) pretreated Red Wine Grape Pomace (RWGP). SBW results in a solid residue rich in lignin and cellulose, target of the cellulase complexes, and a liquor rich in hemicellulose oligomers, target of the hemicellulase complexes. The target characteristics for the complexes are reusability, high enzyme loading, and enzymatic activity, as well as operational and storage stability. Therefore, the complexes were assessed by their retained activity when comparing with the enzyme in its free form. The monomer yield was determined by High-Performance Liquid Chromatography (HPLC), while enzyme leaching was monitored through protein detection assays. A preliminary assessment of the complexes' storage stability was also made.

To develop the immobilization protocols, the project started with the characterization of three available commercial carbohydrase formulations and the analysis of their activity in their free form to establish a control to compare to the immobilization complexes. Two cellulases, CelluClast 1.5L and Cellic cTec2, and a hemicellulase, Viscozyme L, were tested. Protein content was determined by the Bradford assay using Bovine Serum Albumin (BSA) as standard, resulting in 54.8 mg/mL for CelluClast 1.5L, 99.1 mg/mL for Cellic cTec2, and 20.6 mg/mL for Viscozyme L. Total saccharification activities of 51 units/mL in CClast and 137 units/mL in cTec2 were determined for the cellulases. An equivalent activity measurement was determined for the hemicellulase Viscozyme L using two standard substrates, achieving an activity of 2 units/mL in xylan and 0.4 units/mL in arabinogalactan.

Fifteen complexes were performed for the immobilization of cellulase onto mNPs, and two for hemicellulase onto CMPs (HM). From the produced cellulase complexes, the CAS protocols (cellulase immobilized onto APTES-coated SPIONs) were deemed less promising due to the loss of integrity of the matrix. The most promising protocols for cellulase are CDS-g 0, a version of cellulase immobilized onto DMSA-coated SPIONs, and CMm (cellulase immobilized onto CMPs with magnetic cores), while for hemicellulase the most promising protocol is HM 2 (the 2$^{nd}$ protocol of hemicellulase immobilization onto CMPs). However, they all must be reproduced in larger quantities and re-tested in multiple saccharification cycles.



## Keywords

Enzyme immobilization; Cellulase; Hemicellulase; Magnetic nanoparticles; Chitosan microparticles; Lignocellulose saccharification.

## Resumo

O vinho é uma bebida mundialmente apreciada e, em Portugal, a vitivinicultura é um sector muito importante a nível socioeconómico, contribuindo substancialmente para a economia nacional. No entanto, este resulta numa grande quantidade de material residual, intitulado de massas vínicas e rico em celulose, hemicelulose e lenhina.

A celulose e a hemicelulose representam uma fracção significativa da biomassa vegetal, geralmente descartada como ração. No entanto, ambos estes polímeros podem ser hidrolisados atéa os respectivos monómeros (açúcares C5 e C6) por um processo de sacarificação, e em seguida fermentados a múltiplos produtos de valor acrescentado, entre eles bioetanol.

Para a sacarificação, a opção mais "verde" e que oferece maior especificidade é o uso de enzimas, onde após a reação, as enzimas são inactivadas e permanecem no produto. No entanto, essas enzimas são dispendiosas e ainda funcionais após um único uso. Assim, o objectivo deste trabalho é desenvolver protocolos de imobilização para celulases e hemicelulases para possibilitar a sua reutilização, tornando o processo economicamente mais viável.

Os protocolos de imobilização consistiram na ligação covalente de celulase a nanopartículas magnéticas (mNPs), especificamente nanopartículas superparamagnéticas de óxido de ferro (SPIONs), e também de hemicelulase a micropartículas de quitosano (CMPs). Através desta abordagem, após a sacarificação as enzimas fixadas podem ser recuperadas por separação magnética para as mNPs, ou por filtração no caso das CMPs. Para os SPIONs, diversos revestimentos – ácido dimercaptosuccínico (DMSA), (3-aminopropil)trietoxisilano (APTES), e quitosano – foram testados.

O objectivo final dos complexos desenvolvidos neste trabalho será a sacarificação de massas vínicas de vinho tinto, as quais foram pré-tratadas através de um processo de autohidrólise (SBW). O resultado desse processo é um resíduo sólido rico em lignina e celulose, alvo dos complexos de celulase, e um licor rico em oligómeros de hemicelulose, para uso dos complexos de hemicelulase.

As características alvo dos complexos são reutilizabilidade, alta carga e actividade enzimática, bem como estabilidade operacional e de armazenamento. Portanto, os complexos foram avaliados pela sua actividade retida, quando comparados com a enzima na sua forma livre. O rendimento de produção de monómeros foi determinado por cromatografia líquida de alta eficiência (HPLC), enquanto a lixiviação da enzima foi monitorizada por métodos de detecção de proteínas em solução. A avaliação preliminar da estabilidade de armazenamento dos complexos foi também realizada.

Previamente foi necessária a caracterização de três soluções comerciais disponíveis de carbohidrolases e a análise da sua actividade na forma livre, de modo a estabelecer um controlo para comparar com os complexos. Duas celulases, CelluClast 1.5L e Cellic cTec2, e uma hemicelulase, Viscozyme L, foram testadas. O conteúdo de proteína foi determinado pelo método de Bradford usando albumina de soro bovino (BSA) como padrão, e resultando em 54,8 mg/mL para CelluClast 1.5L, 99,1 mg/mL para Cellic cTec2 e 20,6 mg/mL para Viscozyme L. Foram determinadas atividades de sacarificação total de 51 unidades/mL em CClast e 137 unidades/mL em cTec2 para as celulases. Uma medição equivalente de actividade foi determinada para a hemicelulase Viscozyme L usando dois substratos padrão, alcançando-se uma actividade de 2 unidades/mL em xilano e 0,4 unidades/mL em arabinogalactano.

Foram produzidos quinze complexos para a imobilização de celulase em mNPs, e dois para HM (hemicelulase em CMPs). Dos complexos de celulase, seguindo os protocolos CAS (celulase imobilizada em SPIONs revestidas com APTES) são menos promissores devido à perda de integridade da matriz. Os mais promissores são CDS-g0, uma versão de celulase imobilizada em SPIONs revestidas com DMSA, e CMm (celulase imobilizada em CMPs com núcleos magnéticos), enquanto que para hemicelulase o mais promissor é o HM 2 (o segundo complexo de imobilização de hemicelulase em CMPs). No entanto, todos estes devem ser reproduzidos em quantidades superiores, e testados novamente em múltiplos ciclos de sacarificação.



## Palavras-chave

Immobilização enzimática; Celulase; Hemicelulase; Nanopartículas magnéticas; Micropartículas de quitosano; Saccarificação lignocelulósica.

# Contents

# List of figures

# List of tables

## Abbreviations

| | |
|---|---|
| GHG(s) | Green House Gas(es) |
| EU | European Union |
| OPEC | Organization of Arab Petroleum Exporting Countries |
| LCA | Life Cycle Assessment |
| 1GB / 2GB / 3GB | First / Second / Third Generation Bioethanol |
| RWGP | Red Wine Grape Pomace |
| FAO | Food and Agriculture Organization (of the UN) |
| UN | United Nations |
| TSSC | Total Soluble Solid Content |
| SBW | Subcritical Water |
| DP | Degree of Polymerization |
| TSSC | Total Soluble Solid Content |
| C5 / C6 sugar(s) | Pentose(s) / Hexose(s) |
| SHF | Separate enzymatic hydrolysis and fermentation |
| SSF | Simultaneous saccharification and fermentation |
| SScF | Simultaneous saccharification and co-fermentation |
| CBP | Consolidated bioprocessing |
| MESP | Minimal Ethanol Selling Price |
| IUPAC | International Union of Pure and Applied Chemistry |
| CLEAs | Crosslinked Enzyme Aggregates |
| HPLC | High Performance Liquid Chromatography |
| mNPs | Magnetic Nanoparticles |
| SPIONs | Super Paramagnetic Iron Oxide Nanoparticles |
| CMPs | Chitosan Microparticles |
| DMSA | Dimercaptosuccinic acid |
| APTES | (3-Aminopropyl)triethoxysilane |
| EDC | 1-Ethyl-3-(3-dimethylaminopropyl)carbodiimide |
| NHS | N-Hydroxysuccinimide |
| DAS | Dialdehyde Starch |
| CDS | Cellulase immobilized onto DMSA-coated SPIONs |
| CDS-g | CDS followed by a secoundary step of crosslinking with glutaraldehyde |
| CAS | Cellulase immobilized onto APTES-coated SPIONs |
| CMm | Cellulase immobilized onto chitosan microparticles with magnetic cores |
| HM | Hemicellulase immobilized onto chitosan microparticles |
| FPA | Filter Paper Assay |
| FPU | Filter Paper Units |
| LAP | Laboratory Analytical Procedure |
| CClast | CelluClast 1.5L |
| cTec2 | Cellic cTec2 |
| MES | 2-(N-morpholino)ethanesulfonic acid |

# 1. Introduction

## 1.1. The ecological crisis

As a result of population growth and heavy industrialization observed in the last few decades, we now face a fast-paced increase of both the drainage rate of natural resources and the increase of environmental pollution. This led to a point in history where the earth can no longer sustain us, and one of the most evident signals is the trend exhibited by Earth Overshoot Day throughout the years. Earth Overshoot Day is the estimated date by which humanity will have already consumed the number of natural resources – including not only raw materials and food but also water, soil, and clean air – that earth can regenerate each year. There are available records of Earth Overshoot Day since 1961, and its date moves consistently closer to the start of each new year. In 2019, humanity reached Earth Overshoot Day on July 29, which makes the current consumption rate of the resources 1.75 times faster than the regeneration provided by our planet's ecosystems (1) – **Figure 1.1**.

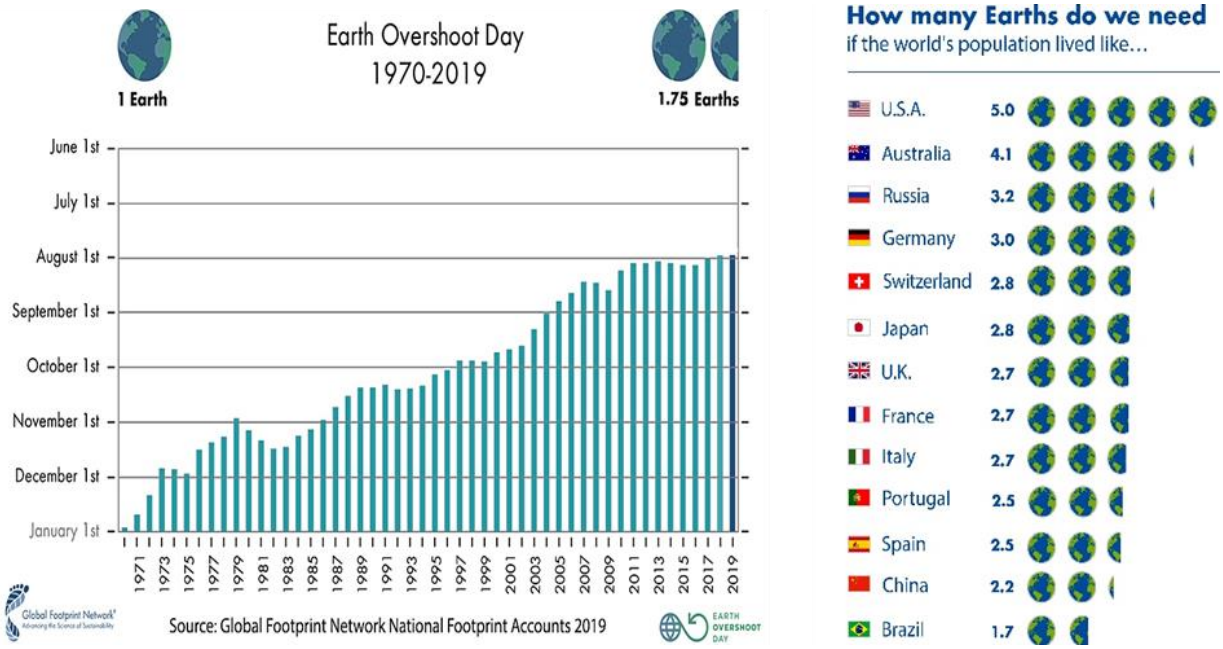


Figure 1.1: Progression of Earth Overshoot Day throughout the last five decades (1970 – 2019), showing the trend of the increasing rate of resources' exhaustion (left) and comparison of the specific rates of resources' exhaustion in various countries (right). Available in (1).

In the words of María Schmidt Zaldívar – Chile's Minister of Environment, and chair of the Climate COP25 (25$^{th}$ UN Climate Change Conference, that took place December 2019 in Santiago de Chile) – "with Earth Overshoot Day occurring ever earlier in the year, and a big part of it being the growing amounts of $CO_2$ emissions, the importance of decisive action is becoming ever more evident" (1).

The global carbon dioxide emissions increased by 60% from 1990 to 2017 (2), – **Figure 1.2** – mostly due to the combustion of fossil fuels, and this increase has devastating ecological consequences [1]: Firstly, of all the anthropogenic carbon dioxide emissions, around 25% were absorbed by the ocean [2]. This allowed for a decrease of the atmospheric concentration of $CO_2$ but also resulted in oceanic acidification, which had a profound impact on the ecosystems, and consequently on their fauna and flora [2,3]. Secondly, the role of carbon dioxide is also of great importance as part of the greenhouse gases (GHGs) emissions, alongside methane ($CH_4$), nitrous oxide ($N_2O$), and water vapor. These emissions contribute heavily to global warming, one of the major downfalls of human activity, responsible for the increase of the average surface temperature of the earth, and consequently potentiating extreme weather effects – such as droughts and floods, heatwaves, and massive storms – which can threaten not only humanity but most of the known life forms that inhabit the planet. But, most important, from all the GHGs, the increase of $CO_2$ is considered to be the determinant factor of global warming, being responsible for triggering and controlling global warming [4].

Even with the immediate end of $CO_2$ emissions, most aspects of climate change will persist for many centuries [1]. Therefore, action needs to be taken as fast as possible to avoid worsening the damages already done and allow the earth to heal. In order to do that, the European Union aims to, by 2050, accomplish a zero-net of GHGs' emission, to achieve the status of climate-neutral by 2050 [5]. To reach this goal, there was developed a set of binding legislation with a 3-phase targeted program: by 2020 must be achieved a 20% decrease in greenhouse gas emissions (relative to 1990 levels), 40% (relative to 1990 levels) by 2030, and finally, by 2050 the climate-neutral status must be reached [5].

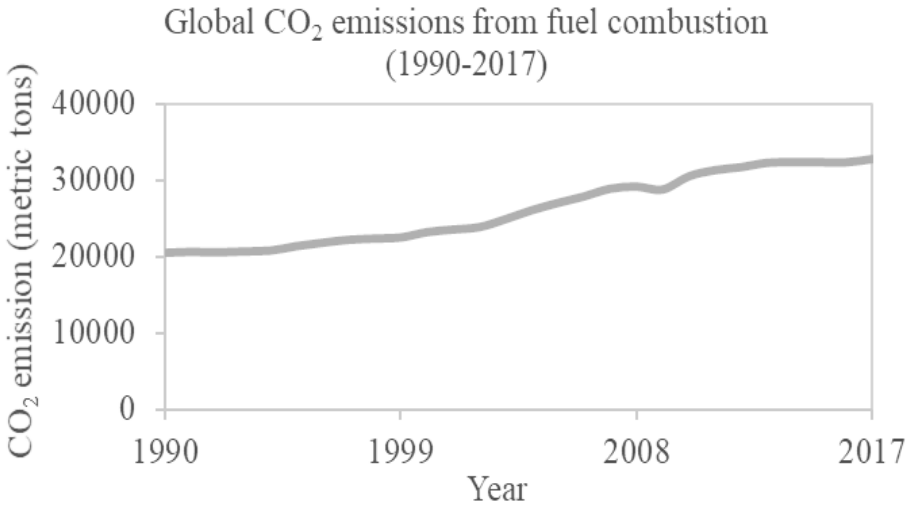


Figure 1.2: The Global $CO_2$ emissions from fuel combustion, 1990-2017. Reproduced based on data from (2).

According to recent data, the EU is on track to meet its target of 20% reduction for 2020, since between 1990 and 2017 it was registered a 20.25% reduction of the emission of GHGs by the EU (2), with an estimated 23% reduction by 2018 [5] – **Figure 1.3** – and it is now working towards the 2030 goals.

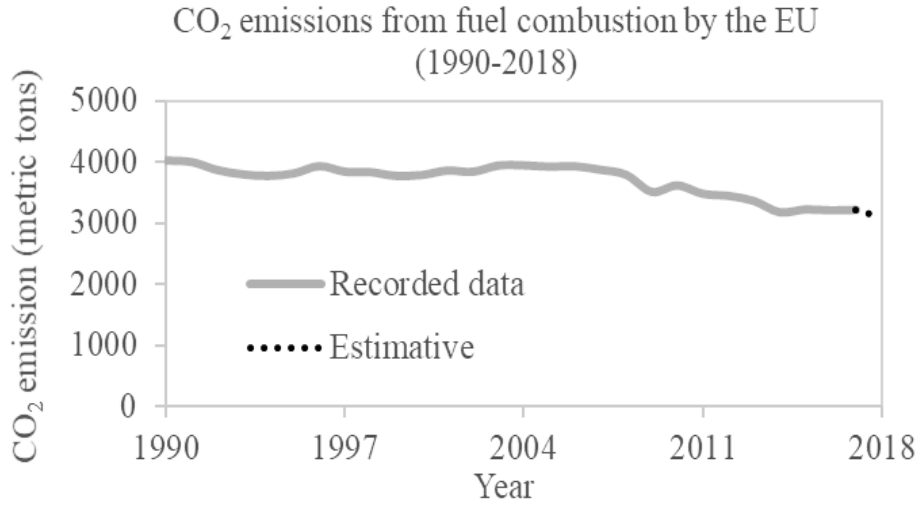


Figure 1.3: EU $CO_2$ emissions from fuel combustion, 1990-2018, based on data from (2) for 1990-2017, and the estimated value for 2018 from [5].

### 1.1.1. The role of fossil fuels

As one of the most concerning environmental aspects is the growing $CO_2$ emissions, a promising approach to reduce the current environmental impact is using "greener" (more environmentally friendly) fuels to replace petroleum-based fuels.

Globally, in 2017 there were produced 32840 metric tons of $CO_2$ from fuel combustion alone, 35% of which originating in the use of oil as an energy source. It was also determined that one-fourth of the total emissions derived from the transport sector (2) – **Figure 1.4**.

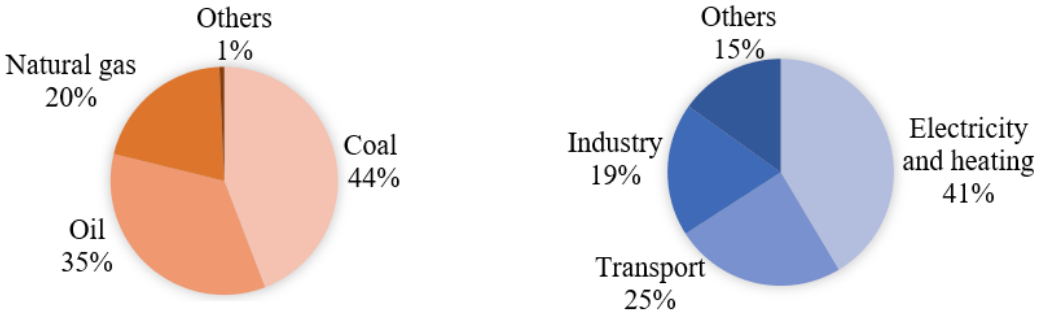


Figure 1.4: Global $CO_2$ production in 2017 due to fuel combustion – Segmentation by energy source (left) and activity sector (right). Graphics were constructed using the data available in (2).

The current overuse of petroleum-based products leads to a net production of GHGs (including not only carbon dioxide ($CO_2$), but also methane ($CH_4$), nitrous oxide ($N_2O$), and water vapor), inevitably contributing to an increase in global warming [4]. Furthermore, the emissions of sulfur dioxide ($SO_2$) and nitrogen oxides in general ($NO_x$) that derive from the combustion of fossil fuels leads to acid depositions after settling. This deposition will contaminate water and soil, impacting both land and water ecosystems. And since these compounds are released as gases, the emissions can travel long distances before ultimately settling, spreading through the whole globe. Also, these nitrogen and sulfur emissions are amongst the primary causes of atmospheric pollution, annually responsible for an estimated 4-5% of the global burden of disease [6].

Another important point to consider is that, due to their nature, traditional energy sources are inconsistently localized through the globe, which can present high costs of transportation and force many countries to rely completely on an external energy source in order to function [6], which can have devastating results for the country's economy. For instance, in 1973 the Organization of Arab Petroleum Exporting Countries (OPEC) announced an oil embargo directed at the countries perceived as supporting Israel during the Arab-Israeli war (Yom Kippur war), selectively boycotting those nations' oil supplies. This led to an aggressive oil price increase of 400% and, consequently, a heavy blow to the industrialized world, with devastating consequences for the global economy [7]. This awoke a generalized interest in alternative fuels in the hope of minimizing the impact of the oil shortage on the global economy. So, by the end of the 70s, many countries had directed efforts into the search for alternative, preferably renewable energy sources, to break free from the oil monopoly hold of the OPEC [7].

Lastly, since fossil fuel is a limited resource, thus bound to end, another fuel source was impending. By 1998, the sum of all known petroleum reserves worldwide was estimated to be depleted in less than 50 years, assuming the consumption rate of that time [8]. Now, 22 years later and after an exponential growth of the fossil fuels' consumption rate, many countries rely on modern technology to increase the efficiency of bioenergy conversion. To achieve this, there is a wide range of biofuels being developed and perfected towards economic viability, to compete with (and ultimately replace) fossil fuels [9]. This is done not only by optimizing the biofuel production process, but also by designing modern biofuel production plants that allow co-generation of power and heat [9]. There are even some options of simultaneous co-production of added-value products, making the overall process more lucrative [10].

Therefore, the change from traditional to more sustainable energy sources is appealing in many sectors:

- Ecological: reduction of GHG emissions, mitigating the contribution to global warming.
- Public health: hopefully reducing the annual burden of disease caused by air pollution.
- Resource management: slowing down the use of limited fossil fuel reserves.
- Energy independence: allowing independence from countries with natural petroleum reserves.
- Economical: by cutting back the importation costs of petroleum and producing fuel at a national level, there will be an improvement in the countries' economy. Additionally, there is still the option of simultaneously producing other added-value products and the co-generation of heat and power.

## 1.2. Biofuel

Biofuels are defined as fuels that are produced from biomass – a renewable source, sustainable, and locally available – and, ideally, they are non-polluting. Biofuels can be liquid or gaseous and are usually used for the transport sector [11,12]. Liquid biofuels can then be divided into three categories: biodiesel (from natural oils), biocrude (from synthetic oils), and alcohols. The most widely used are, by far, bioethanol and biodiesel [11]. Bioethanol is currently the most used biofuel, either as a gasoline additive or even substitute, while biodiesel is used for complementing or replacing petroleum-based diesel [11]. However, it should be noted that the energetic content of biodiesel is similar to diesel, but (bio)ethanol only has around two-thirds of the energy content of gasoline [13].

### 1.2.1. Life Cycle Assessment

Life cycle assessment (LCA) is the study and evaluation of the environmental effects of a substance or product during its entire lifetime [14]. Therefore, it is an important parameter to consider, since the goal of biofuel, in general, is to reach a lower or even negative emission of $CO_2$, when considering the entire life cycle of bioethanol – **Figure 1.5** – from biomass to combustion [8]. Thus, a negative emission is possible because the LCA accounts for the carbon dioxide uptake during the growing process of the biomass. Thus, if the emissions from bioethanol combustion are low enough to be countered by the $CO_2$ consumption during growth, there is a negative $CO_2$ balance, meaning that the biofuel cycle ends up actively removing $CO_2$ from the atmosphere [8,13,14].

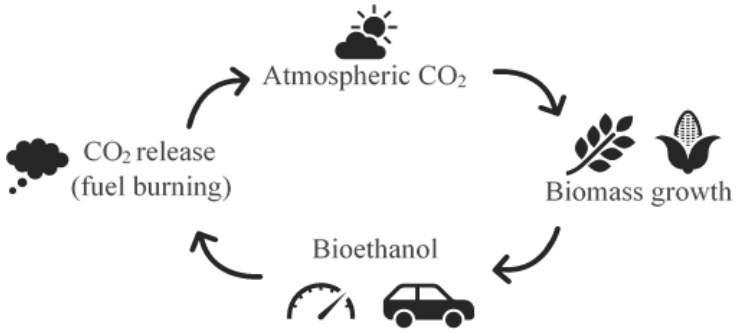


Figure 1.5: The $CO_2$ life cycle of a biofuel. Atmospheric $CO_2$ is absorbed by biomass growth. After bioethanol production and combustion, there is the re-release of $CO_2$ back into the atmosphere. If the released $CO_2$ during the fuel combustion is less than the uptake made by the biomass, it is a case of a negative emission cycle.

Biodiesel presents good results of ecological impact. One of those examples is a study of the life cycle of soybean-derived biodiesel, which concluded that by replacing the petroleum diesel in regular buses with B100 (100% biodiesel [15]), there is a reduction in the life cycle emissions of 35% in carbon monoxide, 8% in sulfur oxides, and 78.45% in carbon dioxide [8,13]. However, the best example of the possibility of an overall negative carbon dioxide balance is the study of the life cycle of E85 bioethanol (a blend of gasoline with 70-95% bioethanol [15]) from different biomass sources used in vehicles with engines adjusted to the use of fuels with high bioethanol content. The best results in GHG emissions (accounting for $CO_2$, $CH_4$, and $N_2O$), when compared with the life cycles of gasoline, showed a reduction of around 115% GHGs in two types of bioethanol, derived from different biomasses: one of them from switchgrass and the other from hybrid poplar trees [13,14].

Thus, biofuels are a sustainable option for a more environmentally conscious fuel, provided that the overall production system is not only designed but also maintained and managed responsibly [9].

### 1.2.2. Biodiesel

Biodiesel is a monoalkyl ester of fatty acids, resulting from transesterification (or esterification) of a long-chain fatty acid by using low molecular weight alcohol (usually methanol) in the presence of catalysts – **Figure 1.6** [8,11,12]. The long-chain fatty acids used are from renewable lipid feedstocks, like animal fat [9,16], waste oils [12,17], or vegetable oils (usually extracted from seeds) [18,19].

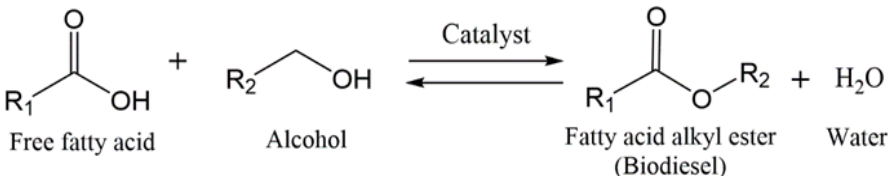


Figure 1.6: Scheme of biodiesel production: Transesterification of a free fatty acid into a fatty acid alkyl ester (biofuel molecule), using a low molecular weight alcohol in the presence of catalysts. Reproduced from [12].

### 1.2.3. Bioethanol

Bioethanol is ethanol (ethyl alcohol) that is produced through alcoholic fermentation of simple sugars, monomers, or dimers, which derive from biomass [11]. It is the most popular biofuel in the transport sector [10] and, in 2019, around 110 billion liters were produced (3). The current titans in bioethanol production are the USA and Brazil (3) – **Figure 1.7** – providing for a combined 84% of total production.

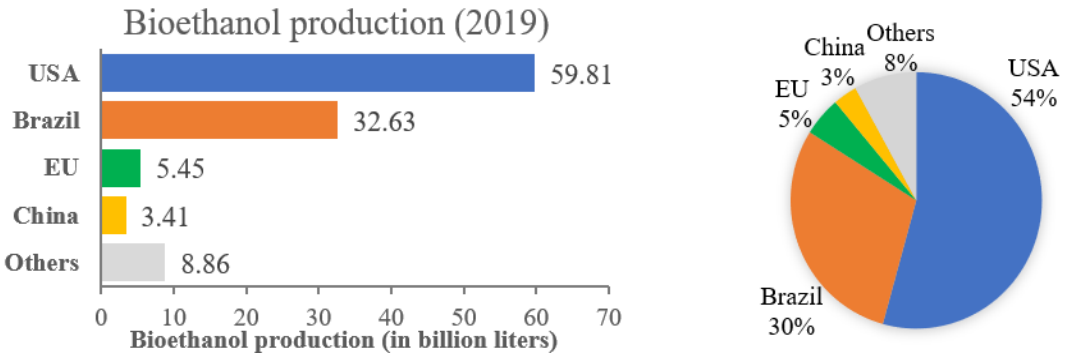


Figure 1.7: Absolute (left) and relative (right) values of bioethanol production in 2019, by countries/regions. Reproduced based on the data available in (3). Conversion of units assuming 1 US gallon = 3.7854 L.

Ethanol contains oxygen and is characterized by the high latent heat of vaporization, and both characteristics are pertinent to the eco-friendly combustion, its distribution, and storage.

There are two ethanol forms, hydrated and anhydrous. The hydrated form commonly contains 5% water and is usually the final product from the fermentation of biomass after distillation. It can be used as a straight spark-ignition fuel in warm climates or added to diesel as a 15% additive. Anhydrous ethanol, on the other hand, is 100% ethanol and is produced by an additional dehydration process that is required for blending with gasoline, which makes for the most common use of produced bioethanol. However, bioethanol can also be used as a straight fuel if in its anhydrous form (E100) [15].

Bioethanol is usually incorporated in a final product of 5% ethanol to 95% gasoline, according to the EU's quality standard EN228. This blend is covered by all vehicle warranties and requires no engine modifications at all. However, if engine modifications are made on the vehicle, bioethanol can then be used at higher levels. The category of bioethanol-blend with higher bioethanol content is the previously mentioned E85, containing 70-95% ethanol mixed with gasoline [15].

There are three generations of bioethanol, 1st [20], 2nd [21], and 3rd [22], and this classification is based on the biomass used as a source for fuel production.

## 1.3. The role of biomass in bioethanol production

Biomass can be composed of multiple organic products, from either vegetable or animal origin. It is renewable and can be used for energy production, either through thermal, chemical, or biochemical processes. Plants are the most common source of biomass, comprising what is considered waste (such as branches and foliage from parks and forests) as well as residues from other industries (such as crop residues from the food industry or pulp remainders from the paper industry). However, biomass can also originate from purposely grown crops. There is a wide range of sources, and its selection is mainly dependent on what is the most common, easily available and cheapest at that time and place [9,11,23].

The most used biomasses for the production of bioethanol are soybean [8], switchgrass [24], corn cob [24], wheat straws [25], sugar beets [26], and sweet sorghum [27]. Sugar cane [28], rapeseed (canola) [29,30], sunflower stalks [31], paper waste [32] and, more recently, algae [33] are also popular.

As mentioned earlier, depending on the biomass used as a source for bioethanol production, the resulting bioethanol can be classified as 1st generation (1GB) [20], 2nd generation (2GB) [21] or 3rd generation (3GB) [22] bioethanol.

First generational bioethanol uses biomass sources rich in starch or soluble sugars, cereal grains being the most used biomass sources. Since the production of bioethanol by the USA is mainly derived from corn, while Brazil relies more on sugarcane, the current bioethanol production heavily relies on biomass with high quantities of starch (USA) and soluble sugars (Brazil). Thus, most of the bioethanol being produced nowadays is a 1$^{st}$ generation bioethanol [20]. However, the main disadvantage of 1GB is that its production relies on biomass that can also be used as food. And in a world where the population keeps growing, there will be exponentially less food. Therefore, soon we will not be able to sustain the production of a biofuel that is in direct competition with the food supplies [9,20–22].

The second generation arose as an alternative, using exclusively non-food sources. 2GB bioethanol relies essentially on lignocellulosic raw material – mostly from fibrous/woody vegetable biomass – but can also be obtained from unused by-products from other industries, such as whey (cheese production) and crude glycerin (biodiesel production) [21]. Still, 2GB can compete indirectly with food supplies, as a large-scale production may require more land use. This can be overcome by the selection of fast-growing crops that are able to be cultivated in low-quality soil [9,21], such as switchgrass [24]. It can also rely on forest waste, such as sawdust [34] or pine cones [35], or agricultural waste, such as corn cobs [24], wheat straws [25], and sunflower stalks [31].

Finally, the third Generation does not compete with food supplies for land, using algae [33] as biomass, and thus the cultivating premises are aquatic. However, both feedstock and overall production are associated with a high cost, which becomes a determinant factor for the economic viability of 3GB [22].

Thus, after analysing the main characteristics of the three bioethanol generations – **Table 1.1** – 2GB seems the best option to invest in, at the moment. This is based not only on the ecological impact but also from a commercial point of view, since the high overall cost of 2GB production can be lowered by improving the production process, while the high cost of the biomass source of 3GB is mostly fixed, due to its intrinsic properties, such as algae growth rate [22]. Also, it should be noted that the best results on LCA were obtained for bioethanol from lignocellulosic biomass: switchgrass and hybrid poplar trees [14], both being cases of negative emission cycle, actively removing $CO_2$ from the atmosphere.

Table 1.1: Comparison of the three bioethanol generations.

| | **Bioethanol generations** | | |
|---|---|---|---|
| | **1GB** | **2GB** | **3GB** |
| **Biomass rich in** | Starch or soluble sugars | Lignocellulose | Lipids and Carbohydrates |
| **Most common source** | Cereal grains | Agricultural or forest waste | Algae |
| **Competition with food supplies** | Direct | Indirect (land use). But can be overcome by selecting specific sources | None |
| **Source cost** | High | Low | High |
| **Total cost of production** | Low | High | High |

## 1.4. Lignocellulosic biomass

Lignocellulosic biomass – **Figure 1.8** – is mainly constituted by cellulose, hemicellulose and lignin, alongside with ash and some other compounds in lower amounts [11,36]. This main constituents are found in the cell walls of plants, where cellulose and hemicellulose are carbohydrates with structural properties, and lignin is an aromatic polymer, strongly resistant to decomposition, that functions as a binder between plant cells [10,37].

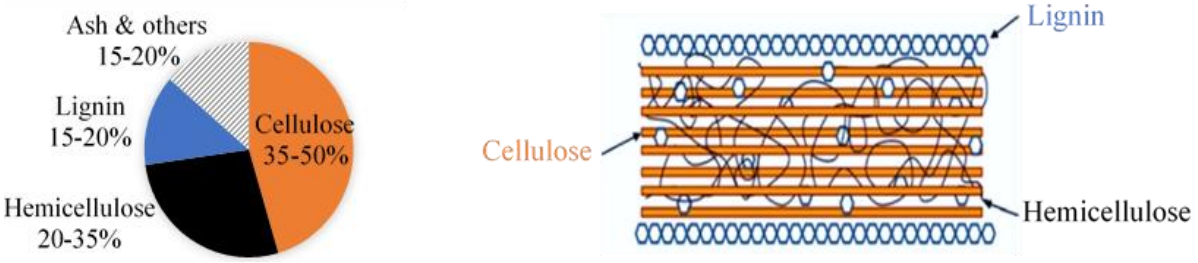


Figure 1.8: Overall composition of lignocellulosic biomass (left) and organization of the three main components of plant cell walls (right). Reproduced from [37].

Due to their location (and consequent abundance), these two sugar polymers make up the majority of vegetable biomass [36]. However, the proportion of these components can vary depending on the source of biomass, the harvest time, and even the genetic variability between plants of the same species [10].

Cellulose is the main component of lignocellulosic biomass and is a remarkably pure organic polymer, consisting of a homopolysaccharide formed by linear chains of D-glucose monomers, linked by β-(1,4)-glycosidic bonds, and strong inter and intrachain hydrogen bonds, therefore being insoluble in water and most organic solvents [11,21,37–40].

On the other hand, hemicelluloses are branched heteropolysaccharides, meaning that they are polymers constituted by multiple sugar monomers. These monomers may include pentoses (xylose and arabinose) and hexoses (mannose, galactose, and glucose), as well as some uronic acids and, in smaller amounts, other sugars, such as fucose and rhamnose, may also be present. Occasionally the hydroxyl groups of the sugar monomers can also be partially substituted by acetyl groups [23,37,41,42]. However, xylose is the most abundant sugar monomer. This is due to the fact that the most common hemicellulose in lignocellulosic biomass is xylan, a branched polymer with a xylose backbone that can have multiple other sugar monomers as branches [23,43], that is believed to have an important role in the maintenance of structural integrity of the cell walls, both by covalent and non-covalent bonds [41].

## 1.5. Grape Pomace

According to FAO (Food and Agriculture Organization of the UN), grapes are one of the most popular fruit crops, with over 79 million tons produced in 2018, mainly by Europe and Asia (4) – **Figure 1.9**.

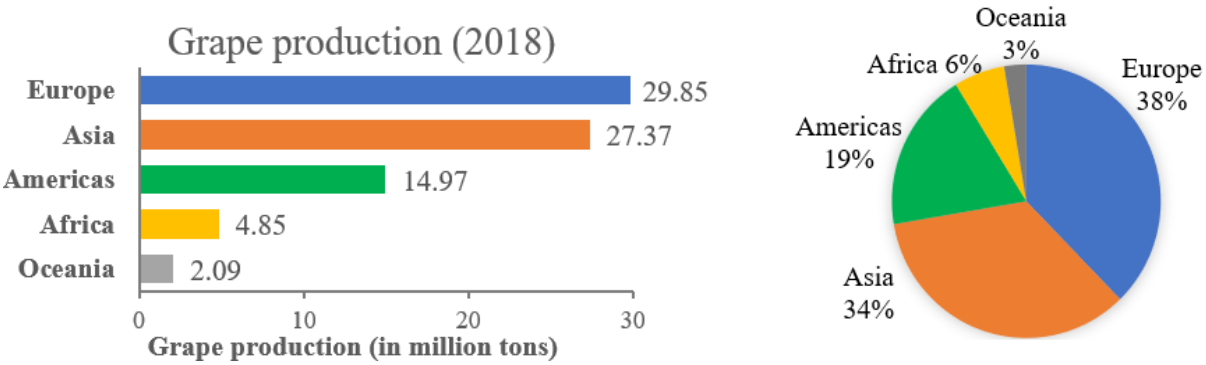


Figure 1.9: Absolute (left) and relative (right) values of grape production in 2018, organized by continental regions. Reproduced based on the data available in (4).

This popularity is due to the grapes' diverse consumption as fresh fruit and multiple processed products such as raisins, jams, jelly, juice, and, especially, wine. Wine is a very appreciated beverage all over the world, and in Portugal, the winemaking sector is of major socio-economic significance, substantially contributing to the national economy [44].

After the winemaking process, pomace is all that remains behind, being composed mainly of fibrous materials such as seeds (≈30%) and stems (≈30%), along with skins and remainders of pulp (≈40%) [45].

Since pomace is essentially considered waste, most of it is re-introduced into the land as compost, completing the carbon cycle. However, with the peak in production around harvest season (from August to October), there is a high intensity of wine production and a consequent high amount of pomace over a very short time span [45].

In 2018, the winemaking industry worldwide used more than half of all the consumable grapes produced that year, adding up to around 44 million tons [46]. After the pressing process, around 20-30% (w/w) of the grapes remains in the form of pomace [45], meaning that in 2018 alone, between 8.8 and 13.2 million tons of grape pomace were produced. Using that much pomace as compost can be detrimental to the environment, where the two main problems would be the lowering of the soil's pH (due to a high content of phenolic compounds), as well as the increase of the soil's resistance to biological degradation (due to the high content of lignocellulosic biomass) [47]. Additionally, there can also occur other problems related to the leaching of numerous compounds into both soil and groundwater, affecting flora and fauna [48].

Fortuitously, grape pomace is being increasingly treated as a by-product, rather than waste: industries ranging from food to pharmaceuticals and cosmetics have shown interest in extractable constituents, mainly polyphenols (for food supplements), and antioxidants (for food preservation and cosmetics) [45]. Still, after the extraction of those components, there is a lot of lignocellulosic biomass that remains [45].

### 1.5.1. Red Wine Grape Pomace (RWGP)

Contrary to white wine production, during the process of making red wine, the pomace is fermented alongside the grape juice and only extracted after the fermentation is over. Therefore, red wine is very poor in TSSC (Total Soluble Solid Content, a measure of the soluble sugar content), as the available soluble sugars were mostly consumed by the fermentative microorganisms during that process [45]. This makes for a pomace with low content in soluble sugars, so the majority of the carbohydrates present is composed of structural sugars, namely in the form of cellulose and hemicellulose – **Figure 1.10**.

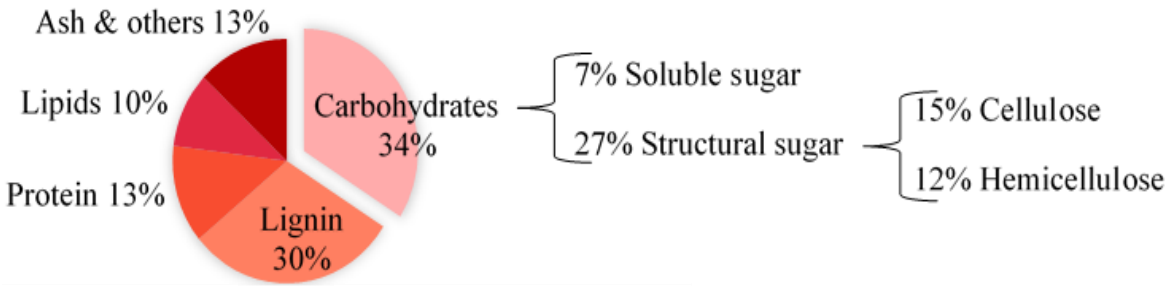


Figure 1.10: Characterization of the Red Wine Pomace used as biomass. Graphic reproduced based on [49].

## 1.6. The three-step process to lignocellulosic bioethanol

Through hydrolysis, both cellulose and hemicellulose from lignocellulosic biomass can be converted into their respective sugar monomers, which can then be fermented into added-value products, including bioethanol [11]. However, the whole production process for lignocellulosic bioethanol –

**Figure** 1.11 – requires three-steps (pretreatment, saccharification/hydrolysis, and fermentation) due to the complexity of the lignocellulosic structure [10,11,23,37,50,51].

The first step is the pretreatment of the biomass. This step is necessary due to the usually high resistance of the lignocellulosic biomass matrix to hydrolysis since the polysaccharides are mostly inaccessible, as they are embedded in a resilient lignin complex. Thus, this step is essential to increase the accessibility to the polysaccharides and, consequently, increase their vulnerability to hydrolysis [36,37]. This is done by breaking down the matrix of the lignocellulosic biomass and disrupting hydrogen bonds in the crystalline sections of cellulose, lowering its degree of polymerization (DP), increasing the fraction of amorphous cellulose, and increasing exposure of surface area of the cellulose for subsequent hydrolysis [36,37,50].

Contrary to cellulose, which has a very high degree of crystallinity, hemicelluloses are relatively easy to hydrolyze due to their branched and amorphous nature [37]. Since the resilience to degradation differs according to the different crystallinities and compositions, during the pretreatment, hemicellulose usually is broken down much faster than cellulose. Thus, this step also facilitates the separation of hemicellulose and cellulose. That happens because, when the hemicellulose is hydrolyzed, this fraction of the biomass becomes water-soluble [42,49,50,52]. However, hemicelluloses are sensitive to parameters such as temperature and retention time, and thus treatment conditions must be well controlled to avoid the formation of unwanted fermentation-inhibitors [37].

There are many pretreatment methods, ranging from physical (including, for example, milling and microwave irradiation) to chemical (the most common being acid or basic treatments), and also physicochemical (such as steam explosion and subcritical water) [37]. However, the methods of pretreatment mainly used are acid hydrolysis, steam explosion, and autohydrolysis (by using subcritical water). Acid hydrolysis has a high environmental impact due to the harsh pH and temperature conditions, as well as a high cost since the acid needs to be neutralized to be disposed of properly. The two best options are therefore steam explosion and autohydrolysis, both hydrothermal procedures, since they only use water. The choice of the best method between these is usually dependent on the biomass being used. The steam explosion has the best results with dry biomass, even though it has attached some negative environmental impacts due to the high energy requirements (which arrive from the high enthalpy of vaporization of water). On the other hand, autohydrolysis is usually the best method for high water content biomass [36,37]. This method uses subcritical water, taking advantage of the adjustability of water properties under subcritical conditions, using high temperatures and sufficient pressure to force the water to remain in the liquid state, leading to a higher ionic product and lower dielectric constant.

The second step in the production of bioethanol is saccharification, characterized by the hydrolysis of the sugar polysaccharides into their respective sugar monomers. Even though there are physical and chemical treatment options to hydrolyze the polysaccharides, those methods are most often highly energy-consuming due to the need for harsh pH and high-temperature conditions. This makes them both economically and ecologically unviable, especially when in large-scale industrial settings [53]. Thus, it is thought that the best strategy to perform the hydrolysis is by enzymatic saccharification, due to benefits such as lower energy requirements (from the milder conditions of temperature and pH), and consequent lower environmental impact, as well as the high specificity to the substrate and good conversion levels achieved [53]. The presence of lignin may hinder the action of the enzyme due to the low accessibility of the substrate, although the pretreatment can help overcome this problem [37].

Finally, the last step of the process of bioethanol production is fermentation: an anaerobic biological process that relies on microorganisms, usually yeast, in order to convert sugars into alcohol (in this case, ethanol) [10,11,23,37,50,51].

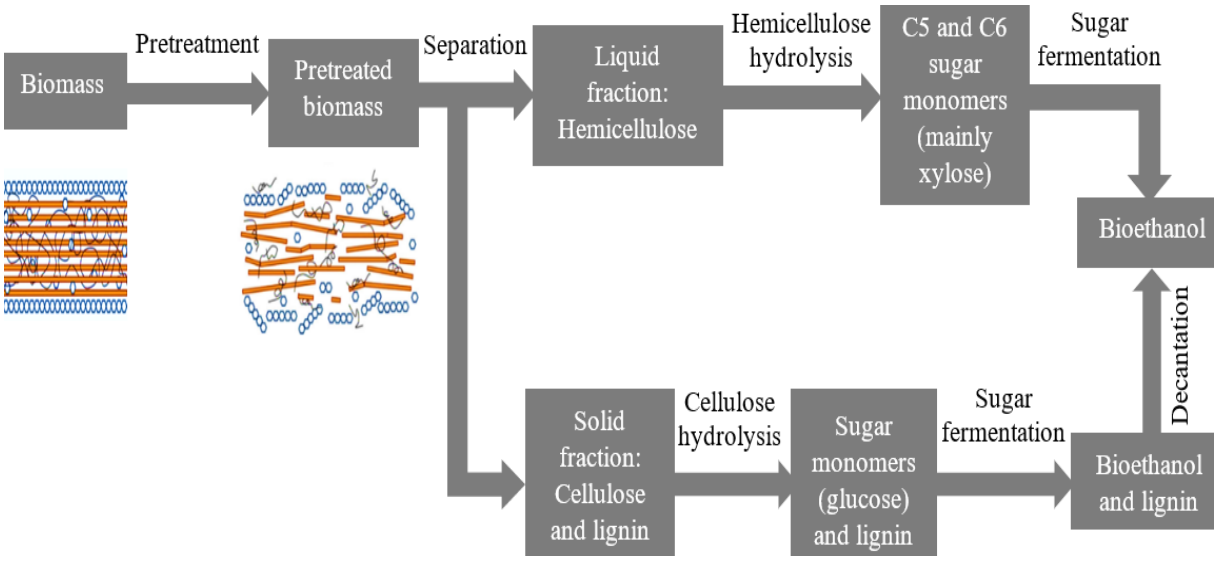


Figure 1.11: Flowchart of the process for bioethanol production from lignocellulosic biomass.

### 1.6.1. Production strategies for lignocellulosic bioethanol production

The process for bioethanol production from lignocellulosic biomass can be approached through four different strategies, as the multiple bioprocesses that take place (enzyme production, cellulose hydrolysis, hexose fermentation, and pentose fermentation) can be performed either separately or simultaneously [21,51,54]. Thus, the possible strategies to approach the process of bioethanol production from lignocellulosic biomass – **Figure 1.12** – are:

- Separate enzymatic hydrolysis and fermentation (SHF)
- Simultaneous saccharification and fermentation (SSF)
- Simultaneous saccharification and co-fermentation (SScF)
- Consolidated bioprocessing (CBP)

Separate enzymatic hydrolysis and fermentation (SHF) is the approach where all the processes occur individually. The second strategy is simultaneous saccharification and fermentation (SSF), where the enzymatic hydrolysis of cellulose to glucose is done simultaneously with the fermentation of glucose to ethanol. The third is the simultaneous saccharification and co-fermentation (SScF), in which enzymatic hydrolysis and fermentation of both hexoses and pentoses into ethanol are performed simultaneously. Lastly, in consolidated bioprocessing (CBP) approach, not only the enzymatic hydrolysis of cellulose and fermentation occur simultaneously, but the enzyme production too [21,54].

Since both SScF and CBP are fairly new approaches, they are not yet fully developed and require further research and optimization [21,54]. Thus, those two processes are not yet implemented to an industrial scale, whereas SHF and SSF are both viable industrial approaches. In some cases, SHF results in higher ethanol yields than SSF [55], but more frequently, the SSF produces higher ethanol yields in a shorter time [56–58], reducing the production cost. Thus, SSF is usually the more cost-effective approach and is, therefore, the preferred approach [21,54]. Nevertheless, the best strategy must be determined for each case, as both methods have different drawbacks: in the case of SSF, there is always a mismatch of the optimal conditions for hydrolytic enzymes and for fermentative microorganisms. Whereas the optimal conditions of pH overlap, the optimal temperature for hydrolytic enzymes is higher than the optimal temperature for fermentation [21]. Thus, depending on the enzymes and fermentation microorganisms used, the process is usually under sub-optimal conditions, and that may lead to lower ethanol yields. On the other hand, the lower efficiency in SHF is explained by an effect of end-product inhibition of the enzymes, which has a negative impact on the overall process. This is avoided with an SSF approach, since in SSF the glucose molecules are readily consumed by fermentative organisms [21]. Nonetheless, the end-product inhibition that occurs in SHF can sometimes be overcome by using enzymatic preparations with higher beta-glucosidase content [21], explaining the reported cases where SHF is considered better. This role of beta-glucosidases will be explored in more detail in **chapter 1.7.1.**

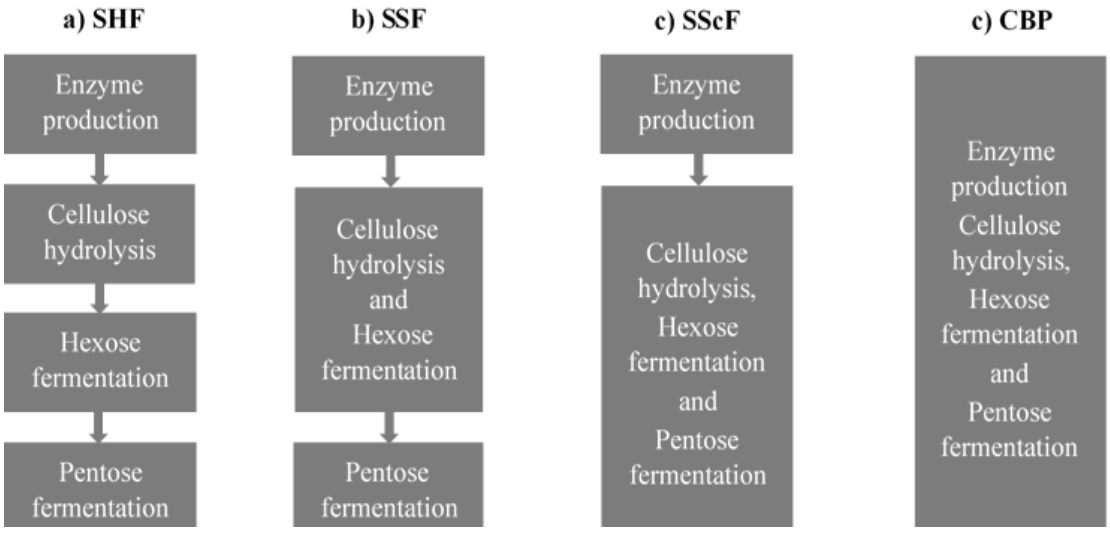


Figure 1.12: The four possible strategies to approach the process of bioethanol production from lignocellulosic biomass: a) Separate enzymatic hydrolysis and fermentation; b) Simultaneous saccharification and fermentation; c) Simultaneous saccharification and co-fermentation; d) Consolidated bioprocessing.

## 1.7. Main enzymes involved in the process

In 2016 G. Liu *et al*. [59] performed a cost evaluation of cellulase for industrial-scale bioethanol production from typical lignocellulosic biomass, concluding that the enzyme's cost can be as high as 0.65€/L, accounting for 48% of the minimum ethanol selling price (MESP).

Since the enzyme cost can represent almost half the price of the final product, a decrease in those costs will heavily minimize the overall price. Consequently, the main barrier to a more economically viable product is the saccharification step due to the high cost of the enzymes (especially cellulase).

So, reducing that expense has been the focal point in optimizing the production of lignocellulosic bioethanol [10,51,59–61], and the reason why the saccharification step is receiving much attention.

### 1.7.1. Cellulases

The hydrolysis of cellulose leads mostly to glucose, which is the most desirable final product, as it can then be applied as a substrate in the microbial production of multiple products, such as biofuel and many value-added chemicals [62]. However, even though glucose is the major product obtained in the saccharification step, small amounts of glucose oligomers, such as cellobiose (disaccharide) and cello-oligosaccharides, are also produced [36,63,64].

The enzymes that are responsible for catalyzing the process of cellulose depolymerization are called cellulases, consisting of a class of hydrolytic enzymes that catalyze the hydrolysis of glycosidic linkages. Cellulases are produced by multiple microorganisms, mainly fungi and prokaryotes, and comprise 3 main groups of enzymes [36,54,63,64]:

- Endoglucanase: EC 3.2.1.4 (5)
- Exoglucanases (also known as cellobiohydrolases): EC 3.2.1.91 (6) and E.C. 3.2.1.176 (7)
- Beta-glucosidase (also known as cellobiase): EC 3.2.1.21 (8)

It is important to note that cellulase action is considered synergetic, as the simultaneous action of the three classes of cellulase provides higher yields than the sequential addition of the three, separately [64].

Endoglucanase attacks the amorphous sections of cellulose, hydrolyzing (1→4)-beta-D-glucosidic linkages and resulting in a fast-paced decrease of the DP of the substrate [36]. This attack occurs in internal positions of the cellulose, cleaving internal bonds of its chains and exposing smaller cellulose polysaccharide units to the attack of other cellulases (5) [36,63,64].

Exoglucanases (cellulose 1,4-beta-cellobiosidase) can attack the crystalline portion of the cellulose chain, hydrolyzing (1→4)-beta-D-glucosidic linkages and sequentially converting small polysaccharide units into cellobiose units and decreasing the DP of the substrate, though at a very slow rate [36]. This occurs on the terminal sections of the exposed polysaccharide units and can take place on the non-reducing end (EC 3.2.1.91) or on the reducing end (E.C. 3.2.1.176) (6), (7), [36,63,64].

Beta-glucosidase (cellobiase) has an important role in the polishing step of the final product by hydrolyzing terminal non-reducing beta-D-glucosyl residues, converting cellobiose and short oligosaccharides into individual units of monomeric glucose. This final step not only decreases the product inhibition of exoglucanases by promoting a product outflow, but also increases the relative percentage of glucose in the final product, which is, as mentioned, the most desirable final product (8), [36,63,64].

### 1.7.1. Hemicellulases

Hemicellulases are a group of enzymes with multiple uses in several industries, in the processing of paper and juice pulps, textiles, animal feed, as well as in agriculture and bioethanol [23,42,43,65]. However, due to the homogeneity of hemicellulose, there is a very large number of enzymes that are implied in the total hydrolysis of that substrate [64].

Since the main type of hemicellulose is xylan (by far the most abundant, present in both hard and softwood), the most studied enzymes and degradation systems are focused on the degradation of xylan [23,42,43,66], and based on many microorganisms (such as *Talaromyces emersonii* and *Penicillium capsulatum*) that possess complete enzymatic systems for xylan degradation [23].

These systems rely on two main groups of enzymes:

- Xylase (endo-xylanase): EC 3.2.1.8 (9)
- β-xylosidase (also known as exo-1,4-beta-xylosidase and xylobiase): EC 3.2. 1.37 (10)

Xylase (Endo-1,4-beta-xylanase) is responsible for the hydrolysis of random (1→4)-beta-D-xylosidic linkages in xylan chains. This is a key enzyme in the process of degradation of polymeric xylan, degrading it into smaller chain oligomers (9), [23,43,66].

Contrarily, beta-xylosidase (Exo-1,4-beta-xylosidase) hydrolyses successive (1→4)-beta-D-xylans, removing consecutive D-xylose residues from the non-reducing terminal of chains (10) , [23,43,66].

## 1.8. Biocatalysis: the role of enzymes as catalysts

Most catalysts used in industry are of inorganic, organometallic, or organic nature. However, the use of biocatalysts – catalysts of a biological nature – is becoming progressively more popular [67].

According to IUPAC, a biocatalyst is "an enzyme or enzyme complex consisting of, or derived from, an organism or cell culture (in cell-free or whole-cell forms) that catalyzes metabolic reactions in living organisms and/or substrate conversions in various chemical reactions" [68]. Therefore, biocatalysis is the production of specific products through chemical transformations that are catalyzed by enzymes.

Enzymes are a greener alternative to their chemical catalyst counterparts – **Table 1.2** – as biocatalysis is a "natural" process that takes place under a milder set of reaction conditions, as regards temperature and pH [53]. It also leads to less waste due to fewer by-products and, thus, present a lower environmental impact. Additionally, they have high specificity for the substrate [53].

However, industrial applications of biocatalysts are limited by practical challenges, such as long term stability and shelf life [69], and high cost, as mentioned, due to costs of production and purification [70]. Also, to make the most of enzyme activity, there is the need to perform the process at the conditions that best suit enzyme function, usually leading to a narrow range of conditions that can be used. There is also the possibility of some substances acting as enzyme inhibitors, which results in a short operational lifetime of the enzyme [70].

From an economic point of view, it is important to optimize the process and the enzyme criteria to achieve a competitive performance against other market options. To that end, the dosage of the enzyme and the overall yield are the main parameters that affect the enzyme cost. Therefore, reducing the enzyme loading (consisting of the ratio between enzyme mass and substrate mass) is a good option to decrease the impact of the enzyme production cost [59].

In theory, enzymes are not consumed in the transformation process. However, over time they may become inactive. This is usually observed with cellulases during the hydrolysis of biomass, where the enzymes become irreversibly adsorbed or bound to solid particles, especially in the presence of lignin, leading to the necessity of a very high cellulase enzyme loading. To circumvent this problem, there are usually two direct options that can be done simultaneously: improving the cellulase performance by tuning the hydrolysis parameters to the optimal conditions and making possible the reuse of the enzymes that remain functional after the process is complete, which is possible by immobilizing the enzymes onto the surface of a retrievable matrix [59].

However, there is another option to enhance the efficiency of the saccharification process that is sometimes used to counter the inactivation of the enzymes that happens by the irreversible interaction with the substrate: the most studied approach is resorting to low-cost additives during the saccharification process [61], namely inexpensive proteins like BSA [39] or soy protein [61]. These work as surfactants, being the general theory that the surfactants bind to lignin, and therefore reduce the chance of binding between cellulases and lignin, avoiding bonds that are unproductive and can result in the enzyme's inactivation [61,71]. However, there is a study where it was demonstrated that the surfactant PEG 4000 prevents cellulase deactivation in both biomass and pure cellulose, suggesting that the deactivation can be induced by cellulose itself, and not only lignin [72].

Table 1.2: Summary of advantages and disadvantages of enzymes, as opposed to chemical catalysts.

| Advantages | Disadvantages |
|---|---|
| High substrate specificity | Short-term operational stability |
| Green option | Lower shelf life |
| Not consumed during the reaction | Low recovery and reusability |
| Less energy cost | |
| Less waste | |
| Performance in different media | |
| Activity and/or specificity can change according to the media | |

To take advantage of the multiple advantages of enzymes and reduce the disadvantages of low recovery and reusability, the process of enzyme immobilization is the golden standard [69,70,73,74].

## 1.9. Enzyme immobilization

Immobilized enzymes are defined as "enzymes that are physically confined or localized in a certain defined region of space with retention of their catalytic activities, and which can be used repeatedly and continuously" [75]. This concept of immobilizing enzymes was born in 1916 by the hand of J. M. Nelson and E. G. Griffin, when it was demonstrated through two of their articles [76,77] that invertase remains active when adsorbed on a solid matrix, such as glass and charcoal. This discovery marks the beginning of the study and development of properties that derive from immobilizing enzymes, leading to many currently available enzyme immobilization techniques.

In industry, immobilized enzymes were firstly used in 1966 to obtain synthetic racemic D-L amino acids by immobilized aminoacylase from *Aspergillus oryzae* [78], and throughout the late 90s, many sectors of the industry followed [69]. Currently, the global need for efficient technologies that are safer and more environment-friendly led to the rising of white biotechnology [67]. This is the biggest branch of modern biotechnology and englobes every industrial setting on which biocatalysts are applied [79]. This branch is exponentially booming since, in the last few years, the use of biocatalysts has been progressively more sought-after for the replacement of chemical catalysts in chemical transformations due to the increasing concern about environmental policies [67]. Now, immobilized enzymes are widely used not only for diverse industrial applications, such as textile [80], detergent [81], and food [82,83] industries but also in biomedicine [82], wastewater treatment [84,85] and energy [86].

The immobilization process has a lot of potential, since it can bring many advantages – **Table 1.3** – to the functional properties of enzymes: Namely by enhancing or altering their properties, such as activity, stability, selectivity, or even solubility. However, like most processes, some drawbacks might exist, and thus the decision on whether and how to immobilize each protein varies from case to case [73].

Table 1.3: Advantages and disadvantages of immobilized enzymes, as opposed to soluble enzymes.

| Advantages | Disadvantages |
|---|---|
| Enhanced enzyme stability | Lower reactional rates |
| Greater resistance to environmental changes | Possible diffusional limitations |
| Facilitated recovery | Immobilization process costs |
| Lower washout probability | |
| Reusable | |
| Easier reactor operation | |
| More robust | |

Perhaps the most important advantage of enzyme immobilization is that converting enzymes into heterogeneous complexes allows for an easy recovery and separation of enzyme and product, allowing for rapid termination of reactions and a greater variety of bioreactor designs [70].

The decision on whether to immobilize an enzyme for an industrial application is usually simple: An immobilization is only considered profitable if the process relies on a cost-effective protocol, producing, at the lowest cost possible, an immobilized enzyme system that can be re-used over long periods of time. This way, the system will outweigh the cost of the immobilization protocol by reducing the amounts of an enzyme that would otherwise be used [73]. Consequently, over the last 40 years, multiple protocols for enzyme immobilization have been reported, but only a few are advantageous enough in order to improve the properties of the enzyme at a beneficial cost for use in an industrial context [87].

## 1.10. Immobilization techniques

There are several methods – **Figure 1.13** – that can be used to immobilize enzymes. These include adsorption, entrapment, and covalent binding and can be divided into physical and chemical methods, as well as reversible and irreversible methods.

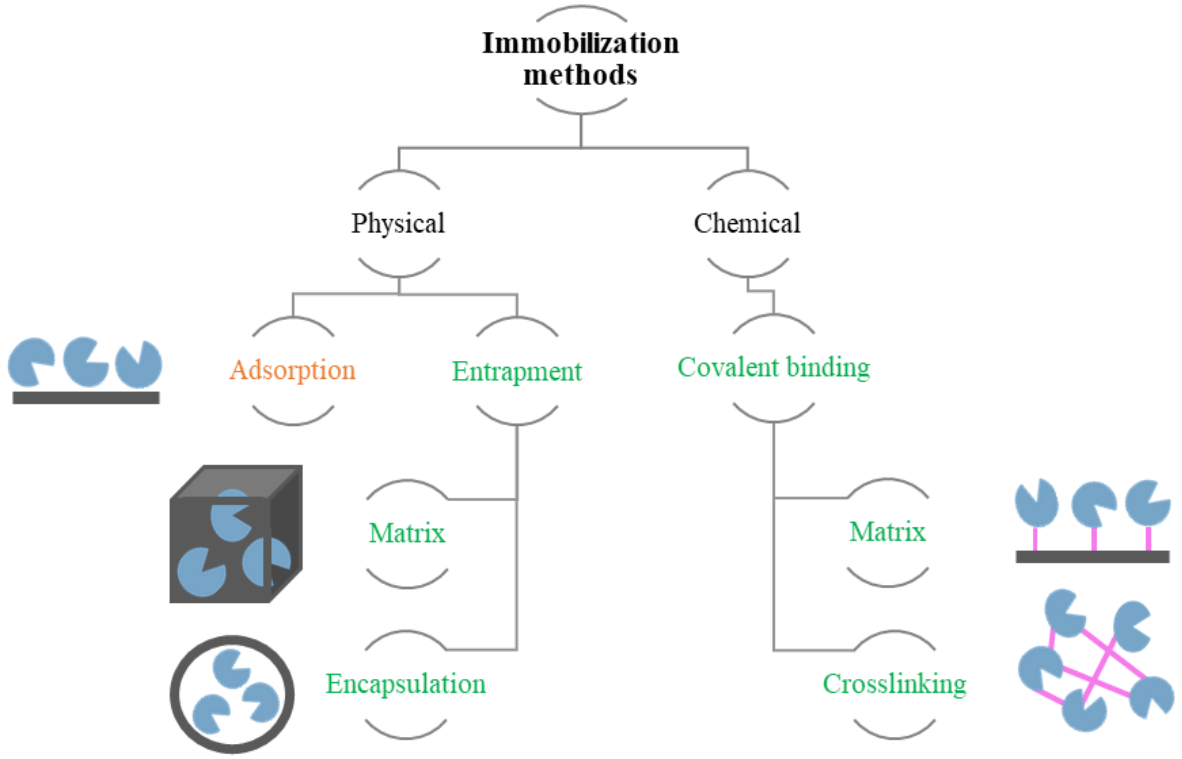


Figure 1.13: Scheme of the usual immobilization methods. Enzymes are represented in blue, the support in grey, and the covalent bonds in pink. The methods written in orange (adsorption) are easily reversible, while the methods in green (entrapment and covalent binding) are considered irreversible.

All methods have their advantages and drawbacks, especially when comparing different enzymes. This is due not only to the unique chemical characteristics of every enzyme – which influences the enzymes' properties in general and, therefore, the interaction between them and the substrate – but also the properties of substrates and products, as they need to interact with the enzyme's active center. Additionally, to decide which immobilization technique will be used, there are many considerations to make regarding the changes in chemical and physical properties that the enzymes will be exposed to when undergoing immobilization since the immobilization processes usually lead to changes in enzyme conformation and in the microenvironment [70,73,78,87–92].

An important criterion that needs to be considered is the size of the substrate. Diffusional limitations are sometimes observed because, for the reaction to occur, the substrate must reach the enzyme's surface.

Thus, the molecular weight of the substrate must sometimes be considered, as the diffusion of larger molecules (e.g. polysaccharides such as cellulose and hemicellulose) will be limited by steric interactions with the matrix, hampering the access of the enzyme to the substrate [87,90].

The concentration of enzyme on the surface is another important factor to be controlled: the goal is to maximize the number of enzyme molecules at the surface to achieve high activity. However, an excess of enzyme molecules at the surface can have adverse effects. This topic will be explored in greater detail in **chapter 2.10.1** and is represented in **Figure 2.5**.

Although the best option for immobilization depends on each specific situation, some general properties of different methods can still be identified.

Entrapment methods are usually the most durable, since the enzyme is permanently trapped and, therefore, there is no leaching. However, there are intrinsic diffusional problems, limiting the interaction between enzymes and substrate. This is particularly true with larger substrates [70,73,78,87–89,92].

Adsorption has been widely popular and, overall, up until the last few years, the most used method of immobilization [39,59,74,77,84,93–104], relying only on ionic bonding as interactive forces [102]. But, with the progress of science and the optimization of protocols, covalent immobilization is becoming more and more popular: with the advance of the immobilization field, the main technique shifted to covalent bonding [39,43,84,94,96,97,99,102,105–114], where usually is used glutaraldehyde as a crosslinking agent [84,115] even though DAS (dialdehyde starch) is also a popular choice [98,115]. This change of preference happened since the covalent method brings multiple advantages over adsorption: in adsorption, the interface between enzyme and support is made by unspecific interactions. Hence, there is a greater range of random binding sites, where some can prove disadvantageous by altering the structure and specificity of the enzyme, impairing the enzyme's ability to function, or the access of the substrate to the enzymes' active site. In some cases – if the surface energy conditions do not favor the enzymes' native conformation – these interactions can even lead to enzyme unfolding and/or aggregation [91]. Also, since adsorption is a reversible interaction, there is usually a great extent of release of the enzyme molecules from the support [87–89].

Covalent binding is the most extensively studied immobilization technique. It consists of the formation of covalent bonds, traditionally between the enzyme and the matrix of the support. This allows retaining the enzyme at the surface of the selected support [73]. However, there is also a sub-class of covalent binding, known as crosslinking or reticulation, that does not rely on a substrate [87,88]. The covalent bonds occur randomly on the side chains of amino acids such as lysine, arginine, histidine, tryptophan, tyrosine, cysteine, serine, threonine, and tryptophan, as well as aspartic and glutamic acids [73,87]. There are, therefore, multiple available options to form covalent bonds. Thus, due to the randomness factor, covalent binding is generally the hardest immobilization technique to reproduce because, to function, the enzymes need to have their active center available to interact with the substrate. Thus, the random location of the bonds formed with the support can influence the activity between replicas [87].

In conclusion, adsorption is simple and cheap, but easily reversible and, therefore, short-lasting. Covalent attachment, on the other hand, is less reproducible and, since the covalent bonds formed will most likely decrease the enzyme's flexibility, it can lead to impaired performance [70,73,78,87–89]. But by being a long-lasting alternative, covalent binding can be very advantageous in the long run.

Finally, as mentioned earlier, crosslinking (also referred to as reticulation) is a sub-type of covalent technique that does not rely on a support matrix and is characterized by the formation of covalent intermolecular bonds between enzymes, either through bi- or multifunctional agents. These bonds give rise to crosslinked enzyme aggregates (CLEAs), making this the only technique that can exist without support [87,88]. However, crosslinking can also be used as a complement to other techniques to increase the stability of already immobilized enzymes. Nevertheless, an excess of reticulation can lead to diffusional barriers, resulting in less efficiency of the overall enzymatic complex, and this is the reason why it is important to optimize the crosslinker concentration for each particular case [87].

Just like the decision on whether to immobilize enzymes, there is no universal best method, and, ultimately, it depends on each particular case. Thus, the optimal immobilization conditions (including the support, method to follow, and reaction conditions) need to be determined through the empirical method of trial and error. For this purpose, multiple parameters need to be tested in an effort to reach high retention of activity, durability and operational stability [70,73,78,87–89,92].

Nevertheless, this criteria must always be checked against the economic viability of the complete process, considering both the investment in the immobilization process and the results of reaction efficiency and reusability.

## 1.11. Immobilization support matrix

The performance of the immobilized enzyme system is influenced not only by the immobilization method but also by the matrix characteristics. Consequently, the choice of support for the enzymes' immobilization is a decision of great importance that may dictate the success or failure of a process that relies on immobilized enzymes – as opposed to the recurrent use of free enzyme – when scaled up for industrial applications. Thus, to enhance the chances of success, there are multiple properties that are considered desirable for a support matrix: These include structural properties such as inertness, stability, physical strength, high affinity to proteins, available reactive functional groups, and hydrophilicity. Additionally, there are also characteristics meeting some biological and ecological concerns, such as being a regenerable material with low ecological impact, non-toxic and biodegradable. Finally, the material must be sufficiently low cost to be economically advantageous. Some supports can even display an aptitude for enhancing enzyme specificity/activity or reducing microbial contaminations [70,73,87].

Regarding the choice of the matrix, there are multiple options, but the most important thing to remember is that, regardless of the selected immobilization technique, it is essential for the matrix to be insoluble in the solvent used for the reaction [89]. Amongst the most commonly used support materials are several natural polymeric materials [69], like cellulose [82,116,117], collagen [118], and chitosan [114,119]. But there are also multiple inorganic supports, as silica [120], glass [121], and metallic nanoparticles like nickel and iron [84,97,98,102,105,111,117].

From all these, magnetic nanoparticles and chitosan microparticles have been shown to be two of the most attractive matrices for the immobilization of enzymes and will be described in more detail.

### 1.11.1. Magnetic nanoparticles

Due to the advances of material sciences, multiple new support matrices were recently identified as compatible with enzyme immobilization and standard enzyme-functioning conditions. Eventually, from all the new supports identified, the ones at the nanoscale became more popular due to their high surface to volume ratio [69,87,90,116,122]. These are commonly called nanoparticles (NPs) and are defined by IUPAC as particles of any shape, with dimensions in the 1-100 nm range [123].

For the past few years, the emerging preference for enzyme immobilization in catalytic and industrial context landed on nano-supports: these are ideal matrices for immobilization, as they maximize the surface area, allowing for higher loading of protein onto their surface and reducing diffusional limitations. It is important to note that diffusion problems increase when dealing with macromolecular substrates, making nano supports especially beneficial in those cases. In fact, the properties of nano supports can lead to a reduction of protein unfolding, thereby improving stability and thus improving the performance of the complex [69,82,84,87,90,116,122,124,125].

Among all the available nano supports, magnetic nanoparticles (mNPs) are the ones receiving more interest, due to advantages such as low toxicity – a key factor in the biomedical field [82,126] – but, mostly, from an industrial point of view, due to their ease of retrieval: This happens because mNPs are composed of metal, such as iron, nickel or cobalt and/or their oxides and, because of that, they respond to magnetic fields [122,125,127,128]. Therefore, these are the ideal matrices for an industrial context due to their low cost and ease of production, and can provide the properties for continuous economic operations, automation, and a facilitated high-purity recovery of the complexes for re-use (by application of an external magnetic field, due to their magnetic properties) [69,73,86,87,92,124].

These mNPs have been applied in environmental [84] and industrial [82] catalysis, where they are extensively studied as support matrix options for the immobilization of enzymes [124,127], as well as multiple applications in biomedicine as biosensors [82,126], used either for diagnosis (as contrast agents in imaging by magnetic resonance), therapy (by controlled drug delivery) or theragnostic (where the nanoparticles act simultaneously as contrast agents and treatment by hyperthermia) [126,129].

It should be noted that the results in the literature for enzyme immobilization onto mNPs are more due to the enzyme's response to the immobilization than due to the matrix itself. However, there was a study on immobilization of cellulase mixtures on mNPs [39] that investigated the effect of particle sizes by comparing the effect of particles with 1000 and 500 nm of diameter, with an increase of 23% of activity on the smaller particles. Therefore, it concluded that the increase of activity was due to the increase of the surface area per mass of particles, allowing for a greater chance of interaction with the enzymes. In that way, the size of the mNP can indeed be considered as an influence for the final complex's success.

The most studied type of mNPs is Superparamagnetic Iron Oxide Nanoparticles (SPIONs). These are $Fe_3O_4$, $\alpha$-$Fe_2O_3$, or $\gamma$-$Fe_2O_3$ nanoparticles with a core diameter between 10 to 20 nm [122,125]. But the small size is not the only reason why SPIONs are such popular support: SPIONs not only are biocompatible and have low toxicity, but also have the most desired magnetic properties: They do not retain residual magnetism, meaning that when the nanoparticles are not exposed to a magnetic field, they are not magnetic [122,125].

Amongst all the iron oxides, magnetite, $Fe_3O_4$, is favored [84,97,98,102,105,111,117] for having the biggest magnetic moment and the presence of iron cations in two valence states (both $Fe^{2+}$ and $Fe^{3+}$), as well as a relatively simple synthesis [122,130].

Magnetic nanoparticles can be synthesized by different methods, such as chemical co-precipitation, thermal decomposition, microemulsion, and hydrothermal synthesis. The adequate method must be determined based on the desired application, as the properties of the resulting mNPs will be highly influenced by the method [125,129]. With the industrial application purpose in mind, only co-precipitation and thermal decomposition are scalable [125]. Between those two, chemical co-precipitation is not only considered the simplest protocol, but also is fast, cheap, does not require high temperature, and the solvent used is water, instead of an organic medium. Also, the resulting nanoparticles are monodispersed. On the other hand, they are highly reactive, which leads to a high probability of aggregation. To counter that, these nanoparticles usually need surfactants to increase stability and remain at the nanoscale [125,129], which will be furthered discussed in **chapter 1.11.2**.

### 1.11.2. Magnetic nanoparticles stabilization

Due to their high surface area to volume ratio and hydrophobic surfaces, mNPs are very popular supports for enzyme immobilization. However, due to those same characteristics they tend to aggregate in clusters of different sizes, resulting in a heterogeneous size distribution. Additionally, some mNPs (particularly $Fe_3O_4$) are easily oxidized, losing their magnetic properties. To minimize that, surface modifications are made with coating agents that increase the stability of the particles by bonding to the particle's surface. Then, by steric or electrostatic repulsion, they disperse the NPs, keeping them in a stable colloidal state [122,125,127,130–133].

Various molecules can be used according to the matrix and desired application, as many functional groups have an affinity to inorganic surfaces. Therefore, coating agents can be natural polymers (such as chitosan [127], which will be referred to in more detail in **chapter 1.11.4**), artificial polymers, as well as small molecules – such as (3-aminopropyl)triethoxylsilane (APTES) [130] and dimercaptosuccinic acid (DMSA) [132], explored in greater detail in **chapters 1.11.2.1 and 1.11.2.2** – or inorganic materials.

Simultaneously, this coating can also be used not only as protection for the magnetic core but also to functionalize the surface of the NP with specific functional groups that may be required for further optimization, including the formation of bonds between the coating agent and proteins, in covalent enzyme immobilization procedures [117,124,125,127,129,130,132,133].

#### 1.11.2.1. DMSA

DMSA – **Figure 1.14** – is a coupling agent commonly used to functionalize the surface of mNPs. It forms very strong and stable complexes with $Fe_3O_4$ [130,131,133] and functionalizes the NPs by covering their surface with both S and COOH functional groups. Depending on the conditions, one or both groups can be available for further functionalization of the complex, which is explored in more detail in **chapter 6.1.1**, and with the possible configurations represented in **Figure 6.1**.

Due to the presence of the COOH functional groups, DMSA is compatible with the crosslink protocol involving carbodiimides (explored in more detail in **chapter 1.11.3.1**) as it can react with primary amines, resulting in a condensation reaction to form amide bonds [130,133].

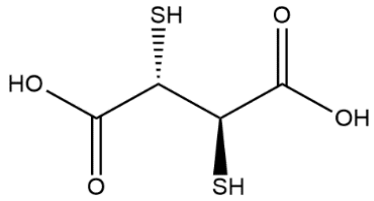


Figure 1.14: DMSA, Dimercaptosuccinic acid.

As mentioned before, the small hydrophilic molecules of DMSA have a high affinity to iron oxide surfaces and, due to their multiple carboxylic groups, are highly reactive towards the mNPs [134]. This can be a problem since due to its high reactivity, DMSA can lead to aggregates between the NPs, leaving the SPIONs less receptive for the functionalization step due to fewer sites available for potential bonding with the crosslinkers and proteins. Additionally, the free S-H groups can react between them, forming both intra- and interparticle bridges, contributing to the creation of aggregates [132]. Thus, it is essential to add a dialysis step after the coating is performed to remove the DMSA that has not reacted directly with the surface of the mNPs [135]. This step will reduce the chance of aggregate formation, which otherwise would lower the efficiency of the following functionalization step.

#### 1.11.2.2. ATPES

APTES – **Figure 1.15** – is an aminosilane coupling agent that is commonly used to functionalize the surface of mNPs [130,136]. Aminosilanes do so by coating the NPs through the formation of Fe-O-Si bonds, while simultaneously aminating the surface of the NP – due to the coupling agent's functional amine group (which can be primary or secondary). Therefore, APTES is compatible with the crosslinker glutaraldehyde, explored in more detail in **chapter 1.11.3.2**.

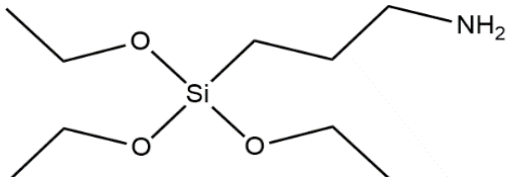


Figure 1.15: APTES, (3 aminopropyl)triethoxylsilane.

### 1.11.3. Surface functionalization

As mentioned earlier, the coating can be used not only as a protection for the magnetic core but also to functionalize the surface of the NP with specific functional groups that may be required for further optimization, including the formation of bonds between the coating agent and proteins, in covalent enzyme immobilization procedures [117,124,127,130,132,133]. To perform that bond between the coated matrix and the protein, a crosslinker is required. A crosslinker is a reagent that reacts with functional groups on two or more molecules to form a covalent linkage between them [137].

There are two main types of crosslinkers, characterized based on their spacer arm size. The spacer arm is the chemical chain between two reactive groups and can range from zero to over 100 Angstrom. Zero-length crosslinkers facilitate the direct bond between the matrix and the protein and do not remain in the final complex, being washed away after the immobilization is finished. On the other hand, spacer crosslinkers remain between the matrix and the protein, acting as the bridge between the two units. The spacer arm's length influences the flexibility of the final immobilization complex, with shorter arms resulting in lower flexibility and higher steric impediment. However, longer arms allow for more sites of potential nonspecific binding [137].

Additionally, bifunctional crosslinking agents, possessing two reactive functional groups, can be classified into two other groups: homobifunctional, and heterobifunctional. In homobifunctional crosslinking agents, the reactive functional groups are the same, while heterobifunctional crosslinkers have intrinsically distinct reactive functional groups at their terminations.

Homobifunctional conjugates are easy to prepare, as the duplicate number of available groups for reacting facilitates the process. Also, they can be used not only as primary crosslinkers (providing the bridge between matrix and proteins) but also as a secondary crosslinker in some immobilization assays (to reticulate the enzyme molecules between themselves), providing more robustness to the final complex. However, some self-conjugation of the NPs is bound to occur, potentially diminishing the conjugates' potentiality. Thus, heterobifunctional crosslinkers are considered the best alternative for a more controlled crosslinking, lowering the probability of unwanted self-conjugations [137].

Glutaraldehyde is a popular homobifunctional crosslinker further explored in **chapter 1.11.3.2**, while carbodiimides – more specifically 1-ethyl-3-(3-dimethylaminopropyl) carbodiimide (EDC) and N-hydroxysuccinimide (NHS) – are heterobifunctional crosslinkers, explored in **chapter 1.11.3.1**.

### 1.11.3.1. Carbodiimides (EDC/NHS)

Carbodiimides are the most used heterobifunctional crosslinkers and cause the conjugation of carboxyl groups (–COOH) to primary amines ($–NH_2$), by forming an amide bond. They are also zero-length crosslinkers, as they do not become part of the final product [133,137]. Said primary amines ($–NH_2$) exist at the N-terminus of each polypeptide chain and in lysine residues, and are usually facing the exterior of proteins due to their positive charge. Therefore, they are usually accessible for conjugation with minimal modification to the original protein structure [73,87].

EDC – **Figure 1.16** – forms an unstable intermediate, activating the carboxylic acid at the matrix's surface. This can then either hydrolyze back into the original state or react with a primary amino group, forming a stable amide bond.

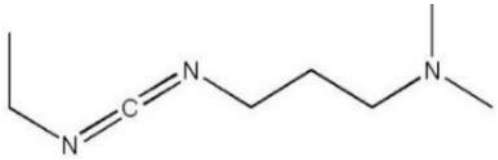


Figure 1.16: EDC, 1-ethyl-3-(3-dimethylaminopropyl)carbodiimide.

NHS – **Figure 1.17** – or its water-soluble analogue, Sulfo-NHS, are added in EDC-coupling protocols to enhance that process. NHS is only used as a complement to EDC and not as an individual crosslinker because its reaction requires a previously activated carboxylic acid group. However, compared to EDC, NHS forms a more stable ester with an extended half-life, less prone to hydrolysis, and can react with primary amines as well [133,137].

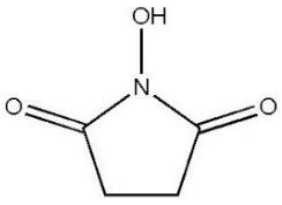


Figure 1.17: NHS, N-hydroxysuccinimide.

### 1.11.3.2. Glutaraldehyde

Glutaraldehyde – **Figure 1.18** – has been used for decades for crosslinking proteins, and is currently the most popular crosslinker due to its low cost, high stability and efficiency [69,73,87,88], as well as solubility in aqueous solvents and the ability to create inter and intra-molecular covalent bonds [124].

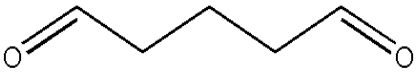

Figure 1.18: Glutaraldehyde.

Being a homobifunctional agent, both the reactive aldehyde groups at each end of the molecule can react with free primary amines. Therefore, glutaraldehyde conjugates are easy to prepare. Still, since it is assumed that both carbonyl groups have the same reactivity, both are equally likely to bind to the matrix or protein during the crosslinking process. Thus, the structure of the final product can vary, and some self-conjugation of the NPs is bound to occur, potentially diminishing the conjugates' potential. Because of this, heterobifunctional crosslinkers are usually considered the best alternative for a more controlled crosslinking, lowering the probability of unwanted self-conjugation [137].

### 1.11.4. Chitosan microparticles (CMPs)

Shellfish is a well-appreciated delicacy all over the world, with the last recorded value of worldwide consumption in FAO being around 13 million tons in 2013 (11).

Approximately 75% of the collected shellfish's total dry weight is considered waste [138], which can add up to more than 10.000 tons of shellfish waste every year [139]. Thus, the treatment of those by-products is of great importance, since if not processed the waste is thrown away at sea, in landfills, or burned, leading to a considerable environmental concern [139].

Chitin, which is a resource with valuable potential, can account for 20 up to almost 60% of that waste's dry weight [138]. It is one of the most widely available biopolymers and polysaccharides found in nature, second only to cellulose, and is found in many organisms, being a part of insects' exoskeletons, as well as cell walls of fungi and algae. Nowadays, commercial chitin is mainly extracted from marine sources, namely crustaceans' and mollusks' shells, thereby repurposing waste from shellfish processing industries, by demineralizing and deproteinating that waste, in order to extract chitin [70,139–143].

Since chitin is water-insoluble, which represents a major large-scale limitation, several water-soluble derivatives are produced, from which the most relevant is chitosan [139,142]. Chitin is a homopolymer of N-acetyl-D-glucosamine (an acetylated amide derivative of glucose), and by a partial N-deacetylation process is converted into chitosan, composed by randomly distributed N-acetyl-D-glucosamine (acetylated) and D-glucosamine (deacetylated) units, bound through β(1→4) linkages. Through this deacetylation process, the degree of acetylation decreases from around 82% (in chitin) to around 20% (in chitosan) [142], and chitosan becomes soluble in aqueous acidic conditions due to the protonatable amino groups in the deacetylated units [70,142,144].

Chitin and its derivates have multiple properties that make them good support for enzyme immobilization: in addition to the advantages of being an inexpensive and renewable material, they have essential ecological properties such as non-toxicity, biocompatibility and physiological inertness, and biodegradability into harmless products, as well as some biological qualities, such as antimicrobial and antioxidant activities [70,139,142]. Because of that, chitosan has been used in multiple fields, including medicine (where it is used as a biomaterial for drug delivery or tissue engineering) and pharmaceuticals (as anti-coagulant agents and cholesterol-lowering supplements) [144,145]. It can be used as well in agriculture as a biopesticide and antifungal treatment [146], in the food industry as a preservative due to its antioxidant and anti-microbial properties [147], or as a fining agent in winemaking [106]. It is also used as a flocculant in water treatments [148].

In the catalytic and industrial domains, since the publication of the works of Stanley and Muzzarelli [149] in 1976, several researchers started actively working on chitin and chitin derivates, especially chitosan, as promising and efficient supports for protein immobilization [150]. Currently, chitosan is used as an immobilization matrix in multiple forms: flakes [151], powder [152], and gels of multiple geometrical forms (with the possibility of a hollow core), like beads [106,112,119,153,154] or fibers, mostly used to be part of membranes [151,155,156]. However, some other more complex geometrical forms are also possible, like nanoflowers [157]. Additionally, chitosan can not only act as a matrix alone but also as a coating of another matrix, like mNPs, in multiple shapes, like magnetic-cored microparticles [127,129] or magnetic-cored nanofibers [158].

In some studies, the immobilization of proteins on chitin/chitosan takes advantage of its ability for chelating heavy metal, where that metal acts as an intermediate with which the protein then interacts [154]. However, the most widely common process to perform the immobilization is using glutaraldehyde as crosslinker [106,112,114,127,150,153,155,156]. This is possible due to another appealing chemical property of chitin and chitosan: an amino group (either acetylated or primary) on each unit. These amino groups make chitosan soluble in aqueous acidic media under pH 6.5 through the formation of $NH_3^+$. This makes chitosan highly reactive to negatively charged entities, leading not only to the ability to chelate heavy metal ions but also the possibility of aggregation with polyanions. Solubility in acidic solutions and aggregation with polyanions are both properties that ensure great gel-forming qualities of chitosan [70]. Additionally, these amino groups are very useful to bind multiple crosslinkers, highly used in processes to covalently bind proteins [142].

## 1.12. Cellulase and hemicellulases as immobilized enzymes

From an immobilization point of view, since cellulases are widely used in multiple fields, is it known that immobilization of cellulase is beneficial, as, in the industrial process, the enzymatic reactions are generally performed under high-temperature conditions. These harsh conditions can lead to a change in the enzyme's structure and the consequent loss of function. That loss of function can thus be overcome by immobilization, because as it has been shown in recent decades, most studies on cellulase immobilization determined that cellulase maintains a high activity for long periods of time when bound, as it improves the enzyme structure, becoming more resilient to the saccharification process harsh conditions [124]. These statements can be proved by multiple examples; for example, in 2009 [74], the hydrolytic activity of free and immobilized cellulase (onto Si wafers) was compared, concluding that the immobilized cellulase produced approximately 20% less glucose. However, the immobilized cellulase eventually becomes advantageous since the immobilization process applied allows the enzyme to be reused six times while retaining the original activity level.

On the other hand, hemicellulase immobilization is less studied, mainly due to the heterogeneity of the substrate, requiring different enzyme complexes according to the hemicellulose sugar constitution [23], and the low fermentability of the resulting sugar monomers by the usual industrial microbial strains [42]. However, there are still a few studies done on one of the usual hemicellulose hydrolytic enzymes. Since the most common type of hemicellulose is xylan, the most studied hemicellulase is xylanase. Xylanase has already been immobilized onto some supports, like agarose beads [113], alginate-polyethyleneimine gel beads [94], and modified graphene oxide nanosheets [43], but most of the studies focus on hemicellulase-cellulases complexes [96,105].

In regard to immobilization of complexes with both cellulase and hemicellulase onto magnetic nanoparticles, in 2017 [96] a commercial enzyme solution containing pectinase, xylanase, and cellulase was immobilized in APTS-$Fe_3O_4$ ($Fe_3O_4$ coated with 3-aminopropyltriethoxysilane), retaining 87% of pectinase, 69% of xylanase and 58% of cellulase activity when comparing with the enzyme's free form. This complex proved efficient up to the 5$^{th}$ cycle. In 2018 [105], another complex of mNPs and three enzymes, xylanase, cellulase, and amylase, was developed through covalent immobilization by glutaraldehyde. In that process, the enzymes were immobilized with an efficiency of 92% for xylanase, 45% for cellulase, and 93% for amylase, and the enzymes presented a maximum of retained activity of 69% for xylanase, 48% for cellulase, and 50% for amylase, after 13 cycles of use. Thus, it is inferred that cellulase is overall the enzyme that comparatively offers fewer promising results, either in retained activity or immobilization efficiency, leading to the need to use more protein, sacrificing around half due to the results in immobilization efficiency. However, this is understandable due to the difficulty of saccharification of cellulose being a lot higher than for other substrates.

It should be noted that all these immobilizations were by covalent bonding, most likely due to the harsh reactional conditions, as previously discussed.

## 1.13. Objectives of this thesis

Wine is a very appreciated beverage worldwide, and, in Portugal, the winemaking sector is of major socio-economic significance, substantially contributing to the national economy. However, it results in a lot of residual material called pomace that is rich in cellulose, hemicellulose, and lignin.

Cellulose and hemicellulose represent a great portion of vegetal biomass, usually discarded as feed. However, both sugar polymers can be hydrolyzed into C5 and C6 monomers by a saccharification process and then fermented into multiple added-value products, like bioethanol.

The greener and more specific option for saccharification is by enzymes. However, after the reaction is over, the enzymes are inactivated and remain in the final product, as there is no way to retrieve them from the solution. Nonetheless, these enzymes are expensive and still functional after single-use.

Consequently, the main barrier to achieving a more economically viable product is the saccharification step due to the high cost of the enzymes (especially cellulase). Thus, reducing that expense has been the focal point in optimizing the production of lignocellulosic bioethanol [10,51,59–61], and the reason why the saccharification step is receiving much attention and is the focus of this thesis.

Thus, this thesis can be seen as an initial step in improving the production of second-generation bioethanol, and 2GB seems to be the best option to invest right now for two reasons: The ecological impact characteristics, making possible the investment in a negative carbon cycle that actively removes $CO_2$ from the atmosphere, and the commercial approach since the high overall cost of 2GB's production can be lowered by perfecting the production process.

With the goal of lowering the cellulase cost, there is an increasing demand for lower-cost immobilization techniques for cellulases, which is demonstrative of the continuously growing applications of these enzymes in multiple industries [124], not only to achieve an efficient and cost-effective process for biomass conversion. However, much research is still needed to optimize a robust procedure that ensures a greener fuel option at a competitive cost [23], thereby contributing to meeting the climate-neutral status that can result from the optimization of biofuel production [9].

So, the goal of this work is to develop immobilization protocols for cellulases and hemicellulases to reuse them, making the saccharification process economically more viable, as since the enzyme cost can represent almost half the price of the final product, a decrease in those costs will heavily minimize the overall price.

This thesis is aligned with those goals. Specifically, it aims to develop immobilization protocols for enzymes to be used in the conversion of pomace, specifically RWGP that was pretreated by SBW. Therefore, the enzymes for which protocols were developed were cellulase (a) and hemicellulase (b): SBW is the best method of pretreatment for high water content biomass, as is the case of grape pomace [36]. This pretreatment is done sequentially by increasing the severity of experimental conditions, as described by B. M. Pedras *et al.* [49]. During this process, at an earlier stage liquors rich in hemicellulose-derived oligomers (b) are obtained, as around 80% of the hemicellulose is solubilized by the SBW process [159]. At a later stage, it is obtained a solid that is rich in cellulose and lignin (a).

Target characteristics of the complexes are high enzyme loading, high enzyme activity, operational stability, and reusability.

To prevent the occurrence of massive internal diffusional limitations, the enzymes had to be immobilized at the surface of the matrix since the reaction of interest involves the conversion of high molecular weight substrates, as is the case of cellulose and hemicellulose.

Also, given the interest in conducting the reaction in an aqueous medium, in which the enzyme is soluble, the enzyme should be immobilized via covalent binding. This is essential for the process since the short-lasting and reversible nature of adsorption, it would most likely be hard to bypass problem as regards reusability, especially given the harsh conditions of the enzymatic saccharification process.

### 1.13.1. Immobilization of cellulase

Two main different immobilization routes, based on the selection of two different crosslinking approaches to the functionalization, were studied to immobilize cellulase onto mNPs –**Figure 1.19**.

The first immobilization method of magnetic cellulase relied on the use of EDC and NHS as crosslinkers, which implicates a DMSA coating of the SPIONs (CDS). In this case, it was also studied the influence of adding an extra crosslink step after immobilization, using glutaraldehyde as a crosslinker between enzymes (CDS-g). The second immobilization method was based on the use of glutaraldehyde as a crosslinker. Two versions of this type of immobilization were studied, using two different coatings for the SPIONs: either an APTES coating (CAS) or a chitosan microsphere (CMm).

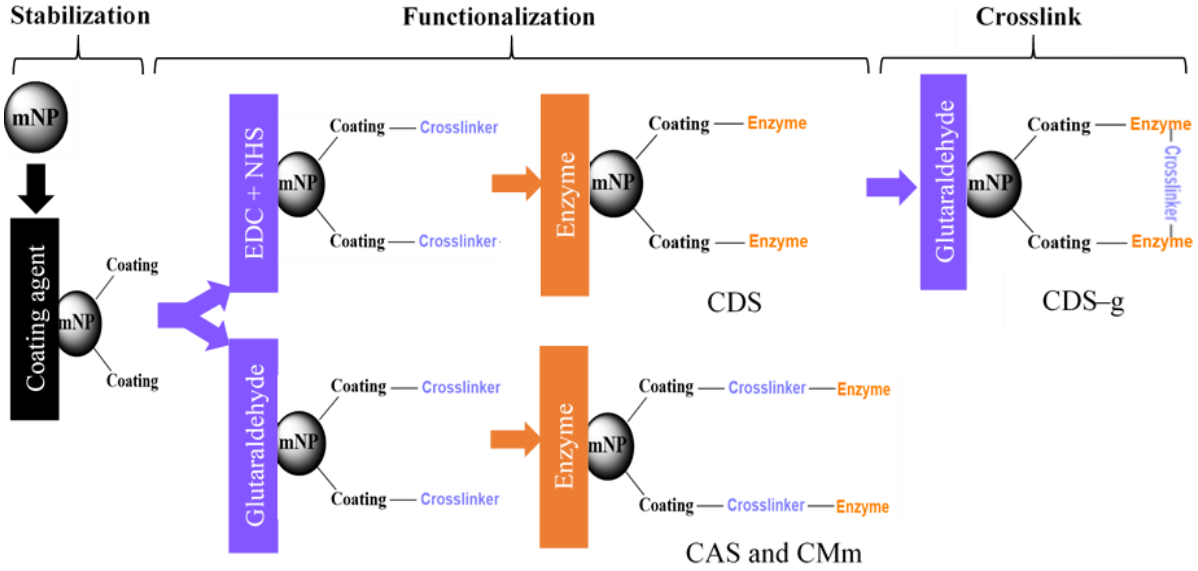


Figure 1.19: Outline of the different immobilization methods studied to immobilize cellulase on magnetic nanoparticles. The final immobilization complex possibilities include CDS (cellulase immobilized on DMSA-coated SPIONs) in 2 versions, simple (CDS) and additionally crosslinked with glutaraldehyde (CDS–g), CAS (cellulase immobilized on APTES-coated SPIONs), and CMm (cellulase immobilized on chitosan microparticles with magnetic cores). Both CDS and CDS–g possesses DMSA as coating agents and rely on EDC/NHS during functionalization, working as a zero-length crosslinker (and therefore those agents do not remain in the final product). Between these two versions, the difference is that CDS–g is subjected to an extra crosslinking step with glutaraldehyde as a secondary crosslinker. On the other hand, both CAS and CMm rely on glutaraldehyde as the primary crosslinker for the functionalization step, which acts as a spacer crosslinker, remaining on the final immobilization complex. These two versions differ on the coating agent used: APTES in CAS, and CMPs in CMm.

## 1.13.2. Immobilization of hemicellulase

For the immobilization of hemicellulase on chitosan microparticles (HM) – **Figure 1.20** – the immobilization approach was similar to the immobilization of cellulase on chitosan microparticles with mNPs at their core (CMm). The main difference is, therefore, the enzyme used in the immobilization, being hemicellulase instead of cellulase, and that the chitosan microparticles used in this immobilization do not have a magnetic core.

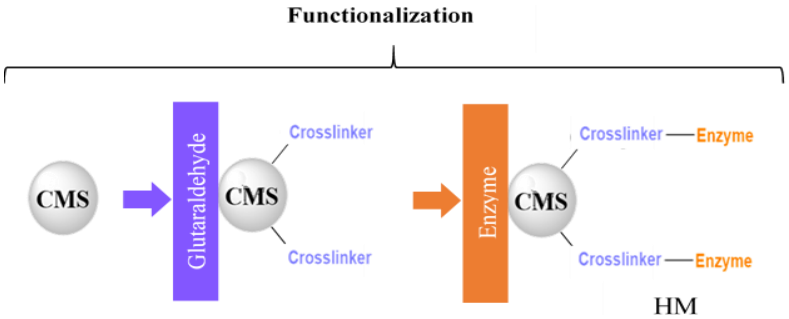


Figure 1.20: Outline of the immobilization method studied to immobilize hemicellulase on chitosan microparticles. The final immobilization complex results in hemicellulase immobilized onto chitosan microparticles (HM) and uses glutaraldehyde as a crosslinking agent, working also as an extender, and, therefore, remaining in the final product.

## 1.14. Thesis outline

Due to the high molecular weight of the substrates to be converted – hemicellulose oligomers and cellulose - and consequent diffusional limitations, the enzymes were immobilized at the surface of the respective matrix. Thus, the selected immobilization method for this thesis was covalent binding, since the short-lasting and reversible nature of adsorption would most likely be a reusability problem hard to bypass, under the harsh conditions of the enzymatic saccharification process, occurring in aqueous media where the enzymes are soluble.

Two different matrices for immobilization were explored, according to the desired application: Differently coated mNPs were used as immobilization matrices for cellulases. These complexes are designed to permeate and attack a solid structure, and to allow facilitated recovery at the end of the process. On the other hand, chitosan microparticles were selected for the immobilization of hemicellulase. This complex is designed to attack soluble carbohydrates in a medium where enzyme recovery should be less challenging than the cellulase complexes.

The mNPs were produced by co-precipitation and stabilized with either DMSA, APTES, or chitosan. The chitosan microparticles, both with and without magnetic cores, were produced in a system of coaxial airflow dripping bead generator to ensure greater control over the shape and size of the final microparticles, thereby increasing their homogeneity.

To determine the best option for the immobilization onto mNPs, both the combination of EDC/NHS and glutaraldehyde were tested as crosslinkers, glutaraldehyde being used not only as a primary crosslinker, providing the bridge between matrix and proteins, but was also as a secondary crosslinker in some immobilization assays, to reticulate the enzyme molecules between themselves, providing more robustness to the final complex. For the hemicellulase immobilization on chitosan microparticles and the cellulase immobilization on magnetic-cored chitosan microparticles, the crosslinker was glutaraldehyde.

Thus, in summary, multiple methods of enzyme immobilization were studied and optimized, as summarized in **Table 1.4**. These included two different matrices (SPIONs or CMPs), each for a specific enzyme (SPIONs for cellulase, and CMPs for hemicellulase), as well as different functionalization agents (EDC/NHS or glutaraldehyde), implying the necessity of different coatings in the stabilization of the matrix (DMSA for EDC/NHS functionalization, and both APTES and CMPs for glutaraldehyde).

Table 1.4: Summary of the different immobilization protocols developed. These include cellulase on DMSA-coated SPIONs (CDS) in 2 versions, simple (CDS) and crosslinked with glutaraldehyde (CDS–g); Cellulase on APTES-coated SPIONs (CAS); Cellulase on chitosan microparticles with a magnetic core (CMm) and hemicellulase immobilized onto chitosan microparticles (HM).

| Experimental immobilization methods | Matrix / core | Enzyme | Coating | Functionalization | Secondary crosslinker |
|---|---|---|---|---|---|
| CDS | SPIONs | Cellulase | DMSA | EDC/NHS | - |
| CDS–g | SPIONs | Cellulase | DMSA | EDC/NHS | Glutaraldehyde |
| CAS | SPIONs | Cellulase | APTES | Glutaraldehyde | - |
| CMm | SPIONs | Cellulase | CMPs | Glutaraldehyde | - |
| HM | CMPs | Hemicellulase | - | Glutaraldehyde | - |

# 2. Methods and materials

## 2.1. Substrate's humidity percentage determination

The humidity of the powdered cellulose was monitored by measuring a 1 g sample on a moisture analyzer *(Kern; DAB 100-3)*. Due to the high sugar content, all the measurements were done on the "soft" setting to avoid caramelization of the sample.

## 2.2. Protein quantification

Two methods were used for protein quantification, Lowry [160] and Bradford [161]. These are two traditional spectroscopic methods and are the most used techniques to determine protein contents, as they are fast and inexpensive [162]. In both methods, bovine serum albumin (BSA) was used as a standard protein for the calibration curves. All the mixing with a vortex was at a low stirring setting to avoid the formation of froth, as it hinders the assay's reproducibility.

### 2.2.1. Lowry assay

The Lowry assay, firstly described by Oliver H. Lowry in 1951 [160] is based on a biuret reaction, which is based on the reaction of $Cu^{2+}$ with peptide bonds, forming a chelate complex between two peptide bonds and a $Cu^{2+}$ with a violet color. However, protein concentrations under 5 mg/mL cannot be determined. Thus, the Lowry method adds the following step with Folin-Ciocalteu reagent, to enhance the color development by reduction of the Folin-Ciocalteu reagent into a blue color, partly dependent on the tyrosine and tryptophan content of the protein, with an absorption peak at 750 nm [162,163]. However, it is recommended to read the absorption at 750 nm for protein concentrations under 0.5 mg/mL or 550 nm for protein concentrations between 0.1 and 2 mg/mL [163].

The assay was done as described in "The Protein Protocols Handbook" [163]. The Lowry reagent was prepared before each assay by mixing equal parts of pre-prepared reagent 2/C (potassium sodium tartrate 2% (w/v) in distilled water) and 3/B (copper sulphate pentahydrate 2% (w/v) in distilled water) and setting up the volume with solution A (30 g/L sodium carbonate + 4 g/L sodium hydroxide in distilled water) to 100x the added volume of the two other reagents before each assay. Usually, the added volumes would be 0.25 mL of solution 2/C and 0.25 mL of solution 3/B, and therefore fill up to 25 mL with solution A. However, the required volume of Lowry reagent to be prepared would be determined depending on the number of samples.

To 200 µL of sample, 1 mL of Lowry reagent was added. The resulting solution was mixed in a vortex and, after 10 minutes, 200 µL of Folin-Ciocalteu reagent 2N *(Sigma-Aldrich; F9252)* diluted 1:2. For each assay, a calibration curve was defined using water as solvent and BSA as standard protein, and the results were measured by UV-Vis absorbance *(Beckman Coulter; DU®800 Spectrophotometer)* at 750 nm after a time frame between 30 to 60 minutes after the addition of the 200 µL of Folin-Ciocalteu reagent 1N and the mixing in the vortex that followed.

### 2.2.2. Bradford assay

The Bradford assay, firstly described in 1976 [161], relies on the binding of a dye, Coomassie Brilliant Blue G250, to protein. This dye binds strongly to specific residues, mostly arginine and lysine residues, and to a lesser degree histidine and aromatic residues (as it is the case of tyrosine, tryptophan, and phenylalanine) [164,165]. Thus, the Bradford assay is ineffective for proteins with low content of arginine [162], and the variation in the content of these residues in different proteins leads to different responses of proteins to the dye. This, therefore, leads to the necessity of always specifying the standard protein when reporting measurements of protein quantification using the Bradford method [165].

The assay was done as described in "The Protein Protocols Handbook" [165]. The Bradford reagent was prepared by dissolving 50 mg of Coomassie Brilliant Blue G250 dye *(Sigma-Aldrich; B0149*) in 25 mL of 95% ethanol, followed by the addition of 50 mL of 85% phosphoric acid *(Supelco; 1.00573)* and the setting of volume up to 50 mL with distilled water. The reagent was filtered through filter paper *(FILTER-LAB "1250"; PN1250090)* and stored in a glass shot, wrapped in aluminum foil, and at 4 ºC.

Before every assay, the portion of the reagent to be used was re-filtered, and 5 mL were added to 100 µL of the sample, followed by mixed the resulting solution in a vortex.

For each assay, a calibration curve was defined using water as solvent and BSA as standard protein, and the results were measured by UV-Vis absorbance *(Beckman Coulter; DU®800 Spectrophotometer)* at 595 nm after a time frame between 20 to 60 minutes after reagent addition.

## 2.3. Sugar quantification

Two methods were used for sugar quantification, a colorimetric phenol sulfuric method [166] to perform bulk quantifications of carbohydrates, and to quantify the content of specific sugar monomers, High-Performance Liquid Chromatography (HPLC) [167,168] was the implemented method.

### 2.3.1. Phenol-sulfuric method

The phenol-sulfuric method is a colorimetric method firstly described in 1956 [166] to perform bulk quantifications of carbohydrates, allowing for fast quantification of reducing sugar content. However, even though this method detects almost all carbohydrates, they vary in absorptivity. Thus, the calibration curve should be based on the main carbohydrate that is suspected to be present. Usually, for analysis of solutions with high content in hexoses, glucose is used as standard at 490 nm, while for solutions of high pentose content, the standard should be xylose at 480 nm [169]. The applied protocol was a specific version of this colorimetric method that was optimized in our lab and described by B. M. Pedras [170]. A glucose calibration curve was constructed using water as solvent and D(+)-glucose monohydrate *(Sigma-Aldrich; 16301)* as carbohydrate standard.

A volume of 1.5 mL of $H_2SO_4$ 96% *(Panreac; 131058)* was added to 500 µL of the sample, followed by 300 µL of 5% (w/v) of phenol *(Sigma Aldrich; 490512)* in distilled water. The resulting solutions were vortexed and incubated at 90 ºC for 5 minutes in a digital dry bath *(Labnet International, Inc.; Accu Block)*, and then cooled down to r.t. by immersion of the tubes in a water bath. The soluble sugars' concentration in the samples is then estimated based on the calibration curve by measuring the UV-Vis absorbance *(Beckman Coulter; DU®800 Spectrophotometer)* at 490 nm.

It is important to note that this method provides an estimate of the soluble sugar content, as it is not specific for the detection of glucose monomers: The concentrated sulfuric acid breaks down any poly, oligo, and disaccharides into monosaccharides [169], so, there is no way to discriminate between partial and complete saccharifications. Therefore, this method was initially used as a fast way to estimate the development of the assays over time, being eventually replaced by HPLC to obtain more precise results.

### 2.3.2. HPLC

HPLC is the high-performance version of liquid chromatography, and it is the standard and most used method for separation and determination of very similar compounds, being even able to, depending on specific experimental conditions, distinguish between many isomeric compounds in chemical mixtures [167].

The assays in this work were all obtained through ion-exchange chromatography, a usual method for carbohydrate identification. For separating mono and disaccharides, as well as some oligomers, the recommended resins are anionic [168].

The assays were run by Nuno Costa at the FCT NOVA, LAQV/Requimte Analysis laboratory, using both a CarboPac PA10 4x250 mm and Aminotrap columns and following the product manual for Carbopac columns [171]. The analysis was done at 25ºC, an eluent gradient of 18 mM NaOH 1 ml/min and an injection volume of 10 µL. The detector used was a pulsed amperometric detector (PAD), and the standards were prepared in $NaN_3$ 20 mg/L solution.

The AminoTrap column is added to ensure the retention of possible interfering amino acids until the monosaccharides have been eluted (12). The CarboPac PA10 column is an anion-exchange column specifically designed for isocratic separations of mono and disaccharides and is usually combined with a PAD (13) – like it was in this analysis – which is a detector specific for sugars and polyalcohols (14).

## 2.4. Enzymatic assays

### 2.4.1. Determination of activity

Filter Paper Units (FPU) is the recommended unit of measurement of total cellulase activity by the International Union of Pure and Applied Chemistry (IUPAC), as characterization of cellulases poses challenges that are rarely encountered while studying other enzymes. These challenges arise particularly from the complexity of the substrate, which is not only insoluble but also structurally variable [172]. Therefore, IUPAC recommends using a method called filter paper assay (FPA), which differs from most enzyme activity characterization methods, as these are usually based on soluble substrate and for initial reaction rates: FPA, on the other hand, is based on a fixed percentage of substrate conversion (4%).

The assay's main goal is calculating the enzyme's concentration that will achieve specifically 2 mg of released glucose from 50 mg of filter paper within 60 minutes of reaction at 50 ºC. The cellulase activity determined by this method is expressed in FPU per milliliter of undiluted enzymatic solution [173].

The values of FPU/mL were assessed based on the "Measurement of Cellulase Activities" LAP, by B. Adney and J. Baker [174]. However, a slight change in protocol was made, replacing the filter paper with long fibers of powdered cellulose *(Sigma Aldrich; C6663)* due to its availability in stock.

Assays were run at 50 ºC with constant stirring at 300 rpm in an incubator *(Heidolph Instruments; inkubator 1000 and unimax 1010*) for 60 minutes. Simultaneously, control assays were run for only enzyme and only substrate in solution, to subtract the stabilizing sugars that are in the enzyme solution, and account for the possible substrate hydrolysis under those conditions. To stop the reaction after that period, the samples were placed in a digital dry bath *(Labnet International, Inc.; AccuBlock)* at 90 ºC for 5 minutes to ensure the degradation of the enzyme.

After cooling down, samples were taken and centrifuged 5 minutes at 12000 rpm *(Heraeus sepatech; Biofuge 13)*. The supernatant was then filtered through 0.22 µm nylon filters *(FILTER-LAB; JNY022013N)*, stored at -4 ºC and then analyzed by HPLC.

The enzymatic activity of cellulases in FPU/mL was calculated for Celluclast 1.5L *(Sigma-Aldrich; "Cellulase from Trichoderma reesei", C2730)* and Cellic cTec2 *(Sigma-Aldrich; "Cellulase, enzyme blend", SAE0020)*. The same activity analysis was done for Viscozyme® L (*Sigma-Aldrich; V2010*), a hemicellulase. Even though it is not the typical activity evaluation performed for hemicellulases, it was done to have a comparative activity value.

Thus, for Viscozyme the same assay was performed under the same conditions but using both xylan (*Sigma-Aldrich; 95588*) and arabinogalactan (*Sigma-Aldrich; 10830*) as substrates. It should be noted that this activity is in units/mL, not specifically FPU/mL, as the substrate is not filter paper nor an equivalent (as is the case of long fibers of powdered cellulose).

### 2.4.2. Enzymatic saccharification

These assays followed the protocol described in the "Enzymatic Saccharification of Lignocellulosic Biomass" LAP described by M. Selig, N. Weiss, and Y. Ji [175], with the slight adaptation of using a buffer at pH 5 instead of the recommended 4.8. That change is explained in more detail in **chapter 3**.

An amount of 150 mg of biomass or 100 mg of cellulose (for CelluClast 1.5L and Cellic cTec2), xylan or arabinogalactan (for Viscozyme L) was weighted on 50 mL shots, and a given volume of sodium citrate buffer 50 mM pH 5 was added, followed by 100 µL of a 2% (w/v) sodium azide solution in distilled water. The final volume of solution was set to 10 mL, assuming a density of 1 g/mL for substrate and, thus, 100 mg would correspond to a volume of 0.1 mL and 150 mg to a volume of 0.15 mL. It should be noted that the volume of buffer for each assay was different since the added volume of enzyme solutions differed according to the enzymatic activity, as the assays were done aiming for a specific amount of FPU/g substrate, and each enzyme has different activities per volume. For the mix, each enzyme added was equivalent to half the target FPU/g, for the total mix activity to add up to the total FPU/g with even contributions of each enzyme solution.

The reaction media (buffer, sodium azide and substrate) was placed in the incubator and brought up to 50 ºC. After 10 minutes of the media in the incubator, the protein was added. Throughout the duration of this thesis, multiple incubators were used according to their availability at that moment. Thus, to

ensure that the variation in the incubator was not an interference with the results, for every saccharification assay of immobilized protein, a control was simultaneously run with the same protein content as the free enzyme.

The assays were run at 50ºC with constant stirring, and samples of 700 µL were taken after different time periods (0, 24 and 72) and placed in the freezer at -4 ºC. After the 3-day assay's samples were collected, they were defrosted and centrifuged 5 minutes at 12000 rpm *(Heraeus sepatech; Biofuge 13)*. The supernatant was then filtered through 0.22 µm nylon filters *(FILTER-LAB; JNY022013N)* and re-stored at -4 ºC. Those samples were then analyzed by HPLC.

Additionally, after the 72 hours saccharification was completed, a 2 mL sample was taken and used for protein quantification.

## 2.5. mNPs

### 2.5.1. Synthesis

SPIONs with an average diameter between 10 to 15 nm were synthesized by chemical co-precipitation using $FeCl_3.6H_2O$ and $FeCl_2.4H_2O$ in a 2:1 ratio. This synthesis followed an optimized protocol, which was developed and described by Paula Soares [176].

This procedure starts with the separate dissolution of $FeCl_3.6H_2O$ and $FeCl_2.4H_2O$ in a total combined volume of 100 mL of ultrapure water. Those solutions are then added to a three-neck round-bottom flask set up – **Figure 2.1** – with mechanical stirring *(Heidolph, Hei-TORQUE 200)* at 1000 rpm. The mix is then exposed to a bubbling process of $N_2$ to create a minimal oxygen atmosphere. Next, 10 mL of 25% ammonium hydroxide *(Sigma Aldrich; CAS 1336-21-6)* is added, and the reaction is stopped after 5 minutes by adding 60 mL of ultrapure water. At this point, SPIONs are already formed and are then subjected to magnetic separation using a strong magnet. After magnetic deposition, the nanoparticles are washed two times with ultra-pure water, one with ethanol, and two more times with ultra-pure water.

The resulting NPs are then stored in suspension on ultra-pure water and, to prevent their aggregation, they were then stabilized with coatings.


Figure 2.1: Setup for SPIONs synthesis. The precursors are placed in a three-neck round-bottom flask, with mechanical stirring on the middle neck. An anaerobic atmosphere is mimicked by bubbling $N_2$ onto the solution by a tube through one of the lateral necks, while the other neck is covered by a cap to maintain the $N_2$ atmosphere.

### 2.5.2. Determination of iron/SPIONs concentration

For the DMSA SPIONs, SPIONs concentration was measured before (to determine the amount of DMSA needed to functionalize the SPIONs) and after coating. For the ATPES SPIONs, however, the concentration is only measured after coating, as there is no pre-determined ratio between SPIONs concentration and the necessary quantity of ATPES.

The concentration of the SPIONs' solution was determined by UV-Vis spectroscopy through the 1,10-phenanthroline colorimetric method. For this method, samples must be submitted to a pretreatment, so the solution was sonicated for 45 seconds, and multiple samples of the SPIONs' solution were collected and treated with HCl 37% *(PanReac; 131020)* for one hour. Since to fit the calibration curve, there might be a need to dilute the samples, usually 1:100, before the treatment with HCl. Therefore, multiple samples of different dilutions were treated. This treatment is an important step of the sample preparation since the colorimetric method applied relied on the reaction of phenanthroline, which reacts with $Fe^{2+}$. Thus, a reducing agent is necessary to assure a complete reduction of all the $Fe^{3+}$ present on the sample [177].

After 1 hour of reaction between the SPIONs and the reducing agent, the reagents required for the colorimetric process were added. Namely, 100 µL of hydroxylamine hydrochloride 100 mg/mL in HCL 0.01 M, 500 µL of phenanthroline 3 mg/mL in HCl 0.01 M and 1.14 mL of ammonium acetate buffer 500 mM in HCL 0.01 M, pH 5. At this point, samples were ready to be measured by the UV-Vis spectrophotometer *(PG Instruments model T90+)*.

The spectrum was measured in a 400-600 nm range, and considering the value of absorbance at the peak at 510 nm (originally 508 nm [177]) for the calibration curve of y= 4,5079 x + 0,0753 [135,178] to measure the iron content in the solution. The SPIONs' concentration was then calculated, based on the experimentally determined proportion of [Fe] = 0.7 [MPs] [129,135,178].

### 2.5.3. Stabilization by coating

#### 2.5.3.1. DMSA

To attain an optimized coating of the SPIONs with DMSA, the iron concentration was determined, allowing to ensure a ratio of DMSA concentration corresponding to 4% of the iron concentration. The mass of DMSA (*Acros organics 98%)* was diluted on 5 mL of KOH 0.1 M, and the pH was set to 5.5.

The pH of the SPIONs' solution was set to 3 by adding one drop of $HNO_3$ *(Merck; Nitric acid 65%)*, and the DMSA solution was added. The resulting solution was then submitted to an ultrasound bath *(BANDELIN; SONOREX SUPER RK 510 H)* for 3 hours, with constant water changes to avoid overheating.

SPIONs were then transferred to a dialysis membrane *(4 RC Dialysis Membrane Tubing 12 to 14 kDa MWCO; Spectrum™ Spectra/Por™)* and left in dialysis with ultrapure water for approximately 3 days to discard the excess DMSA that did not react with the SPIONs. The solvent changes were made 4-5 times a day, and the pH values were controlled after the 2$^{nd}$ day. The dialysis ended when the solvent's pH reached the pH of the ultra-pure water used for the dialysis, and samples were collected to determine the iron and SPIONs concentration after stabilization.

#### 2.5.3.2. ATPES

The ATPES coating is performed on a setup – **Figure 2.2** – with a condenser, mechanical stirring, and an oil bath at 90 ºC. The SPIONs' solution is placed on a 3 headed flask, and 10 mL of glycerol *(pharmaceutical glycerin, vegetal origin, 99.5%)* is added to prevent the NPs' desiccation.

Once the 90 ºC temperature is achieved, nitrogen is bubbled, and the stirring is turned on at 500 rpm. Then, 20 mL of an ATPES 10% (v/v) solution was added, and 2 hours of reaction were timed.

After the reaction is complete, the functionalized SPIONs were washed 2 times with ultra-pure water, once with ethanol, and finally 2 more times with ultra-pure water.

The coated SPIONs were then re-suspended in ultra-pure water, and samples were collected to determine the iron and SPIONs' concentration after stabilization.

Figure 2.2: Setup for ATPES' coating of SPIONs. The precursors are placed in a three-neck round-bottom flask, with mechanical stirring on the middle neck. An adaptor is placed in one of the lateral necks, and both a condenser and the $N_2$ hose for mimicking an anaerobic atmosphere are assembled. The other neck is covered by a cap to maintain the $N_2$ atmosphere. The flask is then set on an oil bath that is maintained at 90 ± 0.5 ºC.

## 2.6. Microparticles

### 2.6.1. Chitosan microparticles

A mass of 0.4 g of chitosan *(batch no. 121128309)* was dissolved in 10 mL of a 2% (v/v) solution of acetic acid in ultra-pure water. The resulting gel was placed in a 5 mL syringe with a diameter of 13 mm. This syringe was then placed in a syringe pump *(kd Scientific)* attached to a system of coaxial airflow dripping bead generator.

Separately, 20 g of NaOH *(Sigma-Aldrich; 221465)* were dissolved in 200 mL of ultra-pure water.

The setup – **Figure 2.3** – was then turned on, dripping the chitosan gel into the NaOH solution, according to the following setup parameters, previously optimized by João Patrício [141]:

- Syringe flow rate: 3.5 mL/h
- Height: 12.5 cm
- Airflow rate: 3 L/min

The resulting microparticles were filtered *(FILTER-LAB "1300/80"; PL1300130)* and extensively washed with ultra-pure water.

The microparticles were then transferred into a falcon and re-suspended in ultra-pure water.

Figure 2.3: Setup of coaxial airflow dripping bead generator system. This system consists in a coaxial airflow dripping bead generator (in red), controlled by an air pump (in blue), and fed by a syringe pump (in yellow). The final part of the setup consists in a precipitation cup filled with NaOH solution, in which the droplets are formed.

### 2.6.2. Chitosan microparticles with magnetic core

The protocol followed was the same as standard chitin microparticles, with the slight alteration that freshly synthesized SPIONs were added to the polymer mix before being set up in the system of coaxial airflow dripping bead generator.

## 2.7. Enzyme immobilization

### 2.7.1. EDC/NHS on SPIONs (for CDS)

The volume corresponding to the necessary SPIONs' mass (40 mg for 1.5:1 protein/mNP ratio and 60 mg for 1:1) was transferred, and the mNPs were re-suspended in 10 mL of solvent (phosphate buffer 0.05 M pH 5.8, distilled water pH ≈5, MES 0.05 M pH 5.5 or PBS 1x pH 7.2). Next, 2.5 mg of EDC *(Alfa Aesar; B25057)* per mg of SPIONs was weighted on an analytical scale *(KERN 770)* and added to the solution. For assays on phosphate buffer, 50 extra mg were added.

Simultaneously, the same mass of N-Hydroxysuccinimide *(Alfa Aesar; A10312)* was diluted on 10 mL of solvent. The two solutions were then combined and incubated on an orbital shaker *(IKA labortechnik; KS125 basic)* for 30 minutes, with mechanical stirring at 400 molt/min.

Using a magnet, the activated matrix was washed 3 times by distilled water, immobilization solvent, and distilled water again, and finally resuspended in 20 mL of solvent. Following, 595 µL of enzyme solution was added, and the solution was incubated for 16 hours on the same orbital shaker.

The solvent of the reaction was collected using a magnet to separate the complexes, and the latter were then washed with distilled water and immobilization solvent, and finally re-suspended in distilled water.

All the solutions after protein addition were collected for protein quantification analysis.

### 2.7.2. Glutaraldehyde on SPIONs (for CAS)

The volume corresponding to the necessary SPIONs' mass (60 mg for 1:3 protein/mNP ratio and 60 mg for 4:1) was transferred, and the mNPs were re-suspended in 10 mL of distilled water.

To that solution, 8 mL of phosphate buffer 0.2 M pH 7 and 12 mL of 25% glutaraldehyde *(Sigma-Aldrich; G6257)* were added, and the resulting solution was incubated on an orbital shaker *(IKA labortechnik; KS125 basic)* for 16 hours, with mechanical stirring at 400 molt/min.

Using a magnet, the activated matrix was washed 3 times by distilled water, immobilization solvent, and distilled water again, and finally resuspended in 20 mL of solvent.

Following, 200 µL of enzyme solution was added, and the solution was incubated for 16 hours on the same orbital shaker.

The solvent of the reaction was collected using a magnet to separate the complex, and the latter was then washed with distilled water and immobilization solvent, and finally re-suspended in distilled water.

All the solutions after protein addition were collected for protein quantification analysis.

### 2.7.3. Glutaraldehyde on chitosan microparticles (for HM and CMm)

A mass of 0.2 g of the saturated weight of chitosan microparticles was added to a solution of 4% glutaraldehyde in phosphate buffer 0.1 M pH 7 (HM 1 -100 mL and HM 2 - 50 mL) and incubated in an orbital shaker *(IKA labortechnik; KS125 basic)* for 3 hours, with mechanical stirring at 300 molt/min.

The activated matrix was then filtered and washed with sodium acetate buffer 50 mM pH 5.5, then 1 M NaCl *(Sigma-Aldrich; 324558)*, and finally with ethylene glycol *(Sigma-Aldrich; 324558)* 30% (v/v) in distilled water. The complex was then resuspended in acetate buffer 50 mM pH 5.5.

The enzyme was then added, and the solution was incubated for 3 hours on the same orbital shaker.

After the process was complete, the complex was filtered and washed again with sodium acetate buffer 50 mM pH 5.5, then 1 M NaCl, followed by ethylene glycol 30% (v/v) in distilled water and, finally, resuspended in distilled water.

All the solutions after protein addition were collected for protein quantification analysis.

## 2.8. Secondary crosslinking with glutaraldehyde for CDS complexes (CDS-g)

The immobilization complex of CDS was re-suspended in a solution of glutaraldehyde (v/v) in sodium phosphate buffer, 0.2 M pH 7 (CDS-g 1 at 0.0625%, CDS-g 2 at 0.125% and CDS-g 3 at 0.5%) and incubated on an orbital shaker *(IKA labortechnik; KS125 basic)* for 2 hours and a half, with mechanical stirring at 400 molt/min.

After the process was complete, the complex was filtered and washed with sodium phosphate buffer 0.2 M pH 7 and resuspended in ultra-pure water.

All the washing solutions were collected for protein quantification analysis.

## 2.9. FTIR

The composition of multiples samples was analyzed by Fourier-Transformed Infrared Spectroscopy (FTIR) with a universal ATR (Attenuated Total Reflection) accessory.

Infrared spectroscopy is a widely used fingerprint method that allows the identification of functional groups. By this method, multiple substances can be identified, characterized, and quantified by the way their components interact with infrared light [179]. ATR enables the analysis of either liquid or solid-state samples to be examined directly, with no requirement of previous preparation. Thus, by reducing the preparation requirements, it enhances spectral reproducibility [180].

FTIR spectroscopy was done by a FTIR spectrometer with UATR *(PerkinElmer; Spectrum two)* and using the software PerkinElmer Spectrum Version 10.5.2.

## 2.10. Evaluation criteria for the immobilization complexes

The complexes were tested to determine the best balance between desired qualities that derive from immobilization, like high complex stability, and the disadvantages that also arise from that procedure, like the loss of activity. Thus, some characteristics were tested to assess the best course of optimization. As these parameters are intertwined – **Figure 2.4** – they require a certain compromise between them.

All those parameters are further explained bellow but, overall, the main goals are to:

- Maximize the immobilization efficiency and the enzyme loading onto the support (minimizing the protocol's cost by respectively lowering the waste of enzyme and the quantity of required support).
- Minimize the enzyme leaching after use (thus maximizing operational stability).
- Maximize the retention of activity at 24 hours (with lower activity at 72 than at 24 hours).
- Maximize the complexes' stability in solution during storage.

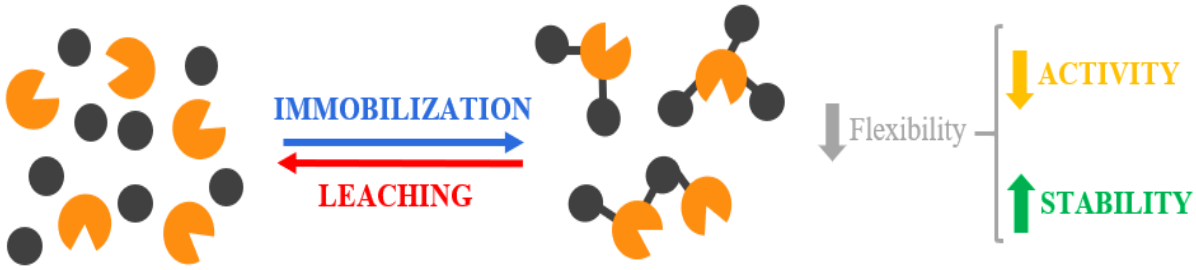


Figure 2.4: Immobilization process – The main criteria being evaluated (in uppercase), and the relationship between them: Protein immobilization (blue) and protein leaching (red) are inverse reactions, while the activity loss (yellow) and the stability enhancement (green) derive directly from the loss of flexibility (gray) that originates from the immobilization itself.

### 2.10.1. Immobilization efficiency

The immobilization efficiency (in percentage) – **Equation 2.1** – allows determining how much of the added enzyme became immobilized onto the carrier. The higher the immobilization percentage, the less enzyme goes to waste and, thus, the more efficient the immobilization protocol will be. This parameter was determined based on the washing solvent after the immobilization process is complete. Thus, it is an indirect quantification that does not compromise the integrity of the complex.

$$\text{Immobilization efficiency (\%)} = \text{ci} - \frac{\text{cwashing}}{\text{ci}} * 100 \quad [102] \qquad \text{Equation 2.1}$$

Based on that formula, the immobilization activity during this work was calculated by **Equation 2.2**.

$$\text{Immobilization efficiency (\%)} = 100 - \left(\frac{\text{remaining protein in washing solvent}}{\text{added protein}} * 100\right) \qquad \text{Equation 2.2}$$

### 2.10.2. Protein leaching (after a 72 h use)

Leaching is the term employed for the loss of soluble material from a carrier into a liquid [181]. In this case, specifically, it is evaluated the leaching of the protein, from the carrier, into the reaction media.

Covalent bonding immobilizations provide strong linkages between enzymes and carrier matrices, therefore reducing the enzymatic leaching in aqueous media when compared to other immobilization methods [127]. However, with repeated use of the complex, the strength of the bonds tends to decrease over time, leading to the detachment of the proteins into the solution. Additionally, it is possible for the enzyme to suffer a distortion of its structure (and consequently, it can interfere with the active site, leading to some degree of enzyme inactivation by reduced catalytic efficiency) [105].

Due to this leaching process, the leached protein will not be retrieved from the solution along with the carrier during the carrier's recovery. This will most likely have an impact on the conversion yield, as once the enzyme becomes free from the carrier, it can regain the flexibility that was sacrificed in the immobilization, therefore enhancing the conversion, and influencing the overall results. Thus, protein leaching (in percentage) – **Equation 2.3** – is an important quantification to perform. The quantification of protein in solution is done on samples of the reaction media after the retrieval of the immobilization complexes so that no immobilized protein is considered.

$$\text{Protein leaching (\%)} = \frac{\text{protein in reaction media after saccharification (72h) and complex retrieval}}{\text{protein added as part of immobilization complexes (0h)}} * 100 \quad \text{Equation 2.3}$$

### 2.10.3. Retained activity (after 24 h and 72 h)

With the covalent immobilization, there is typically a very high decrease in the enzymatic activity due to the loss of flexibility that is imposed on the enzymes [70,73,78,87–89]. Thus, it is essential to quantify the activity that is retained after the immobilization – **Equation 2.4** –, which was done by comparing the yield of glucose from the immobilization complex with the control of the same protein quantity as the free enzyme.

$$\text{Retained activity (\%)} = \frac{\text{activity of immobilized enzyme}}{\text{activity of enzymes in free form}} * 100 \quad [97] \quad \text{Equation 2.4}$$

The retained activity at 24 hours is the most important value to determine the saccharification efficiency of the complex and the success of the immobilization. On the other hand, the activity at 72 hours is used as a measure to ensure that the activity measured at 24 is, in fact, activity retained by the immobilized enzymes, and not due to the leaching of protein, becoming free and regaining the original flexibility. Thus, the value of the retained activity at 72 hours is not important itself if verified that it is lower than at 24 hours. However, if it is higher, then it is an indication that the activity measured at 24 hours was most likely due to leaching of protein and not due to an efficient immobilization protocol. This comparison helps to determine if the leached protein influenced or not the activity detected at 24 hours, since the protein leaching provides information of how much protein was leached, but not if that leached protein was functional and, therefore, if it influenced the results of the activity.

### 2.10.1. Protein loading onto the support

The protein loading onto the support is the ratio of protein attached to the support, expressed in (w/w) – **Equation 2.5**.

$$\text{Protein loading (w/w)} = \frac{\text{protein}}{\text{mNP}} \ (\text{w/w}) \text{ in immobilization} * \frac{\text{immobilization efficiency (\%)}}{100} \quad \text{Equation 2.5}$$

This is an important parameter, as the protein loading influences the activity, due to the quantity of interaction between enzymes that are allowed and modeled by different loadings [91,182] – **Figure 2.5**.


Figure 2.5: Influence in the quantity of interaction between enzymes in lower (left) and higher (right) loadings onto the matrix. The matrix is represented in black, the enzymes in light blue, and the covalent bonds between them in gray.

The goal is usually to maximize the number of enzyme molecules at the surface, to achieve higher activity per gram of complex, and thus a high enzyme loading will lead to a lower need for support production and, consequently, a more economical procedure. Additionally, the interaction between enzymes can lead to a more stable complex [91,182]. However, an excess of enzyme molecules at the surface can have adverse effects, either due to interactions between the enzyme molecules that can affect their conformation, or by physically affecting the accessibility of the substrate to the enzymes' active center, due to the proximity between them [91,182].

Therefore, a higher enzyme loading and consequent higher interaction between enzymes can either lead to positive or negative effects, depending on the case [91,182]. Thus, even though in the case presented in the consulted literature [182], the crowding effect was negative, being more favorable a lower loading, it is noted that for other enzymes or even under different conditions, the effects may shift to positive [91,182]. Consequently, there is no direct way to estimate the influence of protein loading without the empirical method of trial and error [91,182].

### 2.10.2. Stability of the immobilization complex in solution (storage)

The leaching of protein was also studied in some immobilization complexes to determine their stability in solution during storage. This storage was done at 4ºC in aqueous media.

Commercial solutions of protein are usually sold with soluble sugars to stabilize the protein structure [183], but in the case of the immobilization complexes, the immobilization to the matrix also enhances the stability of the protein, substituting the need for stabilizing sugars.

# 3. Results and discussion: Determination of saccharification conditions

The reported optimal conditions for Cellic cTec2 are 45-50 ºC and pH 5.0-5.5 [184], while for CelluClast 1.5L the temperature range is 50-60ºC and pH 4.0-6.0 (15). Finally, for Viscozyme L the declared optimal conditions are 25-55 ºC and a pH range of 3.3-5.5 (16). Hence, to simultaneously fit the specifications of all enzymatic solutions in the study and allow for simultaneous and comparable studies, the saccharification conditions were set at pH 5 and 50 ºC for every enzyme and substrate.

In the literature, some immobilization protocols for cellulase and xylanase reported that the optimal conditions of the immobilized enzyme shifted slightly after immobilization, with complexes showing slightly higher activity at higher pH (e.g. from 5 to 6 [111]) or temperature (existing reports of an upsurge of 5% activity by increasing the temperature from 50 to 55 ºC [115] or 55 to 60 ºC [97]).

However, most of the consulted literature either did not consider that factor, or ensured that not only the optimum conditions for the immobilized enzymes were coincident with their free form for temperature [102] and pH [97,105], but also that the complexes had a very broad range of pH: There are reports were the complexes remain active at pH 9 with only slightly less activity as the optimum pH [102], and even reports of remaining active at pH 12, were despite those harsh conditions the complex still showed slightly over 50% activity, comparing with its optimal conditions [105].

Thus, all the immobilization complexes performed during this work were evaluated under the same conditions as their free counterparts to get more accurate comparisons between the different immobilization complexes, which depending on the protocol, might exhibit slightly different optimum conditions. This way, that possible variation was considered minor and excluded from consideration.

# 4. Results and discussion: Cellulases

## 4.1. Substrates' humidity

The humidity of the cellulose substrate was measured, as cellulosic fibers are hydrophilic and therefore tend to absorb humidity. Moisture can influence the characteristics of fibers, namely their mechanical properties [185], and can thus influence the saccharification results. Therefore, it was important to monitor the fibers' humidity, to ensure a small variation of this value and a fairly homogeneous substrate.

Throughout this work, the cellulose maintained a constant humidity percentage of 5.50±0.12%, which was considered an excellent value as it has a small variation as intended, and these fibers usually have between 5-10% humidity [185].

## 4.2. Comparison of the available commercial cellulosic enzyme solutions

### 4.2.1. Protein quantification

The quantification of protein content was performed by two methods: Lowry and Bradford assays. Both used BSA as standard protein, and the estimations of the solutions' protein content were compared with available literature quantifications for the same commercial enzymatic solutions – **Table 4.1**.

Table 4.1: Comparison of values for protein content in some of the available literature for CelluClast 1.5L (left) and Cellic cTec2 (right). The values that were determined in this work are highlighted in bold.

| CelluClast 1.5L Protein (mg/mL) | Method | Year and reference |
|---|---|---|
| 130 | ninhydrin method | 2017, [186] |
| 129.3 | Bradford, P-cellulase | 2014, [103] |
| 125 | Lowry | 2014, [36] |
| **111.4** | **Lowry** | **2019** |
| **54.8** | **Bradford, BSA** | **2020** |
| 26.7 | Bradford, BSA | 2019, [189] |

| Cellic cTec2 Protein (mg/mL) | Method | Year and reference |
|---|---|---|
| 220 | Not mentioned | 2019, [187] |
| **202.7** | **Lowry** | **2019** |
| 181 | Lowry | 2014, [36] |
| 180 | Not mentioned | 2019, [188] |
| 109 | Bradford, BSA | 2019, [189] |
| **99.1** | **Bradford, BSA** | **2020** |

Overall, the values obtained by Lowry's method are slightly over twice as much as the results obtained by Bradford's method. However, when comparing the same method with the available literature, the values within each method are in reasonable agreement. Thus, it is believed that this variation in results can be justified by the difference in the two used methods for analysis.

Lowry is a highly sensitive method, as it relies on a two-stage reaction (a biuret reaction allied with the addition of Folin-Ciocalteu reagent, to optimize the color development [162]). However, one of Lowry assay's disadvantages is the wide range of substances that may interfere with the assay, which includes some buffers, drugs, nucleic acids, and reducing agents, like sugars [163,190]. Even though usually the interference of these agents can be minimized and considered negligible by diluting the sample [163], since the enzymatic solution is stabilized by sugars and the enzyme will also produce additional soluble sugar, it is likely these can be present in such a concentration that results in interference to the assay. Thus, the main advantage of the Bradford assay is the compatibility with reducing agents that are incompatible with the Lowry method [165,190]. However, as a disadvantage, there is a slight nonlinearity in the pattern of response, including in the calibration curve, due to the reagent itself. Nevertheless, this problem can easily be overcome since the curvature is only slight [161,165] and can be avoided by remaining in the lower range of the calibration curve [190]. In this case, under the protein concentration equivalent to an absorbance of 0.6.

The Bradford assay can be performed using multiple standards. BSA is the most widely used protein standard since it is inexpensive and easily available in its pure form. Thus, the argument for the use of this protein as standard is that due to its common use as standard, the results obtained can then be directly compared with the great majority of the available literature. And, for this reason, BSA was defined as

the protein standard to be used during this work. However, specifically in Bradford assays, BSA can sometimes not be the adequate protein to serve as a standard. The Coomassie blue dye, used in the Bradford method, binds more strongly to specific residues: mostly arginine and lysine residues, and, to a lesser degree, histidine and aromatic residues (tyrosine, tryptophan, and phenylalanine) [164,165]. This makes the Bradford assay ineffective for proteins with low content of arginine [162], and thus the variation in the content of this residue in different proteins leads to the necessity of always specifying the standard protein when reporting measurements of protein quantification when using this method. Furthermore, as BSA is a protein with a higher than usual content of the amino acids that react with the dye, consequently, the response of BSA can vary from other proteins, risking the possibility of under-estimating the protein content of the sample [165,190].

In a 2014 study [103] involving Celluclast 1.5L, for the determination of protein concentration, Bradford assay was used, and three standard proteins were tested, BSA, p-cellulase, and p-β-glucosidase. The calibration curves obtained – **Annex 1** – show that BSA consistently presents half the absorption than the other two. This confirms that by using the BSA calibration line, the Bradford assay will underestimate the protein concentration of the cellulase solution. That ratio is especially important when considering the comparison of BSA and p-cellulase on those calibrations' curves, as the protein in the study in this thesis will be more similar to the latter.

Thus, since the Bradford assay using BSA as standard tends to underestimate the protein content due to the high response of the standard to the assay, and the Lowry assay tends to overestimate the protein content due to the stabilizing sugars' interference, it can only be assured that the real value lies somewhere in between. However, all the calculations will be made according to the results obtained by the Bradford method to ensure that the sugars (either stabilizing from the enzyme solution or produced during the saccharification) do not interfere with the protein quantification. Additionally, Bradford's method is faster, as the results can be visually estimated after 5 minutes, while the Lowry method requires a minimum 40 minutes of incubation before knowing if the dilution will fall within the range of the calibration curve [162,165,190].

### 4.2.2. The overall composition of the commercial cellulase solutions

The main constituents of the available cellulase solutions were analyzed – **Figure 4.1**. These consist of protein (mainly cellulase, but there can also exist remains of other proteins that remain after the process of cellulase extraction), relying on the values of protein quantified by Bradford assay, and sugars (that are added to act as stabilizing agents [183]). Thus, the glucose content was determined by HPLC. The components' percentage was calculated based on the enzymatic solutions' average density, namely 1.22 g/mL for CelluClast 1.5L [191] and 1.15 g/mL for Cellic cTec2 (17).

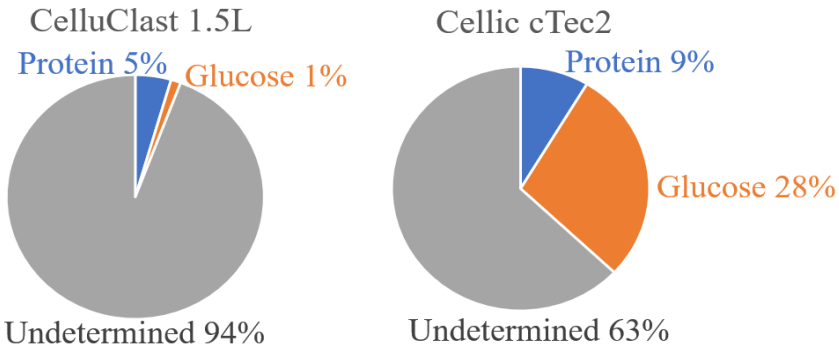


Figure 4.1: Characterization of the main components (protein and glucose) on the available commercial cellulase solutions, CelluClast 1.5L (left) and Cellic cTec2 (right).

Only glucose was measured, as it would be the only sugar that could interfere with the assay's result. However, other sugars can be used as stabilizing agents. For example, fructose is also used, and was identified in higher concentration than glucose in Viscozyme L (a hemicellulase solution analyzed in **chapter 5.2**). Thus, even though the concentration of stabilizing glucose is low in CelluClast 1.5L, it does not necessarily mean that that enzymatic solution has fewer stabilizing agents in solution.

### 4.2.3. FPA: Determination of total cellulase activity

The filter paper assay (FPA) and respective data processing followed the protocol for measurement of cellulase activity as defined by National Renewable Energy Laboratory [174].

Multiple assays were run for 60 minutes at 50 ºC with different enzyme concentrations to establish a calibration line for each enzymatic solutions' activity under those conditions – **Figure 4.2**.

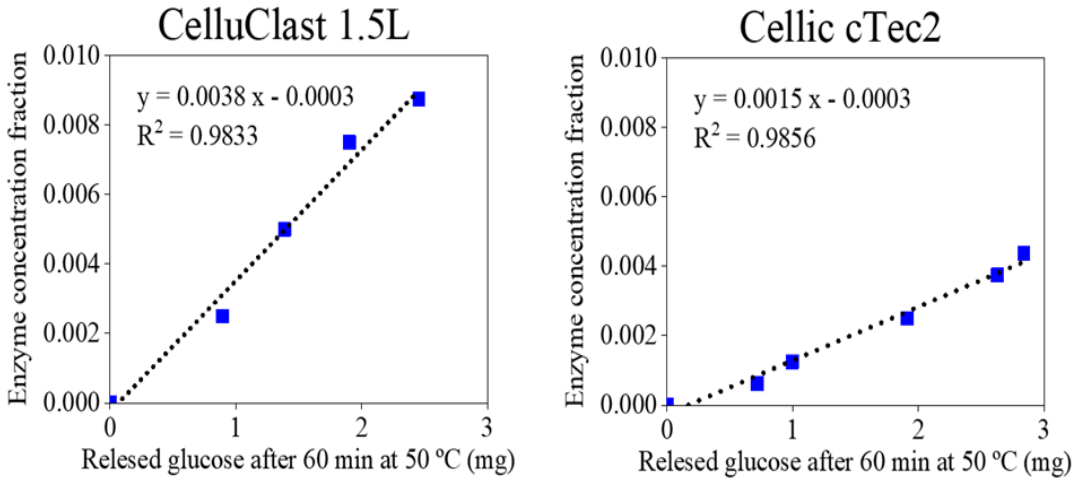


Figure 4.2: FPA for the determination of total cellulase activity in FPU (unit/mL) for CelluClast 1.5L (left) and Cellic cTec2 (right).

The enzyme fraction corresponds to the fraction of the original solution that is added to the assay, being a measurement of the enzyme's dilution relative to the original enzymatic solution.

These calibration curves allowed the calculation of the value of enzyme concentration fraction that, under these conditions, will achieve specifically 2 mg of released glucose. The activity of the original enzyme solutions – **Equation 4.1** – can then be calculated by dividing a constant – **Equation 4.2** – by the enzyme fraction that is calculated from the calibration line [174].

$$\text{FPU (unit/mL)} = \frac{0.37\ \mu\text{mol min}^{-1}\ \text{mL}^{-1}}{\text{fraction that releases 2 mg of glucose from 50 mg of cellulose in 60 min at 50 ºC}} \quad \text{Equation 4.1}$$

$$\text{Constant} = \frac{\frac{2\ \text{mg of glucose}}{0.18016\ \text{mg glucose}\ \mu\text{mol}^{-1}}}{60\ \text{min} \times 0.5\ \text{mL of enzyme solution}} = 0.37\ \mu\text{mol min}^{-1}\ \text{mL}^{-1} \quad \text{Equation 4.2}$$

Thereby, based on these formulas and the experimental calibration lines, activities of 51 unit/mL and 137 unit/mL were obtained for Celluclast 1.5L – **Equation 4.3** – and Cellic cTec2 – **Equation 4.4** – respectively.

$$\text{CelluClast 1.5L:}\ \frac{0.37\ \mu\text{mol min}^{-1}\ \text{mL}^{-1}}{0.0038 \times 2 - 0.0003} = 51\ \text{unit/mL} \quad \text{Equation 4.3}$$

$$\text{Cellic cTec2:}\ \frac{0.37\ \mu\text{mol min}^{-1}\ \text{mL}^{-1}}{0.0015 \times 2 - 0.0003} = 137\ \text{unit/mL} \quad \text{Equation 4.4}$$

These results are congruent with some of the literature available, even though the values found in the literature for these solutions cover such a wide range of results – **Table 4.2**.

Table 4.2: Comparison of FPU values in some of the available literature for CelluClast 1.5L (left) and Cellic cTec2 (right). The values that were determined in this work are highlighted in bold.

| CelluClast 1.5L FPU (unit/mL) | Year and reference | Cellic cTec2 FPU (unit/mL) | Year and reference |
|---|---|---|---|
| 84 | 2015, [192] | 223 | 2015, [192] |
| 65 | 2014, [193] | 205 | 2019, [187] |
| 63.8 | 2014, [103] | 203 | 2017, [194] |
| 60 | 2013, [195] | 189 | 2015, [196] |
| 60 | 2017, [186] | 157 | 2018, [197] |
| 51.4 | 2019, [189] | 150 | 2013, [195] |
| **51** | **2019** | **137** | **2019** |
| 44.7 | 2014, [198] | 117 | 2019, [199] |
| 42.4 | 2012, [200] | 115.3 | 2019, [189] |

The wide range in literature can derive not only from the variation on the operator and the lot of enzyme solution but also the method used for quantification of the resulting glucose. Still, other factors that may influence the values obtained in this study may be that the substrate solubility or constitution may have been slightly different, as the substrate used was powdered cellulose instead of the recommended filter paper. Nevertheless, since all the assays of cellulose saccharification in this work are run with the same substrate, the deviation from the standard substrate will not interfere with the conclusions drawn from the method. This is assured, as IUPAC recognizes that, due to the empirical nature of this assay, the results are more comparative than qualitative, and multiple investigators prefer alternative cellulose substrates instead of filter paper [172]. So, the values in this study are significant from a comparative stand, as in the words of IUPAC, "these assays will more likely be of continued value to biotechnologists than to enzymologists - who will find these methods lacking in theoretical definition" [172].

The pronounced difference between the determined FPU for Celluclast (51 units/mL) and Cellic cTec2 (137 units/mL) was not unexpected since cTec2 has a much higher protein concentration (with CClast having 55 mg/mL and cTec2 99 mg/mL), so it was safe to assume that with almost twice the protein content, that solution would most likely result in higher activity per volume. Additionally, the higher activity of cTec2 may also be explained by the fact that CClast consists solely of endoglucanase (3.2.1.4), while cTec2 is an enzyme blend of multiple enzymes. This can have a great influence, as the cellulase action is considered synergetic, causing higher conversion yields through the simultaneous action of the three classes of cellulase (like in cTec2) than a single class (like in CClast) or even the sequential addition of the multiple enzyme classes, separately [64].

### 4.2.1. Enzymatic saccharification

Enzymatic saccharification assays were run with both enzymes at 60 FPU/g, as well as a mix of both enzymes, with 30 FPU/g each – **Figure 4.3** – in agreement with the LAP analytical standards of the National Renewable Energy Laboratory [175]. It should be noted that these results were for comparison between the 3 options, so these results were obtained by the phenol sulfuric method for a faster and cheaper sugar quantification, roughly estimating the overall conversion of cellulose. Thus, even if the maximum value of conversion obtained reached 100%, the conversion would not necessarily be a complete saccharification (which would result in exclusively glucose monomers), as the quantification method also accounts for multiple oligomers, as long as those are small enough to become soluble.

The assay was stopped after 120 hours, as the values started to stabilize (in average value and by the decrease in the standard deviation), implying that the reaction has achieved the maximum conversion possible under those conditions. In the followed protocol, the recommended reaction time is anything between 72 and 168 hours [175], but from these results, it can be inferred that around the 72 hours mark, the reaction has already stabilized. Therefore, this was established as the standard saccharification period during the rest of the thesis.

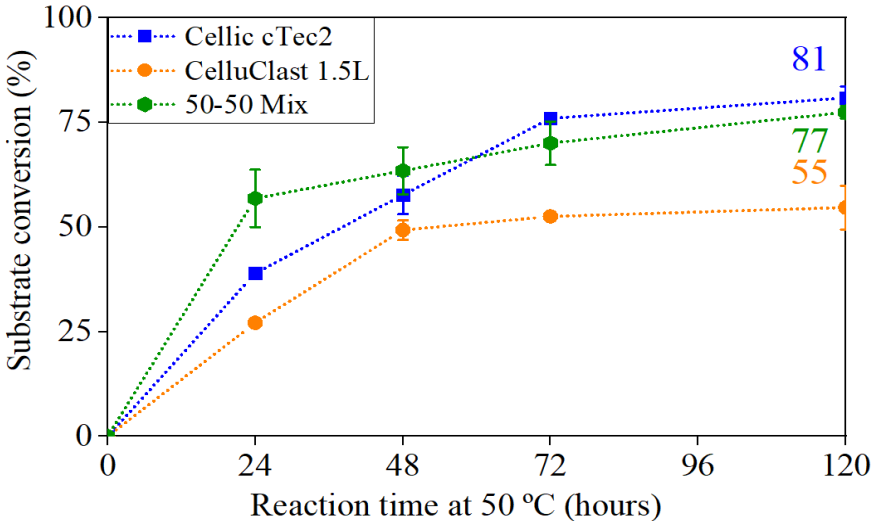


Figure 4.3: Enzymatic saccharification of pure cellulose at 60 FPU/g. Results of Cellic cTec2 (in dark blue), CelluClast 1.5 L (in orange), and a mix of both, with each at 30 FPU/g (in green). Data points and error bars represent average and standard deviation, respectively, of 3 replicate experiments.

However, there was no need to consider the hypothesis of a possible complete saccharification, as it was indubitably never achieved. These assays ended with a maximum of 80.9±5.2% of substrate conversion by Cellic cTec2, followed by the 50-50 mix of Cellic cTec2 and CelluClast 1.5L with 77.5±2.8%, whereas CelluClast only achieved a maximum substrate conversion of 54.7±1.5%. Still, these results were not unexpected, as since the study system is a SHF, it is natural that a complete conversion is never achieved due to the effect of end-product inhibition of the enzymes [21,54].

The approximate 81% of substrate conversion of Cellic cTec2 is congruent with the information provided on the application sheet for Cellic cTec2, where it is showed that the maximum conversion achieved by this enzyme (after both 3 and 7 days) is around 80% of cellulose conversion, regardless of the enzyme loading [184]. The same data is not available in the application sheet for CelluClast. However, in a 2015 article [192], the maximum conversion that was achieved with CelluClast 1.5L was 52% after 96 hours, which is consistent with the 54% conversion obtained in this assay.

### 4.2.2. Final selection of the best cellulase solution

It was demonstrated in previous literature [93,100] that recycling free Celluclast 1.5L could be achieved by recovering the liquid phase after the cellulose conversion (although that would also mean the recovery of the sugar product and, consequently, exponentially increasing the effect of end-product inhibition in following rounds). However, those studies also demonstrated that the same is not possible for Cellic cTec2: in that case, a considerable portion of at least 20-30% of the enzyme remains bound to the final residue, making the recovery of cTec2 more challenging [100]. However, since the enzymatic activity of enzymes is greatly impaired due to covalent immobilization, the comparative saccharification activity of cTec2 was high enough to select the first as the best enzyme to proceed to the immobilization.

Additionally, cTec2 was also the option that resulted in the more economic advantage: a 50 mL solution of Celluclast 1.5L costs 123 € (18), resulting in 2.46 €/mL, while the same volume of cTec2 costs 111 € (17), accounting to 2.22 €/mL. Therefore, cTec2 is not only cheaper by mL, but it also presents more than double the activity (137 unit/mL, while only 51 unit/mL for CClast), resulting in roughly half the overall cost.

## 4.3. Saccharification in biomass and pure cellulose

The main part of the assays was made using pure cellulose as a substrate, to better evaluate the efficiency of the developed enzymatic immobilization complexes. This was a practical decision to reduce the variability that is intrinsic to the biomass, since the proportion of its components varies depending on factors like harvest time and genetic variability between plants of the same species [10],

and slight variations during SBW treatments to which the original source of biomass is exposed [49]. However, a few assays were run to determine the efficiency of the free enzyme on the biomass for which it is ultimately intended: SBW pretreated RWGP, described by B. M. Pedras *et al.* [49] – **Figure 4.4**.

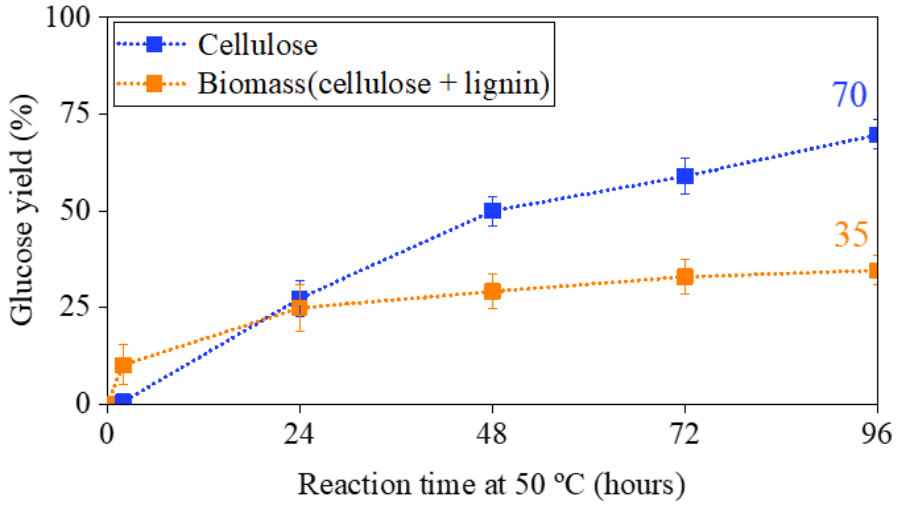


Figure 4.4: Comparison of the enzymatic saccharification of pure cellulose (in dark blue) and SBW pretreated RWGP (in orange) by cTec2 at the recommended dosage of 60 FPU/g substrate. Data points and error bars represent average and standard deviation, respectively, of 3 replicate experiments.

The reaction was stopped at 96 hours, even though it was already determined that around 72 hours, the conversion of the substrate is already stabilized when the substrate used is pure cellulose. The extra day was given to ensure that the conversion when using biomass would also stabilize, since due to the presence of lignin, this conversion could be slower, as lignin hinders the access of the enzyme to the available cellulose in the biomass.

The value for biomass was adapted to consider the glucose yield instead of overall biomass conversion, as according to the characterization made by B. M. Pedras *et al.* [49], the original RWGP, before treatment, has a composition of 30% lignin and 15% cellulose. Since this source is pretreated by SBW until only lignin and cellulose remain, the pretreated lignocellulosic biomass that was used as a substrate in the assay is roughly composed of 66.67% lignin and 33.33% cellulose. Hence, from the 150 mg of biomass added, it was considered that there were available 50 mg of cellulose, from which only approximately 35% was converted into glucose monomers.

The final glucose yield values after 96 hours of reaction at 50 ºC were 69.7±3.8% for cellulose and 34.6±3.8% for the biomass. The low glucose yield of biomass, when compared with the pure cellulose, can be attributed to the presence of lignin, which, as previously mentioned, hinders the accessibility of cellulase to the substrate and leads to unproductive binding and enzyme deactivation [61,71].

Finally, it must be noted that these results of biomass saccharification do not show a significant variation because the same batch of pretreated lignocellulosic biomass was used in the replicate experiments. Thus, even though these results show low variation, it was still defined that the substrate used in the assays will be pure cellulose.

## 4.1. Enzyme loading for enzymatic saccharification

The enzyme loading of enzymatic saccharification quantifies the added enzyme per quantity of substrate. It can be represented by mass, usually expressed by % (w/w), or activity, usually expressed by FPU/g substrate. For this work, the loading was expressed in FPU/g since the enzyme is extracted from cells, and therefore there can be residual proteins in the solution. Thus, expressing the enzyme loading by its activity, a characteristic exclusive of cellulase, can be more accurate than by % (w/w), as the Bradford assay performed to determine the protein concentration in solution quantifies all the protein, and not specifically the enzyme.

To ensure an optimum contact between the substrate and the enzymes, the enzymatic hydrolysis of lignocellulosic biomass is typically carried out at 5-8% (w/w) solids [201]. However, for cTec2 the recommended dosage for the hydrolysis of biomass is 1.5% (w/w) solids for low cellulose content, 3% (w/w) solids for mid cellulose content, and 6% (w/w) solids for high cellulose content [184].

The followed saccharification protocol [175] recommends a protein loading of 60 FPU/g of biomass. Thus, for the saccharification of SBW pretreated RWGP by cTec2, based on the previously determined values of FPU (137 units/mL of enzymatic solution) and protein content (99.1 mg/mL, determined by Bradford method, using BSA as standard), this dosage corresponds to around 66 µL of enzymatic solution for 0.15 g of biomass = 6.54 mg of protein for 150 mg of substrate = 4.4% (w/w) solids.

Therefore, the recommended dosage in the followed protocol [175] was slightly under the standard 5-8% guideline for general lignocellulosic biomass saccharification [201] and slightly over the recommended dosage of 3% (w/w) solids for cTec2 in biomass with mid cellulose content [184]. As the SBW pretreated RWGP is a biomass with twice the lignin than cellulose content (roughly 67% to 33%), this may be classified as either a low or mid cellulose content biomass. However, it is thought that this slightly higher dosage may be beneficial since it may counter the potential deactivation induced by the high percentage of lignin: Since the general theory of enzyme inactivation during the saccharification process of lignocellulosic biomass attributes this inactivation to the presence of lignin in the biomass (as the binding between cellulases and lignin is unproductive and can result in the enzyme's inactivation [61,71]), an above-average content of cellulase in a substrate with a pre-determined very elevated content of lignin is most likely very beneficial to counter the resulting high enzyme inactivation.

Hence, it was determined that for biomass, the indicated dosage of 60 FPU/g, correspondent to 4.4% (w/w) solids, was adequate due to the high content of lignin on the pretreated RWGP.

However, as mentioned, the main part of the assays used pure cellulose as a substrate to reduce the variation of results. The recommendation of 60 FPU/g of cellulase for the saccharification of pure cellulose [175] approximately corresponds to 45 µL of enzymatic solution for 0.1 g of cellulose = 4.46 mg of protein for 100 mg of substrate = 4.5% (w/w) solids for pure cellulose. This loading dosage was tested in pure cellulose, as well as double and triple the dosage, to ensure at what value were the best conditions achieved –**Figure 4.5**.

Additionally, since the cellulose conversion of the cTec2 and CClast 50-50 mix had results very close to cTec2 (in Figure 4.4), this mix was also tested at a 2x recommended dosage.

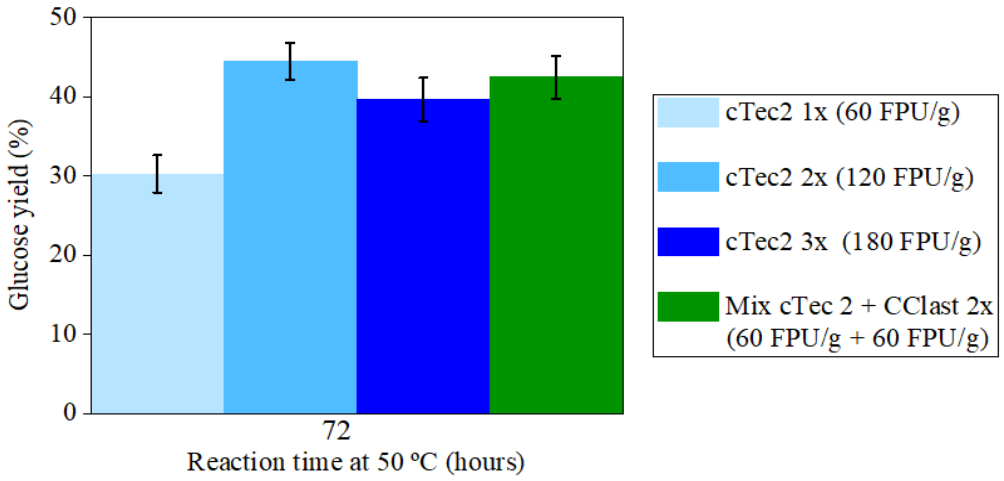


Figure 4.5: Comparison of the influence of different enzyme loadings on the enzymatic saccharification of pure cellulose: Cellic cTec2 at 60 FPU/g (light blue), 120 FPU/g (medium blue) and 180 FPU/g (dark blue) and a 50-50 mix of Cellic cTec2 and CelluClast 1.5L with each at 60 FPU/g, adding up to a total of 120 FPU/g (green). Data points and error bars represent average and standard deviation, respectively, of 3 replicate experiments.

It should be noted that, while the results presented in Figure 4.3 were expressed in the conversion of the substrate, the results presented in Figure 4.5 are expressed in glucose yield, representing exactly how much of the substrate was converted into glucose monomers. Thus, the higher results of conversion

obtained in Figure 4.3 for cTec2 at 60 FPU/g substrate after 72 h (of around 75%) when comparing with the results for the same enzyme at the same loading in Figure 4.5 (of around 30%) can be explained by the quantification of conversion of cellulose into soluble glucose oligomers, that are accounted for in Figure 4.3, and not in Figure 4.5.

In conclusion, even though the recommended loading for pure cellulose is 4.5% (w/w) solids in the LAP [175], based on these results, it was determined that the best enzymatic loading when using pure cellulose as substrate was 120 FPU/g of cellulose, making up for a 9% (w/w) solids.

Additionally, once again, the mix resulted in slightly less conversion than the same enzyme loading of only cTec2, confirming that cTec2 alone is the best option.

# 5. Results and discussion: Hemicellulase

## 5.1. Protein quantification

The quantification of the enzyme solutions' protein content was determined as 20.6 mg/mL by the Bradford method, using BSA as standard.

## 5.2. The overall composition of the commercial hemicellulase solution

The main constituents of the hemicellulase solution consist of protein (mainly hemicellulases, but there can also exist remains of other proteins that remain after the process of extraction), quantified by Bradford assay, and sugars (that are added to act as stabilizing agents [183]). The components' percentage was calculated based on the enzymatic solution's average density of 1.2 g/mL (19).

The content of multiple carbohydrates was determined by HPLC, due to the complex heterogeneous composition of the hemicellulosic biomass: Since multiple sugars could interfere with the results of the saccharification process, a complete examination was performed – **Figure 5.1**.

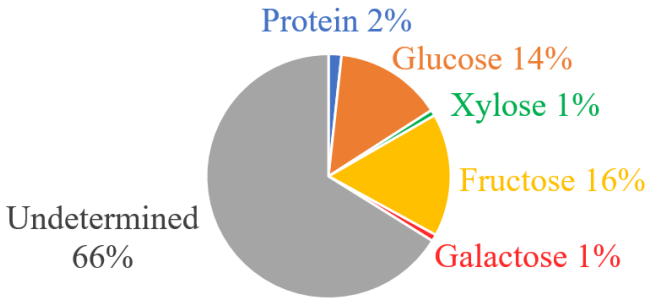


Figure 5.1: Characterization of the main components of Viscozyme L: protein (in blue) and multiple carbohydrates (glucose in orange, xylose in green, fructose in yellow, and galactose in red).

## 5.3. Determination of activity

To allow for the comparation of Viscozyme's activity with the cellulases, the same protocol was used to determine an FPU-equivalent measure of activity.

Viscozyme L is announced as a "Multi-enzyme complex containing a wide range of carbohydrases, including arabanase, cellulase, β-glucanase, hemicellulase, and xylanase" (19), so its activity was tested in two substrates: xylan and arabinogalactan. Since xylan is the most abundant polymer in hemicellulose, as mentioned in the introduction, the activity of Viscozyme L was firstly determined using xylan as a standard substrate – **Figure 5.2**.

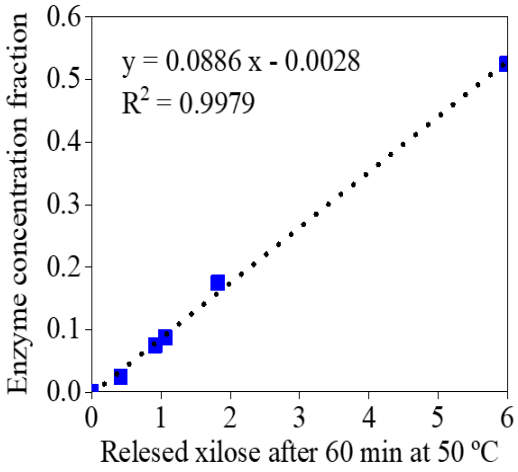


Figure 5.2: Viscozyme L activity determination, using xylan as standard substrate and following the same protocol as FPA, used for cellulase. Data points represent the average of 2 replicate experiments.

It was determined that Viscozyme had a very low activity of 2 unit/mL – **Equation 5.1** – when comparing to the 51 units/mL of CelluClast 1.5L and 137 units/mL of Cellic cTec2.

Due to the slim percentage of only 2% of the solution being identified as protein, while CClast had 5% and cTec2 had 9%, it was expected for Viscozyme to present a lower activity than the cellulases. But, since in the description of the solution, xylanase is specified in particular (19), it was expected for the activity of Viscozyme on xylan to reach a more significant result.

**Viscozyme L (in xylan):** $\frac{0.37\ \mu mol\ min^{-1}\ mL^{-1}}{0.0886 \times 2 - 0.0028} = 2$ unit/mL Equation 5.1

However, Viscozyme L has been reported as having a low yield in the saccharification of sugar polymers into xylose, an average yield in arabinose, and a very high yield in galactose and glucose [95]. Nevertheless, even though this enzyme yields very low quantities of xylose monomers, it is reported that by HPSEC it is possible to infer a high quantity of degradation products with high molecular weight than xylose. Thus, this suggests that Viscozyme L is indeed capable of incomplete saccharification of xylan backbones, mostly degrading it into oligomers and not completely into xylose monomers [202]. To understand this, it must be considered that, as mentioned in **chapter 1.7.1**, there are two main groups of xylan-degradative enzymes: xylanase (endo-1,4-beta-xylanase), responsible for random hydrolysis of linkages in xylan chains, resulting in smaller chain oligomers (9), [23,43,66], and beta-xylosidase, that sequentially degrades successive linkages of xylan chains into monomeric xylose (10), [23,43,66]. Thus, the declared results suggest a lack of beta-xylosidase in Viscozyme L.

On the other hand, Celluclast 1.5 L was indicated as the tested enzyme solution with the highest xylose yields [95]. Additionally, it was reported that co-incubation of Viscozyme L with Celluclast 1.5 L showed a weak synergistic interaction in catalyzing liberation of xylose [202]. Most likely, because Celluclast 1.5L is supposedly rich in beta-galactosidades, reported in that study as the reason for its higher yield of xylose [202]. Thus, it was considered the use of Celluclast 1.5L as a supplement for Viscozyme. However, this would require either a single saccharification assay with both enzymes (and the respective optimization of the ratio between the two commercial enzymatic solutions) or two separate assays, firstly with Viscozyme to degrade the xylan into xylose oligomers, followed by another cycle with Celluclast to degrade further those oligomers into monomers (since only monomers are accounted for by HPLC). Therefore, as a least time-consuming option, it was determined that the Viscozyme activity should be determined using arabinogalactan as substrate – **Figure 5.3** – instead of xylan.

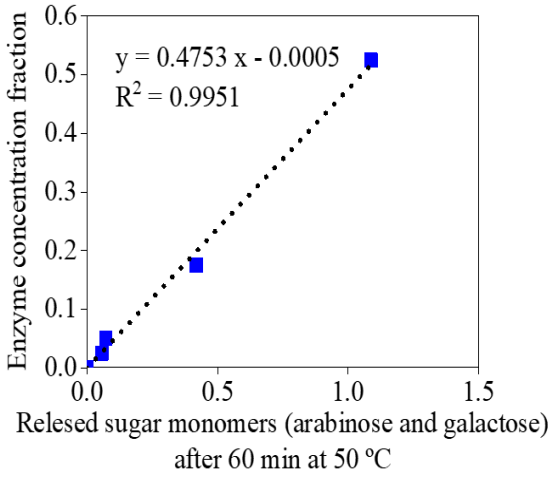


Figure 5.3: Viscozyme L activity determination, using arabinogalactan as standard substrate and following the same protocol as FPA, used for cellulase. Data points represent the average of 2 replicate experiments.

However, surprisingly, the activity in arabinogalactan is 0.4 units/mL – **Equation 5.2.** This activity is even lower than using xylan as substrate, with the undiluted enzymatic solution not being able to reach the 2 mg mark after 60 minutes at 50 ºC.

**Viscozyme L (in arabinogalactan):** $\frac{0.37\ \mu mol\ min^{-1}\ mL^{-1}}{0.4753 \times 2 - 0.0005} = 0.4$ unit/mL Equation 5.2

The structural base of arabinogalactan is a backbone of mainly (1-3)-linked beta-D-galactopyranose, frequently branched with side chains of more galactopyranose, along with L-arabinofuranose and D-glucuronic acid, whin an average ratio of galactose:arabinose:glucuronic acid of 5:1:0.08 [203].

Even though Viscozyme L is announced as a "Multi-enzyme complex containing a wide range of carbohydrases, including arabanase, cellulase, β-glucanase, hemicellulase, and xylanase" (19), and has indeed some activity towards arabinogalactan, the previous assumption that it would be more active in arabinogalactan than xylan was incorrect. So, contrarily to the reported results, it was determined that instead of having a very high yield in the saccharification of sugar polymers into galactose and an average yield in arabinose [95], (which would make Viscozyme L an enzyme better fit for the hydrolysis of arabinogalactan), the enzyme actually led to a higher yield in the hydrolysis of xylan, even though it was reported that Viscozyme L resulted in a low yield in xylose [95].

# 6. Results and discussion: Immobilization complexes produced

## 6.1. FTIR analysis

### 6.1.1. Conformation of the DMSA-coated SPIONs

Dimercaptosuccinic acid (DMSA) forms very strong and stable complexes with $Fe_3O_4$ – **Figure 6.1** – and allows the functionalization of the nanoparticles by covering the surface with both S and COOH functional groups where, depending on the conditions, both can be available for further functionalization of the complex [130,131,133].

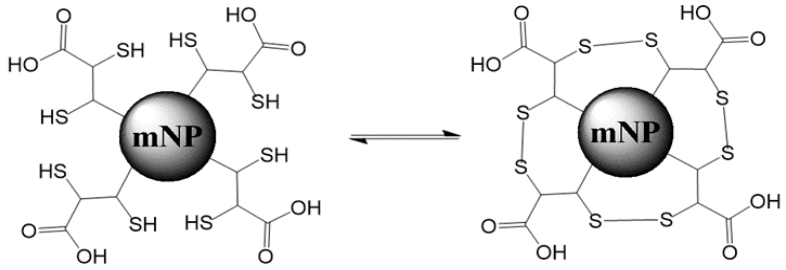


Figure 6.1: Possible configurations for DMSA-SPIONs.

FTIR analysis – **Figure 6.2** – was made to determine the conformation of the DMSA coated SPIONs, concluding that the complex is in a sable crown formation. That conclusion was drawn since the stretching of thiols (S-H) usually appears between 2550 to 2620 $cm^{-1}$ [204], and it was not identified in the performed analysis. It is believed that the absence of S-H stretching vibrations is due to the dialysis, which contributes to intraparticle disulfide bridges instead [135]. On the other hand, the stretching of disulfides (S-S) appears near 600 to 620 $cm^{-1}$ [204], where it can be masked by the accentuated peak of Fe-O that usually occurs close to 569 $cm^{-1}$ [131] and is here detected at 544 $cm^{-1}$.

Thus, the SPIONs are most likely in a crown formation since S-H functional groups were not detected, but the COOH were, based on the peaks at 3197 $cm^{-1}$, 1598 $cm^{-1}$, and 1371 $cm^{-1}$: The wide band with a peak at 3197 $cm^{-1}$ is compatible with the O-H stretching, characterized by a wide band between 3200 and 3570 $cm^{-1}$ [204], more specifically being from an acid OH, which usually appears between 2500 to 3400 $cm^{-1}$ [205] as well as overlapping vibrations for the water in the sample [131]. The peak at 1598 $cm^{-1}$ is consistent with carboxylic acids, which are found between 1725–1700 $cm^{-1}$ [204], since the conjugated carbonyl (C=O) stretching is usually found at 1690 $cm^{-1}$ [205], but can range from 1650-1800 $cm^{-1}$ [205]. The peak at 1371 $cm^{-1}$ is consistent with C-O bonds in acyl groups, which are usually detected around 1100-1350 $cm^{-1}$ [205]. Together, these two peaks around 1600 and 1400 $cm^{-1}$ are therefore attributed to the asymmetric and symmetric carboxylate stretching [131,134,135]. Both these bands shifted slightly to lower frequencies due to the bond of the DMSA to the nanoparticles, making the carboxyl group dissociated and coordinated with the surface of iron oxide [134].

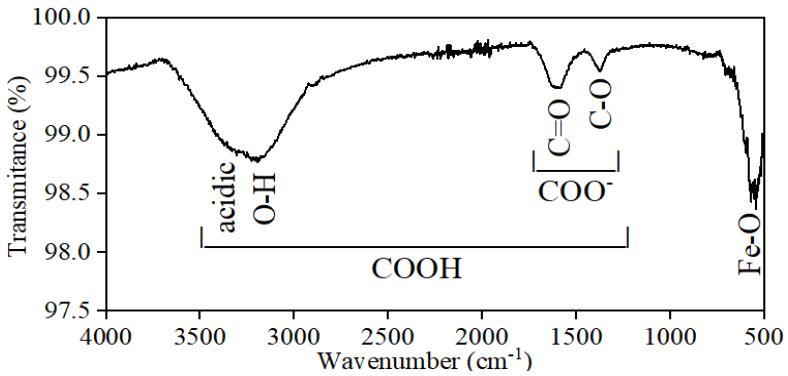


Figure 6.2: FTIR spectrum of a batch of fresh DMSA-coated SPIONs, in distilled $H_2O$. The main peaks (broad around 3197 $cm^{-1}$ and narrow at 1598, 1371, and 544 $cm^{-1}$) have their respective functional groups signaled. Data points represent the average of 2 replicate analysis.

### 6.1.2. Stability of the matrix in solution over time

To ensure the quality of the DMSA-coated SPIONs, it was necessary to determine the best storage and the required frequency of production of new batches of SPIONs. Thus, the quality of the SPIONs over time was investigated after 5 weeks of storage under different conditions: storage in distilled water at 4 ºC and -4 ºC, as well as lyophilized, stored at r.t. and -4 ºC. These samples were analyzed visually to evaluate their homogeneity and by FTIR – **Figure 6.3** – to evaluate shifts in composition. For the analysis, the frozen sample was defrosted at r.t., and the lyophilized samples were re-suspended in ultra-pure water. By visual examination of the homogeneity of the nanoparticles, it was clear that the ones in the frozen sample were agglomerated and did not remain in suspension. Both lyophilized samples were able to be re-suspended, even though they were deposited after around 10 minutes. Overall, the only sample able to remain in suspension indefinitely was the sample stored in ultra-pure water, at 4 ºC.

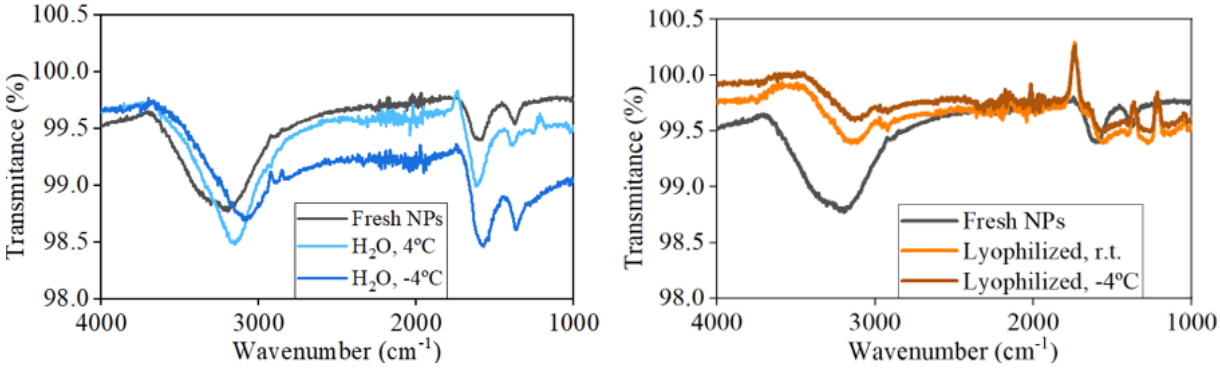


Figure 6.3: FTIR analysis of SPIONs after 5 weeks storage under different conditions: ultra-pure water (left) at 4ºC (in light blue) and -4ºC (in dark blue), and lyophilized (right) stored at r.t. (in orange) and -4ºC (in brown). The spectrum of a fresh batch of SPIONs is represented (in black) to allow for the comparation of profile changes after the 5 weeks of storage. Data points represent the average of 2 replicate analysis.

Through FTIR analysis of all samples, two distinct patterns were easily detected: the SPIONs stored in ultra-pure water (both at 4 and -4 ºC) suffered a slight blue shift, especially of the O-H peak (the broad area around 3197 $cm^{-1}$), but they still matched the original FTIR profile. On the other hand, both lyophilized samples suffered the largest profile change, showing not only a slight blueshift in the O-H area but also losing the profile of the peaks corresponding to the carboxylic acids of the coating. Thus, it was inferred that the coating is most likely degraded by the lyophilization process, making storage under those conditions unfeasible.

Since the sample with the closest FTIR profile to the original was stored in ultra-pure water at 4 ºC and it coincided with the observations of the visual examination, it was determined that a visual examination was enough to evaluate the quality of the nanoparticles and FTIR of the APTES-coated SPIONs was deemed unnecessary, respecting the same storage conditions and time frame of producing monthly batches of SPIONs, to ensure their quality.

## 6.2. Cellulase immobilized onto DMSA-coated SPIONs (CDS)

The immobilization time should be determined based on the protein in the study. However, in the available literature, the immobilization times can range from intervals of 3 hours [97], 6 hours [111] or 7 hours [102], to overnight [105] and 24 hours protocols [39]. So, the immobilization time of 16 h (overnight) was selected, not only to keep the protocol close to the protocol of Catarina Chaparro for antibody immobilization onto DMSA-coated SPIONs through the use of EDC/NHS [135], from which this was adapted but also because it was the more favorable option from a practical point of view.

The same dilemma is applied for the protein/mNP ratio: It is dependent of the enzyme understudy, but the literature values found for cellulase immobilization can go from ratios as high as 3:1 (1500 mg enzyme : 500 mg mNPs ) [97] and 4:1 (72 mg enzyme : 18 mg NP) [111] to as low as 1:3 [97] and 1:30 (8 mL of 0.25 mg/mL cellulase solution : 60 mg mNPs) [102]. Thus, the immobilization ratio was originally set at 1.5:1, even though the 1:1 ratio was also tested.

### 6.2.1. Immobilization CDS 1 to 7: preliminary testing

The preliminarily evaluated characteristic was the efficiency of the immobilization, to determine if the overall process of immobilization was happening, and which batches to continue studying.

Since proteins contain multiple amine and carboxyl groups, if the EDC-NHS step was simultaneous to the protein addition, it would cause random polymerization of proteins, hindering the immobilization to the support [137]. Thus, it is important to only add the enzyme once the EDC and NHS have already reacted with the SPIONs and the resulting activated SPIONs were thoroughly washed, to avoid unwanted crosslinking. So, the immobilization is made as a two-step process: First the functionalization of the SPIONs with the crosslinkers, and then adding the protein. Thus, the target pH can be set at different values for each step, allowing for a better optimization fitting the reaction taking place at each step. Therefore, CDS 1 through 6 – **Table 6.1** – tested multiple media during the immobilization process.

Since the main crosslinker in play is EDC, and its reaction is most efficient in conditions around pH 4.5, and the media must be devoid of carboxyl and amine functional groups, the most recommended buffer for EDC crosslinking reactions is MES [137]. However, due to the availability in the lab at the time, the first buffer tested was sodium phosphate buffer 0.05 M, pH 5.8, as the EDC crosslink reaction can still be performed in phosphate buffers, as well as media up until neutral pH (maximum of pH 7.2). However, in these conditions, the efficiency is lower, so a good immobilization may require an increase in the amount of EDC [137]. Thus, the EDC quantity was increased in those assays (CDS 1 and 2).

Ultrapure water was also tested (CDS 1 and 2), and the pH was measured before and after the reaction steps in question. It showed minimal variation, so it could be considered an adequate solvent as it was showed that there is no need to use specifically a buffer.

On the other hand, even though the recommended pH for EDC crosslinking is around 5, the compound N-hydroxysuccinimide (NHS) is used in EDC-coupling protocols to create a more stable intermediate and facilitate the EDC reaction. These esters are specific for primary amines ($-NH_2$) and are efficient between pH 7 to 9, with higher efficiency achieved at neutral conditions [137]. Therefore, in theory, the target pH for the first step is pH of 7.2, as it is the pH overlap in both crosslinkers (EDC from 4.5 to 7.2 and NHS from 7 and 9). With that in mind, PBS 1x pH 7.2 is the recommended buffer for protocols of EDC+NHS crosslinking [137] and was also tested as solvent (CDS 4 and 5).

However, it must be noted that even though pH 7.2 is more desirable for the crosslinking reaction, the optimum pH for the enzyme is around pH 5. Thus, performing the whole immobilization at pH 7.2 might be the better option for the immobilization to occur, but it can alter the enzyme's conformation. Therefore, MES buffer 0.05 M, pH 5.5 was also tested (CDS 5 and 6), as not only it is the recommended buffer for the use of the main crosslinker EDC but is also more compatible with the enzyme and can ensure that the enzyme is immobilized in the correct conformation to perform the saccharification.

Table 6.1: Comparison of the immobilization efficiency results of CDS 1 to 6 to determine the influence of the media during the two steps: EDC/NHS activation and enzyme immobilization.

| Batch | Buffer used:<br>1st step<br>2nd step | Immobilization efficiency (%) |
|---|---|---|
| CDS 1 | Phosphate 0.05M, pH 5.8<br>Phosphate 0.05M, pH 5.8 | -0.07 ± 0.33 % |
| CDS 2 | Phosphate 0.05M, pH 5.8<br>distilled water, pH 5.2 | 14.80 ± 0.79 % |
| CDS 3 | distilled water, pH 5.2<br>distilled water, pH 5.2 | 1.24 ± 0.76 % |
| CDS 4 | PBS 1x, pH 7.2<br>PBS 1x, pH 7.2 | 42.36 ± 1.62 % |
| CDS 5 | PBS 1x, pH 7.2<br>MES 0.05 M, pH 5.5 | 31.43 ± 1.93 % |
| CDS 6 | MES 0.05 M, pH 5.5<br>MES 0.05 M, pH 5.5 | 47.13 ± 1.27 % |

From these 6 batches, only CDS 2, 4, 5 and 6 were considered as having a high enough immobilization efficiency to proceed with the study of said complexes.

Considering that the best immobilization efficiency results were obtained when both steps were performed with MES buffer as a solvent (with a pH of 5.5), the immobilization complex CDS 7 was performed with the goal of comparing it with CDS, and determine if the NHS is necessary – **Table 6.2** – since NHS is used as a complement to EDC, and its range is reportedly 7.2 to 8.5 pH [137].

Table 6.2: Comparison of the overall results of CDS 6 and CDS 7 to determine the influence of using NHS as a complement for the EDC, in the EDC/NHS crosslink method.

| Batch | Crosslinker | Immobilization efficiency (%) |
|---|---|---|
| CDS 6 | EDC and NHS | 47.13 ± 1.27 % |
| CDS 7 | EDC only | 48.27 ± 1.08 % |

As CDS 7 achieved an equally high immobilization efficiency, it was also deemed worthy of continuing the study.

### 6.2.2. FTIR as confirmation of immobilization

FTIR was necessary on the presumed successful CDS complexes – **Annex 2 to 6** – as the process of cellulase immobilization onto DMSA-coated SPIONs via EDC/NHS crosslinking was not described in the literature. Thus, it must be confirmed that the process achieved immobilization, and its implications on the overall complex's structure. Since the remaining complexes produced (CAS, CMm and HM) had some literature background ensuring some success, FTIR was not performed for them.

This analysis was performed to ensure that the enzyme was immobilized, and that it maintained the same profile since a change in conformation would alter the FTIR profile and probably the enzyme's activity. The studied CDS complexes – **Figure 6.4** – resulted in the same profile, thus one can be elected as a representative.

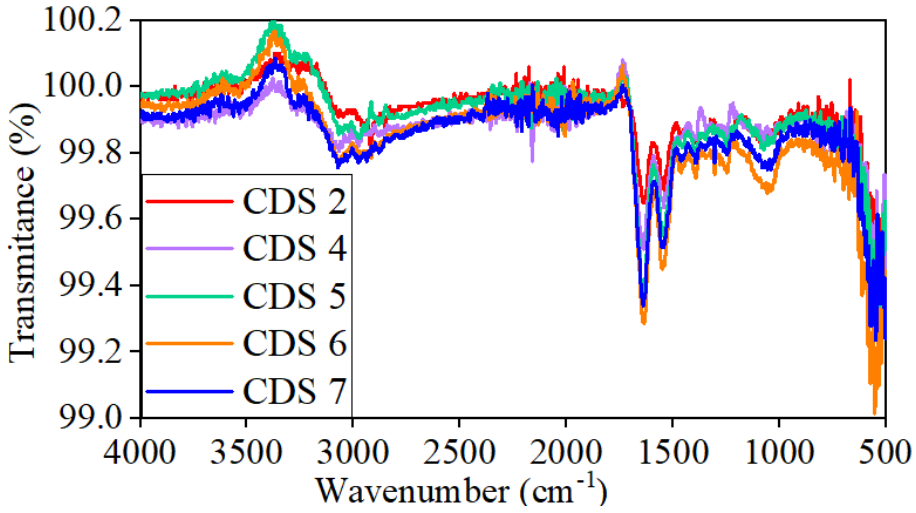


Figure 6.4: Overlap of the FTIR spectra of CDS successful immobilization complexes: Comparison of the profiles of CDS 2 (in red), CDS 4 (in purple), CDS 5 (in light green), CDS 6 (in orange), and CDS 7 (in blue). Data points represent the average of 2 replicate experiments.

Consequently, to confirm the immobilization process, a comparison was made of the profiles of the matrix, the commercial enzymatic solution, and one of the CDS complexes (acting as the representative of the profile of all CDS immobilization complexes) – **Figure 6.5**.

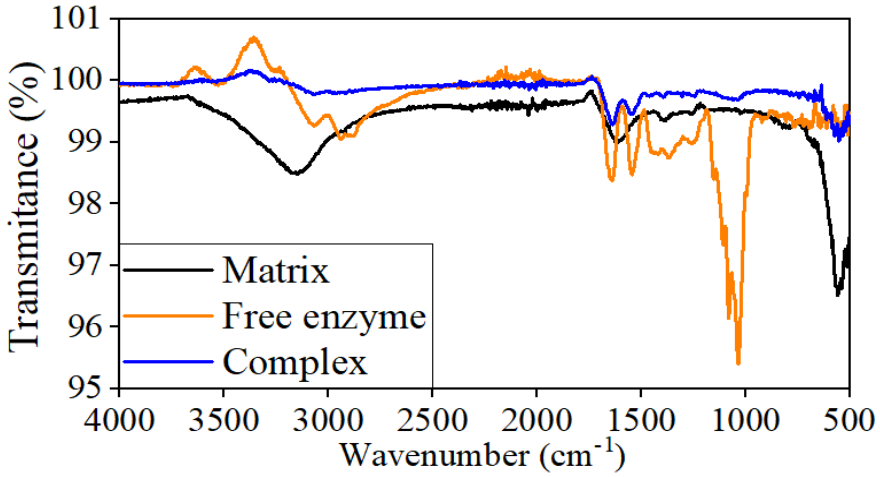


Figure 6.5: FTIR spectra for the confirmation of immobilization: Comparison of the profiles of the SPIONs matrix (in black), Cellic cTec 2 enzymatic solution (in orange), and the immobilization complex (in dark blue). This specific spectrum belongs to CDS 6, but simultaneously represents the profile obtained in all the analyzed CDS immobilizations: 2, and 4 to 7 (individual comparison spectra are available in annexes). Data points represent the average of 2 replicate experiments.

It is noticeable that the profile of the immobilized enzyme corresponds to a juxtaposition of the profiles of both free enzyme and matrix, as expected. This can be pointed out for the double peak around 1642 $cm^{-1}$ and 1542 $cm^{-1}$ that is highly pronounced in free enzyme and detected in the complex. On the other hand, the Fe-O peak detected at 544 $cm^{-1}$, characteristic of the matrix, is also detected on the complex, though with less intensity. Thus, it can be confirmed that the enzyme was immobilized into the matrix, composing a new profile that incorporates the major characteristics of both constituents.

It should be noted that since the enzymatic solution is of commercial origin, its constitution is not fully known, so the analysis of its FTIR profile is merely to compare with the complex. It was noted that a massive peak (around 1050 $cm^{-1}$) in the solution was not found in the complex. However, since there are effectively peaks in common, the absence of this one in the complex is most likely due to the presence of the stabilizing agents in the commercial enzyme (that are not immobilized into the matrix and are therefore washed away during that process), since to have such an intense signal it must belong to a major component of the overall solution.

### 6.2.1. Immobilization CDS 1 to 6

In the first set of CDS immobilizations – **Table 6.3** – the complexes CDS 1 and CDS 3 were deemed not good enough to proceed into the saccharification phase, due to the very low protein immobilization percentages obtained (-0.07±0.33% for CDS 1 and 1.24±0.76% for CDS 3).

Table 6.3: Comparison of the overall results of CDS 1 to 3 to determine the influence of the media during the two steps: EDC/NHS activation and enzyme immobilization.

| Batch | Buffer used: 1st step 2nd step | Immobilization efficiency | Retained activity 1st use, 24 h | Retained activity 1st use, 72 h | Protein leaching 1st use, 72 h |
|---|---|---|---|---|---|
| CDS 1 | Phosphate 0.05 M, pH 5.8<br>Phosphate 0.05 M, pH 5.8 | -0.07 ± 0.33% | - | - | - |
| CDS 2 | Phosphate 0.05 M, pH 5.8<br>Distilled water, pH 5.2 | 14.80 ± 0.79% | 53.32% | 60.60% | 88.88 ± 0.03% |
| CDS 3 | Distilled water, pH 5.2<br>Distilled water, pH 5.2 | 1.24 ± 0.76% | - | - | - |

Even though CDS 2 did not achieve a good immobilization percentage either (14.80±0.79%), it was tested in the saccharification phase to determine if the immobilized enzyme was still active.

From an activity point of view, CDS 2 appeared to be a very promising complex. Presenting a retained activity of 53.32% after 24 hours of saccharification assay, this would be an excellent result, as the usual best-reported values for cellulase retained activity are in these order of percentages, like 48% [105] and 58% [96] of cellulase activity when compared to its free form.

However, the retained activity of CDS 2 at 72 hours (61%) is higher than at 24 hours (53%). Thus, it is highly probable that the high glucose yield after 24 hours derived from the enzymes being released from the matrix, regaining their original flexibility and, thus, the standard activity of the free enzyme. This is supported by the value of leached protein, as 89% of the immobilized enzyme remained in solution after the retrieval of the complex, reinforcing the idea that CDS 2 is a very ineffective protocol.

For the second half of the CDS immobilizations – **Table 6.4** – CDS 5 should theoretically be the complex with the best results since during the 1st step, as recommended for EDC/NHS protocols, maintains the 7.2 pH, and the change of solvent into MES for the 2nd step ensures the enzyme conformation at pH 5. However, between these 3 batches, it was the protocol with the lowest immobilization percentage, showing an immobilization efficiency of 31.43±1.93%, while CDS 4 reached 42.36±1.62%, and CDS 6 was able to achieve an immobilization efficiency of 47.13±1.27%.

Table 6.4: Comparison of the overall results of CDS 4 to 6 to determine the influence of the media during the two steps: EDC/NHS activation and enzyme immobilization.

| Batch | Buffer used:<br>1st step<br>2nd step | Immobilization efficiency | Retained activity<br>1st use, 24 h | Retained activity<br>1st use, 72 h | Protein leaching<br>1st use, 72 h |
|---|---|---|---|---|---|
| CDS 4 | PBS 1x, pH 7.2<br>PBS 1x, pH 7.2 | 42.36±1.62% | 40.11% | 20.69% | 29.76±0.04% |
| CDS 5 | PBS 1x, pH 7.2<br>MES 0.05 M, pH 5.5 | 31.43±1.93% | - | - | - |
| CDS 6 | MES 0.05 M, pH 5.5<br>MES 0.05 M, pH 5.5 | 47.13±1.27% | 41.36% | 20.72% | 29.57±0.07% |

Thus, from all the CDS complexes performed until this point, CDS 4 and 6 were selected as the most promising and, thus, selected to move on to the test of activity in cellulose saccharification.

After the saccharification assay, both these immobilization batches were considered promising, since similar values of both immobilization efficiency and retained activity are reported in the literature: for example, in 2018 [105], complexes of mNPs and cellulase were developed. Those complexes were established through covalent immobilization, like in this work, but it should be noted that, in that case, the functionalization was made by glutaraldehyde and not EDC/NHS, as there were found no reported cases of cellulase immobilized with those crosslinkers. However, in the mentioned article, cellulase was immobilized with an efficiency of 45%, which is congruent with the obtained results.

### 6.2.2. Immobilization CDS 7

As mentioned before, considering the best immobilization efficiency, results were obtained when both steps were performed in MES buffer (with a pH of 5.5). Thus, CDS 7 – **Table 6.5**– was performed to determine if the addition of NHS is necessary for the immobilization protocol since it is used as a complement to EDC, and its range is reportedly 7.2 to 8.5 pH [137].

According to those results, it was determined that removing NHS from the process resulted in a nearly insignificant improvement in immobilization percentage (increasing from 47.1±1.3% in CDS 6 to 48.3±1.1% in CDS 7) and negligible variation on the 1st use leaching (29.57±0.07% in CDS 6 and 30.43±0.74% in CDS 7) and long-term stability (23.45% in CDS 6 and 24.66% in CDS 7). However, it was decided that the addition of NHS is beneficial to the process, regardless of the pH is far from the optimal pH for its reaction, due to the decrease in retained activity when comparing CDS 6 and CDS 7, both at 24 and 72 hours, with 41.4% in CDS 6 and 36.6% in CDS 7 at 24 hours, and 20.7% in CDS 6 and 17.5% in CDS 7 at 72 hours.

Table 6.5: Comparison of the overall results of the 1st saccharification cycle of CDS 6 and CDS 7, to determine the influence of using NHS as a complement for the EDC, in the EDC/NHS crosslink method.

| Batch | Crosslinking agent | Immobilization efficiency | Retained activity 1st use, 24 h | Retained activity 1st use, 72 h | Protein leaching 1st use, 72 h | Protein leaching 1-month storage |
|---|---|---|---|---|---|---|
| CDS 6 | EDC+NHS | 47.13±1.27% | 41.4% | 20.7% | 29.57±0.07% | 23.45±0.09% |
| CDS 7 | EDC only | 48.27±1.08% | 36.6% | 17.5% | 30.43±0.74% | 24.66±0.08% |

Hence, these results suggest that using NHS as a complement is indeed beneficial, but most likely not by enhancing the protein binding, but its quality: It is suspected that the use of NHS leads to a more favorable immobilization process by modelling the enzyme's binding site to the matrix in a different way than EDC. Thus, slightly less enzyme was immobilized, but in a more favorable configuration, that allowed for more flexibility of the enzyme or facilitated the access of the substrate to the immobilized enzymes' binding sites.

### 6.2.3. Immobilization batch CDS-g 0

This batch is the control for CDS-g 1 to 3, to test the influence of adding glutaraldehyde as a secondary crosslinker. However, since this control would follow the same parameters of CDS 6, the protein/mNP ratio (w/w) during crosslinking was altered to test its influence – **Table 6.6 and Table 6.7**.

The study of the influence of the ratio during functionalization was done by reducing the ratio from 1.5:1 to 1:1, and with the goal of potentially reducing protein waste during the immobilization process.

Thus, it was necessary to lower the ratio of all the CDS-g protocols, allowing to compare two different parameters of this complex: compare CDS-g 0 with CDS 6 to see the influence of the ratio, and by lowering the ratio of all the CDS-g complexes, it still allows to check the influence of the glutaraldehyde by altering only that parameter between them.

It should be noted that, since it relies on a small modification to CDS 6, the CDS-g batches did not require FTIR analysis, even though they are still CDS complexes and, thus, unreported in the literature.

Table 6.6: Comparison of the overall results of CDS 6 and CDS-g 0 to determine the influence of lowering the protein/mNP ratio (w/w) from 1.5:1 to 1:1 in the immobilization process efficiency, and complex activity.

| Batch | Protein/mNP ratio (w/w) | Immobilization efficiency | Protein/mNP approximate final ratio | Retained activity 1st use, 24 h | Retained activity 1st use, 72 h |
|---|---|---|---|---|---|
| CDS 6 | 1.5 : 1 | 47.13±1.27% | 0.7 : 1 | 41.36% | 20.72% |
| CDS-g 0 | 1 : 1 | 58.43±0.27% | 0.6 : 1 | 25.37% | 17.48% |

Relative to the immobilization efficiency of the protocols – **Table 6.6** – CDS 6, with a (w/w) ratio of 1.5 protein /mNP, can be seen as the better protocol, because even though it has a lower percentage of immobilization efficiency (leading to slightly more enzyme waste), it also culminates in a higher enzyme loading onto the nanoparticles, which is one of the aims for the immobilization complexes.

Regarding activity – **Table 6.6** – CDS 6 also takes the lead since CDS-g 0, achieving 25% retained activity, has a significantly lower performance than CDS-g 6, with 41%.

However, from a perspective of complex stability– **Table 6.7** – CDS-g 0 is superior since the protein leaching after 1 use is lower (with 30% in CDS 6 and 20% in CDS-g 0). This tendency is also found after 1 month of storage, where 14% leaching was detected on CDS-g 0, while CDS 6 accused 19%.

Due to the COVID-19 quarantine it was not possible to run a 2nd round on batch CDS 6, as its integrity was deemed compromised after all the time spent in the fridge. Thus, with only one round of comparison, it cannot be conclusively determined that CDS 6 did not have future potential since it has such a promising activity that maybe can compensate for the protein leaching, providing that the leaching was insignificant in the second round (which has been observed in other complexes).

Table 6.7: Comparison of the protein leaching results of CDS 6 and CDS-g 0 to determine the influence of lowering the protein/mNP ratio from 1.5:1 to 1:1 in protein stability.

| Batch | Protein leaching 1st use, 72h | Protein leaching 1-month storage |
|---|---|---|
| CDS 6 | 29.57±0.07% | 18.56% |
| CDS-g 0 | 19.80% | 13.73% |

However, based on the available information, the best protocol appears to be CDS-g 0, as a complex with reasonable potential in immobilization efficiency, slightly higher loading, and lower retained activity, but more promising stability.

### 6.2.4. Immobilization batch CDS-g 1 to 3

Citrate buffer 0.05 M, pH 4.8 is the standard buffer for cellulose saccharification, according to the Laboratory Analytical Procedure (LAP) for Enzymatic Saccharification of Lignocellulosic Biomass [175]. However, since carbodiimides catalyze the formation of a bond between a carboxyl group (–COOH) and a primary amine ($–NH_2$) [137], and citrate buffer has carboxyl functional groups, those can compete with the SPIONs, potentially accelerating the leaching process. Therefore, an alternative buffer was selected to perform the cellulose saccharification, using CDS 4, 6 and 7. The selected buffer was MES 0.05 M pH 5.5, as it has a similar pH and the immobilization complexes remained in solution longer in MES buffer (around 3 days), contrary to citrate buffer (that lead to precipitation of the complexes overnight).

However, after analyzing the saccharification results in MES, the activity values were low, both in the immobilization complexes but also in the control assay with free enzyme: While the free enzyme assays usually have around 30 and 60% of glucose yield after 24 and 72 hours respectively, during this saccharification in MES the free enzyme only reached 22 and 52% for the same time frames, losing, respectively, a comparative 27 and 13% of yield. Thus, it was concluded that the citrate buffer should remain the standard buffer for cellulose saccharification assays. Consequently, in the immobilization batches of CDS-g – **Table 6.8** – was studied the option of adding an additional step of glutaraldehyde crosslinking between enzymes after those were already immobilized onto the magnetic nanoparticles via EDC/NHS immobilization. This immobilization scheme has the potential to obtain better results than using only glutaraldehyde from the start, as the symmetry from glutaraldehyde can induce indiscriminate binding, leading to clusters of both enzymes or nanoparticles or multiple chain bonds [137], hampering the homogeneity of the resulting immobilization complexes. On the contrary, the EDC/NHS bonding is specific, increasing the chance of a preferential connection between enzyme and nanoparticles, as well as smaller clusters [137] and, therefore, a better homogeneity in the final immobilization complexes.

Since the enzyme was previously crosslinked to the matrix, it was determined that most likely the glutaraldehyde percentage (v/v) that was required to crosslink the enzymes would be lower than the usual recommendation. Thus, the tested percentages of glutaraldehyde (v/v) were correspondent to 1/8, 1/4, and the recommended concentration of 0.5% for glutaraldehyde crosslink of previously immobilized proteins [206], along with CDS-g 0 to provide control of 0% glutaraldehyde.

Table 6.8: Comparison of the overall results of CDS-g 0 to 3, to determine the influence of using different glutaraldehyde percentages (v/v) as a secondary crosslinker.

| Batch | Glutaraldehyde's percentage (v/v) | Immobilization efficiency | Retained activity 1st use, 24 h | Retained activity 1st use, 72 h | Protein leaching 1st use, 72 h |
|---|---|---|---|---|---|
| CDS-g 0 | 0 (control) | 58.43±0.27% | 25.37% | 17.48% | 19.80% |
| CDS-g 1 | 0.0625% (1/8 of recommended) | 61.44±0.14% | 15.88% | 9.36% | 19.46% |
| CDS-g 2 | 0.125% (1/4 of recommended) | 61.98±0.18% | 8.75% | 6.42% | 13.00% |
| CDS-g 3 | 0.5% (recommended [206]) | 62.45±0.22% | 6.73% | 4.23% | 10.36% |

When comparing to the results obtained in CDS-g 0, CDS-g 3 suffered a sacrifice of roughly 75% of retained activity (from 25% in CDS-g 0 to 7% in CDS-g 3), accompanied by an improvement of around 50% in protein leaching (from 20% in CDS-g 0 to 10% in CDS-g 3). So, from a relative comparison between the percentage of retained activity versus protein leaching, CDS-g 3 shows the best statistical results. However, a retained activity of 7% is too small for this complex to be considered.

Consequently, it was deemed that the best batches were CDS-g 0 and CDS-g 1 since, as expected, the higher glutaraldehyde percentages (in this case CDS-g 2 and 3) led to such a loss of flexibility that the retained activity suffered greatly, and that was not compensated by the results of protein leaching.

CDS-g 1 sacrificed a comparative 37% of its retained activity to CDS-g 0 (from 25% in CDS-g 0 to 16% in CDS-g 1), with the minimal improvement of the protein leaching (from 20% in CDS-g 0 to 19% in CDS-g 1). Thus, based on the results of the 1st saccharification round, it appears that the secondary crosslinker was not an efficient addition to the protocol, as the leaching of protein is almost identical, and there is a noticeably decreased activity. However, since the crosslinking was an optimization aimed at long-term, a 2nd round of saccharifications was performed in both CDS-g 0 and 1 – **Table 6.9**.

However, the data from the 2nd round cannot be fully trusted, as due to the COVID-19 quarantine, this batch remained in the freezer for a long time, and it may have had its integrity compromised. Since it was not as old as CDS 6, a 2nd saccharification assay was performed. However, it is possible that the very low activities obtained were a consequence of the time the complex spent in between assays.

Table 6.9: Comparison of the 1st and 2nd saccharification rounds of CDS-g 0 and CDS-g 1.

| Batch | Retained activity 1st use, 24 h | Retained activity 1st use, 72 h | Protein leaching 1st use, 72 h | Retained activity 2nd use, 24 h | Retained activity 2nd use, 72 h | Protein leaching 2nd use, 72 h |
|---|---|---|---|---|---|---|
| CDS-g 0 | 25.37% | 17.48% | 19.80% | 1.5% | 1.6% | 4.14% |
| CDS-g 1 | 15.88% | 9.36% | 19.46% | 1.4% | 3.0% | 3.52% |

Nevertheless, storage stability assays were also performed to quantify the protein leached after 1 month and after the quarantine – **Table 6.10**.

Table 6.10: Comparison of the protein leaching of CDS-g 0 and 1, after storage during 1 and 4 months, to determine the influence of using glutaraldehyde as a secondary crosslinker in the complexes' stability over time.

| Batch | Protein leaching 1-month storage | Protein leaching 4-month storage |
|---|---|---|
| CDS-g 0 | 13.73% | 5.39% |
| CDS-g 1 | 0% | 1.88% |

After 1 month of storage, there is a pronounced difference between CDS-g 0 with 14% of leaching, while there was no detected leaching in CDS-g 1. Thus, after 1-month storage, it is very noticeable the difference between using glutaraldehyde as a secondary crosslinker. This tendency was maintained after the 4-month period with, as expected, higher leaching in the absence of glutaraldehyde as a secondary crosslinker (with CDS-g 0 over 5% protein leaching while CDS-g 1 slightly under 2%). However, although the protein leaching during that period is small, the protein may suffer a loss of activity.

Nevertheless, it appears that the secondary crosslinking step is not a satisfying addition to the immobilization protocol developed so far, as even though it showed some improvement in stability, it did not appear to be sufficient to compensate for the disadvantages of the additional loss of flexibility.

## 6.3. Cellulase immobilized onto APTES-coated SPIONs (CAS)

Since there are already some examples of cellulase immobilization onto APTES-coated SPIONs, three different protocols from the literature were tested out – **Table 6.11** – with slight alterations that will be further explained below. These complexes were all reproduced to choose a base protocol to then optimize. Therefore, there is a simultaneous variation of multiple parameters that can then be optimized individually once the base protocol is determined.

Table 6.11: Summary of the parameters applied in the three batches of CAS produced and the achieved immobilization efficiency and complexes' protein loading onto SPIONs.

| Batch | Reference protocol | Glutaraldehyde | Crosslinking time | Protein/mNP ratio (w/w) | Immobilization efficiency | Protein/mNP approximate final ratio |
|---|---|---|---|---|---|---|
| CAS 1 | [206] | 10% (v/v) | 16 + 5 h | 1:3 | 33.55% | 0.3 : 1 |
| CAS 2 | [111] | 70 mM (0.66% (v/v)) | 3 + 3 h | 4:1 | 12.03% | 0.5 : 1 |
| CAS 3 | [97] | 30 mM (0.28% (v/v)) | 1.5 + 1.5 h | 1:3 | 20.23% | 0.2 : 1 |

CAS 1 was based on an overall protocol from a 2020 immobilization manual by Springer Nature [206] for glutaraldehyde crosslinking in aminated supports like it is the case of APTES-coated SPIONs. CAS 2 was based on a protocol from a 2019 immobilization article [111], and CAS 3 was based on a protocol from a 2018 immobilization article [97].

The protocol for CAS 1 was deemed promising since the 10% (v/v) glutaraldehyde was congruent with one article in the literature that claims to have immobilized peroxidase in a way that maintained approximately its full activity after up to 100 cycles [84]. However, in that case, not only were the mNPs not coated by any stabilizing agent, being directly activated with glutaraldehyde instead, but also the immobilized enzyme was peroxidase, which is submitted to less hard conditions during its cycles: uses of only 4 or 6 hours at 25 ºC and a pH of 6. For CAS 1, since there was no information of the reaction time, the same time regime used for DMSA-coated SPIONs was implemented, the crosslinking protocol being divided into an overnight (16 h) activation with a crosslinker, followed by washing of the activated support and addition of the protein that was immobilizing for 5 more hours. Otherwise, the parameters applied were all congruent with the ones suggested by the protocol, except for another slight change: The protocol instructed a ratio of 30 mL of enzyme solution for 10 g of support. In order to scale down, it was expected to use 60 mg of SPIONs to 180 µL of protein, resulting in approximately 18 mg of protein and consequently a protein/mNP ratio of 1:3.(3). Therefore, the added protein was rounded up to 20 mg (202 µL) to have a 1:3 protein/mNP ratio.

The protocol for CAS 2 was selected since the resulting complex was described as having a very high retained activity of 93%, and the protocol for CAS 3 was selected since the article already covered the optimization of multiple factors, namely glutaraldehyde concentration, protein/mNP ratio and crosslinking time, being the more extensively studied protocol available. In both these immobilizations, an alteration was made to allow for a more controlled immobilization of the enzyme: The protocols described a single step crosslinking, where both glutaraldehyde and cellulase were simultaneously added. This can lead to an increase of the probability of formation of CLEAs (Crosslinked Enzyme Aggregates), which due to the fact they are not bound to the retrieved support, are not recycled along with the rest of the immobilized protein. This CLEAs' formation is undesirable, as not only do the involved enzymes lose flexibility due to inter and intra protein crosslinking, thus hindering their activity, but they are also irretrievable as well. Thus, to avoid the formation of CLEAs, the activation step with glutaraldehyde and the protein addition were done separately by splitting the mentioned crosslinking time in half for each step.

The immobilization results of the three complexes are presented below, in **Table 6.12**.

Table 6.12: Summary of the achieved immobilization efficiency and complexes' protein loading onto SPIONs for the CAS immobilization protocols.

| Batch | Protein/mNP ratio (w/w) | Immobilization efficiency | Protein/mNP approximate final ratio |
|---|---|---|---|
| CAS 1 | 1:3 | 33.55% | 0.3 : 1 |
| CAS 2 | 4:1 | 12.03% | 0.5 : 1 |
| CAS 3 | 1:3 | 20.23% | 0.2 : 1 |

All the immobilization efficiencies were lower than expected, since in 2018 [105] complexes of mNPs and cellulase were developed through covalent immobilization, and the functionalization was made by glutaraldehyde. In this article, cellulase was immobilized with an efficiency of 45%, which is higher than CAS 1 (34%) CAS 2 (12%), and CAS 3 (20%).

Even though CAS 1 had the best immobilization efficiency, CAS 2 showed the highest enzyme loading onto the SPIONs, achieving a protein/mNP ratio of 0.5 : 1, while CAS 1 attained 0.3 : 1 and CAS 3 has the lowest loading of 0.2 : 1. However, the immobilization efficiency of CAS 2 was very low, so it was considered a rather wasteful protocol. Thus, from an immobilization point of view, the most promising protocol is CAS 1. Additionally, it must be pointed out that after the first cycle of saccharification, CAS 2 lost its integrity – **Figure 6.6** – so the waste of protein was not the defining factor in abandoning the protocol of CAS 2.


Figure 6.6: CAS 3 (left) and CAS 2 (right) after 1 saccharification cycle of 72 hours at 50 ºC. The integrity of CAS 3 was maintained, presenting the dark color that is characteristic of the SPIONs' matrix. Contrarily, CAS 2 presents a bright yellow color and, thus, denounces the loss of integrity of the $Fe_3O_4$ that constituted the SPIONs that constitute the core of the matrix.

It is thought that the change in color from the characteristic dark derives from the oxidation of magnetite ($Fe_3O_4$) to goethite (α-FeOOH), a yellow iron oxide. This is a yellow pigment that is usually synthesized by co-precipitation using the residual solution of $Fe_3O_4$, oxidizing it between pH 4 and 9, where the increase of pH leads to an increase of the yellow's brightness [207].

Thus, since the reaction taking place is saccharification, the reaction media becomes increasingly rich in glucose. Those monomers are reducing sugars, thus capable of acting as a reducing agent, donating electrons. Therefore, it is probable that the magnetite that composes the SPIONs was oxidized to FeOOH, for which the literature's proposed reaction is:

$$O_2 + 2\ e^- + 2\ H_2O \rightarrow H_2O_2 + 2\ OH^-, \text{ Followed by } H_2O_2 + 2\ Fe_3O_4 + 2H_2O \rightarrow 6\ FeOOH \quad [208]$$

CAS 1 and 3 survived when submitted to 2 cycles – **Table 6.13**. Still, the same type of integrity loss was detected in both CAS 1 and 3 after the 2nd saccharification round. However, that loss of integrity was not as extensive, so it was yet possible to analyze the glucose yield.

It should be pointed out that, in the CDS-g results, the matrix maintained its integrity after the 2nd round. Therefore, the immobilization of cellulase onto DMSA-coated SPIONs seems more durable, and it is assumed that APTES coating is more prone to allow the disintegration of the SPIONs' matrix.

Table 6.13: Comparison of the results for retained activity and stability in 1st and 2nd saccharification rounds for the produced CAS immobilization batches.

| Batch | Retained activity 1st use, 24 h | Retained activity 1st use, 72 h | Protein leaching 1st use, 72 h | Retained activity 2nd use, 24 h | Retained activity 2nd use, 72 h | Protein leaching 2nd use, 72 h |
|---|---|---|---|---|---|---|
| CAS 1 | 20.87% | 11.43% | 0.35% | 2.77% | 3.28% | 0.24% |
| CAS 2 | Not assessed | - | 0% | - | - | - |
| CAS 3 | 47.99% | 49.31% | 35.68 ± 3.78% | 12.03% | 11.77% | 0% |

Due to its loss of integrity, the glucose yield of CAS 2 could not be analyzed, since whatever resulted from the loss of integrity of the matrix was in solution, and could possibly damage the HPLC columns. Thus, that risk was not worth taking as that protocol was immediately abandoned.

On the other hand, CAS 1 and CAS 3 yielded very distinctive results, as CAS 1 retained comparatively less 27% activity than CAS 1 (21% to 48%), but it is accompanied by very low leaching of only 0.35% when compared to the 36% of CAS 3. However, in CAS 3 the retained activity at 72 h is slightly higher than at 24 h, which, alongside the high leaching of protein of around 36% indicates that the leaching of the enzyme may be responsible for such a high retained activity.

Thus, CAS 1 appears to be the most promising immobilization due to its very low leaching and reasonable retained activity. Still, those leaching quantifications in CAS 1 may prove misleading: Since during the 2nd round, CAS 1 had a slightly higher activity at 72 h than at 24 h, it was predictable that the enzyme was probably becoming free of the matrix due to leaching. However, the quantification of protein leaching could not detect any protein in the solution. The assay was performed 3 separate times, including separate calibration lines that were always consistent with previous assays. There were also no dilutions performed, so the change of user error is very slim. Hence, it was considered the hypothesis of enzyme precipitation along with the coating and mixing with the remaining unhydrolyzed biomass. It was already demonstrated in previous literature that a considerable portion of at least 20-30% of Cellic cTec2 remains bound to the final residue, even after the hydrolysis process (thus making the recovery of that enzyme more challenging) [100], so the presented thesis may be valid. The binding between enzymes and residue are unproductive and can also result in the enzyme's inactivation [61,71]. Accordingly, that could explain the decrease of retained activity at 24 hours from the first (21%) to the second (3%) round, with no apparent protein leach between the two cycles. The same can be applied to the other leached protein values that round zero, namely after the 1st CAS 2 cycle and 2nd CAS 1 and 3 cycle. The general theory of enzyme inactivation during the saccharification process of lignocellulosic biomass attributes this inactivation to the presence of lignin in the biomass, which would not exist in this assay with pure cellulose. However, there is a study that reports cellulase deactivation in both biomass and pure cellulose, suggesting that the deactivation is induced by cellulose itself and not lignin [72], which would be applicable in the case.

Compared to the literature, the obtained results are promising: In 2018 [105] cellulase immobilized onto mNPs by glutaraldehyde achieved 45.32% immobilization efficiency and 48% retained activity after 13 cycles. Even though CAS 1 and 3 both show lower immobilization activities (33.55% for CAS 1 and 20.23% in CAS 3), the retained activity of CAS 3 after 1 cycle (48%) is congruent with those results. It should be pointed out, however, that the saccharification times used during this thesis was of 3 days, while this article does not mention the duration of the assays. Therefore, it does not necessarily mean less reusability on the part of CAS 3, versus the mentioned complex. Additionally, in the described article, the quantification method was miller assay, which estimates the presence of general reducing sugars, and not specifically glucose yield, as it was used in this thesis. Therefore, the results of the article are most likely over-estimating the activity of the enzyme, as it considers multiple oligomers, and the HPLC quantification is specific for complete hydrolysis into monomers.

Additionally, comparing the results obtained by CAS 3 with those reported in the article used as a reference for this protocol, it was reported a maximum of around 80% retained activity, while the produced CAS 3 only achieved 49%, and retained more than 90% activity up to 4 cycles of 30 minutes. However, since the saccharification process of this thesis is harsher (3 consecutive days versus 30 minutes cycles), the obtained results are considered very satisfactory, especially when comparing with

the other protocols for cellulase immobilization, as it has the best results for the second round of saccharification, retaining 12% of activity after 24h and a lower activity at 72h and no detected leaching, pointing to a successful immobilization. Thus, it was considered that during the first saccharification round of CAS 3 there was high leaching of protein that resulted in the abnormally high retained activity, when comparing with the other cellulose immobilizations. However, that leaching was of weaker bonds between the matrix and protein, like adsorption and ionic bonds that were strong enough to endure the washing process but too weak to withstand the saccharification conditions. On the second round, only the covalently bond proteins remained, and those did not leach during the second round since they are robustly bound to the matrix.

Ultimately, CAS 3 was deemed the best base protocol and the most promising CAS to optimize to adapt to the conditions of saccharification tested through this thesis. Thus, its stability after 1 month was analyzed**,** presenting a protein leaching of 36.98% after 1 month of storage. Therefore, its storage stability is not the best, when comparing with other immobilization complexes already developed. However, even though this is a very high leaching value that points to a lack of stability of the complex, that high leaching may have been induced by the loss of integrity of the matrix after the 2$^{nd}$ round: with the loss of integrity of the matrix, its ability to connect to the enzymes may have been lost, leading to separation of the protein from the now-damaged matrix, over time.

## 6.4. HM (Hemicellulase immobilized onto chitosan microparticles) batches

This section of the work started by replicating the optimized version of this immobilization performed in previous work in this lab [141], resulting in batch HM 1 – **Table 6.14**.

The parameters used were optimized by João Patrício [141] and, according to his characterization of the microparticles that were produced under what was determined by him as the best set of parameters (described as “standard” and corresponding to a polymer flow of 3.5 mL/h, an airflow of 3.0 L/min airflow and a distance of 12.5 cm from the tip of the bead generator and the surface of the NaOH solution), these microparticles have regular shapes and an average size of 910 ± 88 µm. However, some of the obtained microparticles were not regularly shaped. Thus, it is suggested that the height distance be lowered, not only to avoid the “oval” shape that was detected in some of the microparticles but also to facilitate the production phase, where it was difficult to ensure that the polymer mix would drop into the NaOH solution and not around it, on the table, due to slight air currents that are unavoidable.

During the enzymatic immobilization process, it was noticed a slight darkening of the complex from the white matrix of chitosan after that matrix was produced to a slight yellow after the enzymatic immobilization – **Figure 6.7**.

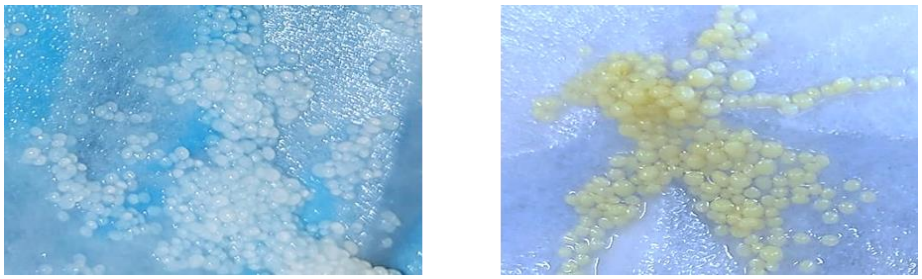

Figure 6.7: Color change caused by enzyme immobilization – Chitosan microparticles before (left) and after (right) enzyme immobilization.

Through the deacetylation process of chitosan production from chitin, the degree of acetylation decreases from around 82% (in chitin) to around 20% (in chitosan), and chitosan becomes soluble in aqueous acidic conditions (bellow at least 6.5 pH) due to the protonable amino groups in the deacetylated units [70,142,144]. Therefore, if chitosan is water-soluble in acidic conditions and the saccharification is done at pH around 5, then in CMPs the glutaraldehyde is essential not only to perform the crosslinking between the matrix and the protein but also for crosslinking the chitosan matrix itself by binding amino groups in the deacetylated units. Thus, this crosslinking of the matrix can explain the slight color change that derives from the immobilization.

However, the most noticeable problem with HM 1 was that the complex gained a brownish-orange coloration during the saccharification process. The color exchange was a lot more dramatic with the elapse of time after the saccharification process, turning completely dark after 72 hours – **Figure 6.8**.

Figure 6.8: Color change caused by glutaraldehyde polymerization – Immobilization complex HM 1 after 72 hours of saccharification at 50 ºC.

However, since the color can be an indicator of the polymerization degree, brownish color is indicative that glutaraldehyde polymerization has occurred [206]. It is probable that this was due to the high temperature achieved during saccharification, as that process occurs at 50 ºC, and it is established that the high degree of polymerization that is achieved after 7 weeks at 30 ºC is obtained in 48 hours when at 50 ºC [209] and thus the conditions during the saccharification reaction are stimulating glutaraldehyde polymerization, and that process is responsible for that change of color.

Thus, assuming that there was excessive glutaraldehyde in the reaction of HM 1, the percentage was lowered from a 4 to 2% glutaraldehyde solution during the first step of the immobilization to produce batch HM 2 – **Table 6.14**.

Additionally, a smaller problem found in HM 1 was that due to the large volume used during the immobilization process, an accurate measurement of the protein in the solution for quantification of the immobilization efficiency was not possible, as the error limit was 23%: Since Bradford's assay detection limit is 20 µg/mL [190], the added 0.125 mL of Viscozyme L, with a predetermined protein content of 20.57 mg/mL, would make up approximately 2.57 mg of protein in a total volume of 30 mL. That results in a concentration of 85.71 µg/mL, the 20 µg/mL that would not be determined due to the method's sensitivity would correspond to (20/85.71) * 100 ≈ 23%.

Therefore, the enzyme quantity was increased from 125 µL, equivalent to 2.57 mg, to 150 µL, equivalent to 3 mg, and the volume of enzyme immobilization was decreased from 30 to 15 mL to lower the error limit from 23 to a possible (20/200) * 100 = 10%. Additionally, to avoid waste of reagents on the first step, the volume used for the activation of the microparticles with glutaraldehyde was reduced from 100 to 50 mL.

Table 6.14: Comparison of the overall results of HM 1 and 2 to determine the influence of lowering the glutaraldehyde percentage during the matrix activation with glutaraldehyde.

| Batch | Protein/CMPs ratio (w/w) | Glutaraldehyde | Immobilization efficiency | Retained activity 1st use, 24 h | Retained activity 1st use, 72 h | Protein leaching 1st use, 72 h |
|---|---|---|---|---|---|---|
| HM 1 | 2.57 mg protein / 200 mg CMPs | 4% | 77 – 100% | 72.1% | 67.7% | 28.28% |
| HM 2 | 3 mg protein / 200 mg CMPs | 2% | 67% | 133.1% | 101.8% | 0% |

Since the 100% immobilization efficiency was inferred from a 0 mg quantification of protein in the solution, with the 23% error limit, the real immobilization efficiency value for HM 1 could be anything from 77 % to 100%. If that is the case, in the worst-case scenario, then we can only assure a minimum of 2.57 mg * 0.77 = 1.98 mg of protein immobilized onto 200 mg of microparticles. On the other hand, in HM 2, from the added 3 mg, only 67 % of immobilization efficiency was achieved. And, in that case, 3 mg * 0.67 = 2 mg of enzyme immobilized onto 200 mg of microparticles. With this in mind, it can be inferred that Viscozyme L achieves the maximum limit of immobilization at a specific ratio of 1:100.

Additionally, the lowering of the glutaraldehyde percentage from 4 to 2% (v/v) seemed to be efficient in lowering the degree of glutaraldehyde polymerization during the saccharification process, as the color change of HM 2 is less pronounced – **Figure 6.9**.

Figure 6.9: No color change that would indicate glutaraldehyde polymerization – Immobilization complex HM 2 after 72 hours of saccharification at 50ºC.

Another interesting result is that with less glutaraldehyde, the enzymes appear to be immobilized in a more stable way, as there is no detected leaching in HM 2 after one use, while HM 1 had leaching of 28.3% under the same conditions. This is probably due to the formation of fewer CLEAs (Crosslinked Enzyme Aggregates), which by not being linked to the retrieved support, are not recycled along with the rest of the immobilized protein. This CLEAs' formation is undesirable, as not only do the involved enzymes lose flexibility due to inter and intra protein crosslinking, thus hindering their activity, but they are also irretrievable as well. To avoid the formation of CLEAs, the activation step with glutaraldehyde and the protein addition is already done separately. However, since glutaraldehyde is a homobifunctional crosslinker with a high affinity to the same functional group either on the mNP or the enzyme, it can always detach itself from the mNP to bind to the functional group of an enzyme, leading to CLEAs anyway. Additionally, the immobilization complex was washed after both steps with 50 mM sodium acetate buffer, pH 5.5 buffer, 1M NaCl, and ethylene glycol (30% v/v in water) to remove unbounded, ionically, and hydrophobically bounded glutaraldehyde and enzymes [210].

The retained activity in HM 1 is a very good result and is in good agreement with some of the literature. In 2018 [105], xylanase immobilized onto mNPs by glutaraldehyde retained 69% of activity. However, it should be noted that, in that assay, only xylanase was used, while HM is based on an enzymatic solution with multiple enzymes, one of which is xylanase. Since the substrate used was xylan, that is the most important one to consider. Another more similar complex was made [115] by immobilizing xylanase onto chitosan microparticles using glutaraldehyde as a crosslinker and retaining 54.2% of its activity. So, overall, HM 1 presents a very high activity and is a promising protocol, even though it was high leaching. This leaching problem may have been solved in HM 2; however, the second round of saccharification should be performed to confirm this supposition.

Regarding the activity results obtained for HM 2 of yields over 100%, it can be pointed out that in some cases, the immobilization can improve the enzymatic activity versus the free version of the enzyme. This is usually by immobilizing the enzyme in "hyperactive" states or by protecting the enzyme from deleterious effects that derive from aggressive reaction media [182]. Since the reaction is at 50 ºC and acidic pH, both those cases are a possible justification for this activity improvement. However, since this was not the case in HM 1, it also must be considered the possibility of some kind of mistake during the quantification process. However, it can be assured that the samples of free and immobilized enzyme were not switched, as even though that would explain the apparent yield over 100%, the values for 0 h of a free enzyme reveal the presence of stabilizing sugars and the 0 h of the immobilized enzyme does not. That means that the sample labelled as free was indeed the free sample, as it accuses the presence of stabilizing sugars that would only be found there and not in the immobilized sample. Thus, it is suspected that, since the HPLC samples were defrosted, diluted 1:10, and the quantification ran overnight, that dilution may have affected the efficiency of the sodium azide, and the results from the free enzyme may have been compromised by microorganisms.

Regardless, it appears that for the immobilization of hemicellulase, the best protocol so far was HM 2. However, a 2$^{nd}$ cycle was not performed due to the very low mass that remained after the saccharification. Thus, to guarantee the superiority of this complex, it must be reproduced in larger quantities and re-tested in multiple saccharification cycles.

## 6.1. Cellulase immobilized onto chitosan microparticles with magnetic cores (CMm)

This complex was tested to better protect the SPIONs from degradation, considering the observed loss of integrity in APTES-coated SPIONs, described in **chapter 6.3**. For that purpose, it was tested the coating of the matrix by chitosan, which results in a more robust coating than DMSA and APTES, as it consists of a sturdy polymer shell instead of superficial molecules. Thus, the immobilization complex retains its magnetic property, allowing for its separation of the solution and remaining unhydrolyzed substrate, but it has more robust protection by the outer layer of chitosan.

The protocol followed was the same as for the immobilization HM 2 – as it was the most successful immobilization complex obtained of enzyme onto chitosan – described in **chapter 6.4**. Thus, the protocol of CMm had the slight adjustment that freshly synthesized SPIONs were added to the polymer mix before being set up in the coaxial airflow dripping bead generator system, and the immobilized enzyme was cellulase instead of hemicellulase. The results of CMm are summarized in **Table 6.15**.

However, it was noted that the SPIONs' addition bestowed to the polymer mix a slightly higher viscosity. Thus, although the magnetic microparticles were produced under the same conditions and parameters as the non-magnetic microparticles, the magnetic ones resulted, on average, in smaller microparticles than the non-magnetic counterpart – **Figure 6.10**.

Figure 6.10: CMPs with magnetic cores (left) and the standard non-magnetic CMPs (right). Both batches were produced on the same day and following the same parameters. Due to the increased viscosity that resulted from the addition of SPIONs to the polymer mix, the size of the magnetic CMPs is, on average, visibly smaller.

Table 6.15: Summary of the results obtained after 1 round of saccharification with CMm.

| Batch | Protein/mCMPs ratio (w/ww) | Immobilization efficiency | Protein/mNP approximate final ratio | Retained activity 1st use, 24 h | Retained activity 1st use, 72 h | Protein leaching 1st use, 72 h |
|---|---|---|---|---|---|---|
| CMm | 1:10 | 59.94% | 0.06 : 1 | 84.88% | 71.83% | 15.64% |

The coating of SPIONs with chitosan is not new and is a clever way of developing a more stable and robust matrix without losing its magnetic properties, which are so useful for retrieval [127].

In 2017/2018 [127,211], cellulase was covalently immobilized onto chitosan-coated magnetic nanoparticles using glutaraldehyde as a crosslinker, and just like in this thesis, the average diameter of magnetic nanoparticles was about 8 nm before coating. That complex had an immobilization efficiency of 67%, while CMm only immobilized 60% of the protein. However, the reported complex retained about 37% of its activity, while CMm was able to retain 85% of its activity and presented leaching of 20% after 15 cycles of 4 hours, while CMm presented leaching of 16% after 1 cycle of 72 hours. Thus, in comparison, CMm achieved a very high retained activity and, even though it still has some significant leaching, overall is a better value, as 16% after 72 hours is lower than 20% after 4*15=60 hours.

This is by far the more promising complex obtained. It only needs some optimization by increasing the crosslinking level, maybe by adding a second step of glutaraldehyde like it was explored in CDS-g 1 to 3 since it was determined in HM that the increase of glutaraldehyde in the first crosslinking step only leads to glutaraldehyde polymerization and the browning of the chitosan microparticles.

Additionally, since the protocol is essentially the same as HM 2, it is interesting to compare the results of both and see the influence of the enzyme used – **Table 6.16**.

Table 6.16: Comparison of the results of the 1st saccharification of CMm and HM 2.

| Batch | Retained activity 1st use, 24 h | Retained activity 1st use, 72 h | Protein leaching 1st use, 72 h |
|---|---|---|---|
| CMm | 84.88% | 71.83% | 15.64% |
| HM 2 | 133.1% | 101.8% | 0% |

With these results, it is confirmed that the immobilization of cellulase is more challenging than hemicellulase, since the same immobilization protocol onto chitosan microparticles (even though CMm had magnetic cores and HM did not) resulted in higher activity and better stability in hemicellulase, while cellulase had lower activity and substantially more protein leaching under the same conditions.

## 6.2. Comparison of the best immobilization methods developed for cellulase

From all the complexes developed (CDS, including CDS-g, CAS and CMm), the best of each group were selected to be compare in order to determine the best protocol for the immobilization of cellulase.

This analysis was made based on the results from the 1st saccharification cycle – **Table 6.17** – and, when possible, the 2nd cycle – **Table 6.18** – as well as the long-term stability of storage – **Table 6.19**.

Table 6.17: Results of 1st cycle utilization of the top protocols of each group.

| Batch | Retained activity 1st use, 24 h | Retained activity 1st use, 72 h | Protein leaching 1st use, 72 h |
|---|---|---|---|
| CDS 6 | 41.36% | 20.72% | 29.57±0.07% |
| CDS-g 0 | 25.37% | 17.48% | 19.80% |
| CDS-g 1 | 15.88% | 9.36% | 19.46% |
| CAS 3 | 47.99% | 49.31% | 35.68 ± 3.78% |
| CMm | 84.88% | 71.83% | 15.64% |

The most promising immobilization method developed for the immobilization of cellulase so far was determined as CMm, as it retains the most activity after 24 hours (while ensuring a lower activity at 72h) and the lowest leaching after the saccharification is completed. However, a 2nd cycle was not performed due to the very low mass that remained after the saccharification. Thus, to guarantee the superiority of this complex, it must be reproduced in a larger quantity and tested through a 2nd cycle.

So, the results of the complexes that were tested on a 2nd cycle are shown in **Table 6.18.**

Table 6.18: Results of 2nd cycle utilization of the top protocols of each group.

| Batch | Retained activity 2nd use, 24 h | Retained activity 2nd use, 72 h | Protein leaching 2nd use, 72 h |
|---|---|---|---|
| CDS 6 | - | - | - |
| CDS-g 0 | 1.5% | 1.6% | 4.14% |
| CDS-g 1 | 1.4% | 3.0% | 3.52% |
| CAS 3 | 12.03% | 11.77% | 0% |
| CMm | - | - | - |

Surprisingly, from the complexes that were indeed tested a 2nd round, the most promising one appears to be CAS 3. These results reinforce the importance of the 2nd round of saccharification to evaluate the best option properly, as CAS 3 appeared to be the worst protocol for cellulase immobilization due to its

very high leaching after the 1st round, where the retained activity at 72 h was higher than 24 h and, thus, pointed to the conclusion that the high retained activity of 48% at 24 h was due to the enzyme becoming free from the support and regain its free activity. However, during the 2nd cycle, CAS 3 stood out by having both a higher retained activity and lower leaching than the remainder of the tested complexes. However, it should be noted that the CDS-g 0 and CDS-g 1 complexes were maintained in the fridge for 3 months before being submitted to a 2nd cycle (due to the COVID quarantine), so the activity results are possibly hindered by that.

Finally, the storage stability was also tested – **Table 6.19**. The stability of CMm after 1 month was not analyzed since it was not possible to go to the lab in either 1 month or 4 months' time frame.

Table 6.19: Storage stability of the top protocols of each group.

| **Batch** | **Protein leaching** **1-month storage** | **Protein leaching** **4-month storage** |
|---|---|---|
| CDS 6 | 18.56% | - |
| CDS-g 0 | 13.73% | 5.39% |
| CDS-g 1 | 0% | 1.88% |
| CAS 3 | 36.98% | - |
| CMm | - | - |

Also, from a stability point of view, it should be pointed out that the matrix maintained its integrity after the 2nd round in both CDS-g and CMm, while in the CAS group, all the complexes lost their integrity, either after the 1st (CAS 2) or 2nd (CAS 1 and 3) cycle. Therefore, it is assumed that APTES coating is more prone to allow the disintegration of the SPIONs' matrix and, thus, not the best option for immobilization. Thus, the high leaching of CAS 3 after 1 month is not surprising, since if the matrix lost its integrity, it is normal that the protein became free from it with time.

Ultimately, it is determined that the best protocol for the immobilization of cellulase are CDS-g 0 and CMm and, to determine which is the absolute best, both require reproduction and re-testing in multiple saccharification cycles. However, CDS-g 1 is also a good option and should also be re-tested to ensure that the reduction of leaching caused by glutaraldehyde was indeed not enough to make up for the activity. Maybe after a few consecutive rounds, the durability is good enough to justify the addition of the second crosslinking step.

# 7. Conclusions

This work started with the characterization of the available commercial enzyme solutions available. The quantification of the protein content was determined by both Lowry and Bradford methods, using BSA as standard. It was noted a high discrepancy between the results determined by Lowry and Bradford assays, with the values obtained by Lowry slightly over twice as much as the results obtained by Bradford. However, when comparing the same method within the available literature, the values of each method seem to be in good agreement. Thus, it is believed that this variation in results can be justified by the difference in the two methods of analysis. It has been reported that the Bradford assay using BSA as standard tends to underestimate the protein content due to the high response of the standard to the assay [164,165,190], especially in proteins with low content of arginine [162]. On the other hand, the Lowry assay tends to overestimate the protein content due to the stabilizing sugars' interference [163,165,190]. Thus, it can only be expected that the real value lies somewhere in between. However, all the calculations in this work were made according to the values obtained using the Bradford method to ensure that the sugars, either used as additives in the enzyme solution or produced during the saccharification, did not interfere with the protein content determinations.

Therefore, as determined by the Bradford assay using BSA as standard, the protein content of the commercial enzymatic solutions available was 54.8 mg/mL for CelluClast 1.5L, making up for 5% of the overall composition of the solution, 99.1 mg/mL for Cellic cTec2, corresponding to 9% of the solution, and 20.6 mg/mL for Viscozyme L, which accounts for 2% of the solutions' composition.

Carbohydrates are usually added to protein solutions to act as stabilizing agents [183], so the quantification of these constituents was also done by HPLC. For the cellulases, CClast, and cTec 2, only the glucose content was analyzed. This is due to the homogeneous nature of cellulose, where glucose is the only stabilizing sugar monomer potentially interfering with the results. The characterization revealed that CClast had a 1% glucose content and cTec2 28% glucose content. However, other sugars can be used as stabilizing agents. Thus, even though the concentration of stabilizing glucose is low in CelluClast 1.5L, it does not necessarily mean that that enzymatic solution has fewer stabilizing agents in solution. For the hemicellulase Viscozyme L, the content of multiple carbohydrates was determined by HPLC, due to the complex heterogeneous composition of hemicellulosic biomass and, therefore, the possibility of multiple sugars interfering with the assay's results. It was determined a total constitution of 32% carbohydrate monomers, composed of 16% fructose, 14% glucose, 1% xylose, and 1% galactose.

By the FPA, the total activity of the enzymatic solutions was determined, resulting in 51 units/mL in Cclast and 137 units/mL in cTec2, which is in good agreement with the available literature (despite its wide range). The pronounced difference between CClast and cTec2 was not unexpected since cTec2 has a much higher protein concentration. Additionally, the higher activity of cTec2 may also be explained by the fact that CClast consists solely of endoglucanase (3.2.1.4), while Cellic cTec2 is an enzyme blend. This can have a great influence, as the cellulase action is considered synergetic, causing higher conversion yields through the simultaneous action of the three classes of cellulase (as cTec2) than from a single class (as CClast) [64].

When submitted to the same conditions using xylan as substrate, Viscozyme L hemicellulase had a very low activity of 2 unit/mL, compared to the 51 units/mL of Celluclast 1.5L and 137 units/mL of cellic cTec2. Lower activity was expected due to the low percentage of only 2% of the solution being identified as protein (while CClast had 5% and cTec 9%), but not as low since Viscozyme L is reported to be a multi-enzyme complex containing a wide range of carbohydrases, including specifically xylanase (8). Based on the literature, it was deemed that maybe arabinogalactan would be a better substrate, as it was reported that Viscozyme L had a very high yield in the saccharification of polymers into galactose and an average yield into arabinose. However, after the same assay using arabinogalactan, it was determined that Viscozyme had an activity of 0.4 unit/mL. So, contrarily to the reported results, it was determined that Viscozyme L was more adequate for the depolymerization of xylan into xylose monomers than the saccharification of arabinogalactan into its respective monomers.

Saccharification assays were run for the individual cellulase solutions and a mix of both at a total of 60 FPU/g of the substrate. After 72 h the values seemed to stabilize, suggesting maximum conversion under those conditions, setting 72 h as the standard time period for all the saccharification cycles performed in this thesis. The maximum substrate conversion achieved was 80.9±5.2% using cTec2,

followed by the 50-50 mix of cTec2 and CClast with 77.5±2.8%, whereas CClast alone achieved a maximum substrate conversion of 54.7±1.5%. It is not unexpected that the maximum conversions never reached 100%, as the system is a SHF, and thus it is natural that complete hydrolysis is never achieved due to the effect of end-product inhibition of the enzymes [50,51].

Finally, the solutions' cost was analysed, and cTec2 was determined to be not only cheaper per mL, but since it also exhibits more than twice the activity of CClast, it resulted in roughly half the overall cost and was therefore determined as the best cellulosic solution.

After the selection of cTec2 over CClast, the enzyme was tested in the saccharification of the pretreated biomass for which it is intended. That biomass is originated from the SBW treatment of RWGP and composed of lignin and cellulose, so its saccharification (in glucose yield) is based on the approximate theoretical cellulose present, which is estimated to be around 33% of the total pretreated biomass. It was determined that using cTec2, around 35% of the total cellulose content was converted into glucose. This value corresponds to 70% yield in pure cellulose, corroborating the notion that the lignocellulosic structure hinders the enzyme activity, even after pretreatment, by hindering the enzyme's access to the substrate and by unproductive binding of the cellulase to lignin.

The enzyme loading of cTec2 for enzymatic saccharification was also studied, both in pure cellulose and pretreated RWPG, to test the dosage of 60 FPU/g of substrate indicated in the protocol used as a reference [16]. It was determined that for biomass, the indicated dosage of 60 FPU/g corresponded to 4.4% (w/w) solids and, even though it was under the standard 5-8% (w/w) guideline for general lignocellulosic biomass saccharification [56], it is around the recommended dosage of cTec2 for mid cellulose content biomass of 3% (w/w) solids [25]. Thus, due to the high content of lignin on the pretreated RWGP (67% lignin and 33% cellulose), this dosage of 60 FPU/g was deemed adequate. On the other hand, for pure cellulose, the recommended value of 60 FPU/g of the substrate, equivalent to 4.5% (w/w) solids, as well as twice and three times that dosage, were tested. From there, it was concluded that the best enzyme loading for cTec2 was 9% (w/w) solids, equivalent to 120 FPU/g, and twice the recommended dose in the reference protocol.

From all the complexes developed to immobilize cellulase, the CAS protocols were deemed less promising due to the loss of integrity of the matrix, either after one (CAS 2) or two (CAS 1 and 3) uses. Ultimately, it was concluded that the best protocols developed for the immobilization of cellulase are CDS-g 0 and CMm, and, in order to determine which is the absolute best, both require reproduction and re-testing in multiple saccharification cycles. However, CDS-g 1 is also a good option and should also be re-tested to ensure that the reduction in leaching caused by glutaraldehyde was indeed not enough to make up for its lower retained activity, as the data may have been compromised by the time that the complex spent in the fridge. Maybe after a few consecutive rounds, the durability is good enough to justify the addition of the second crosslinking step.

The same is applicable to the immobilization of hemicellulase: It appears that the best protocol so far was HM 2. However, it must be reproduced in larger quantities, and the complexes obtained must be re-tested in multiple saccharification cycles.

# 8. Future perspectives

## 8.1. Near future

In order to improve the shape of the chitosan microparticles, it is suggested that the distance between the tip of the bead generator and the NaOH solution be around 7-8 cm. That would avoid the "oval" shape that was detected in some of the microparticles and, additionally, it would facilitate the production phase by ensuring that the droplets of polymer mix would drop onto the NaOH solution and not the surface of the table due to some air currents hard to control in the lab setting.

For the immobilization of cellulase, the best results for the 1st saccharification round are by far those obtained with CMm, which achieved a very high retained activity and, even though it still had some significant leaching. This complex may be further optimized with the goal of increasing the crosslinking level (to lower the leaching percentage). It is recommended that the optimization of CMm is done by adding a second step of glutaraldehyde crosslinking like it was explored in CDS-g 1 to 3 since it was determined in HM that the increase of glutaraldehyde in the first crosslinking step only leads to glutaraldehyde polymerization and the browning of the chitosan microparticles. However, as it was proven by CAS 3, it is essential to test more than 1 round to ensure the quality of a given enzymatic complex. Keeping this in mind, the best protocol for the immobilization of cellulase could be either CDS-g 0 or CMm. To determine which is the absolute best, both immobilization protocols must be reproduced, and the resulting complexes tested in multiple saccharification cycles.

It should be noted that CDS-g 1 is also a good option and should be re-tested to ensure that the reduction in leaching caused by glutaraldehyde was indeed not enough to make up for the loss of activity induced by the decrease of flexibility that derives from the 2nd immobilization step with glutaraldehyde. It is possible that after a few consecutive rounds (more than the 2 rounds tested during this work) the stability of this complex is good enough to justify the addition of the second crosslinking step.

Since due to the COVID-19 quarantine it was not possible to run a 2nd round on batch CDS 6, this batch should be produced again, as the comparison of the quality of the 2nd round against CDS-g 0 could be the determinant factor to decide which of the crosslinking ratios is most beneficial, whether 3:1 used in CDS 6, or 1:2 used in CDS-g 0. Additionally, the level of confidence inspired by the data from the 2nd round of saccharification with CDS-g 0 and 1 can be questioned, since due to the time that these batches remained in the fridge during the COVID-19 quarantine, those complexes may have had their integrity compromised. Therefore, it is also recommended the re-testing of CDS-g 0 and 1 to ensure that the data collected is correct.

The same is applicable to the immobilization of hemicellulase: It appears that the best protocol so far was HM 2. However, a 2nd cycle was not performed, and so to guarantee the superiority of this complex, it must be reproduced in higher quantities and re-tested in multiple saccharification cycles.

Additionally, for the immobilization of hemicellulase it could be interesting to use DAS instead of glutaraldehyde, since according to the literature [27], the complex using DAS has higher stability, as well as an increase in retained activity of 54.2 to 60.8%, than its glutaraldehyde counterpart.

## 8.2. Down the road

To improve the complexes' activity, the best immobilization protocol could be re-produced, this time setting the temperature during the overnight immobilization to 4 ºC, like it was already tested in some literature protocols [82]. In theory, that would avoid protein degradation during the overnight period of the immobilization, as proteins should be kept at 4 ºC, and in this work, the overnight step was performed at room temperature.

After achieving an optimized enzymatic immobilization, assays should be done in SSF since the lower efficiency in SHF can possibly be explained by an effect of enzyme inhibition by end-product, having a negative impact on the overall process. This is avoided with an SSF approach since in the SSF process, the glucose molecules are readily consumed by the fermentative organisms [50]. However, if the mismatch between the optimal conditions of the immobilized enzymes and the fermentative microorganisms result in sub-optimal results, another alternative can also be tested in SHF: an alternative

immobilization, achieved by supplementing the commercial enzyme solution with extra beta-glucosidase, which can sometimes overcome the end-product inhibition that results from SHF [50].

Another way to enhance the economic viability of the enzymatic hydrolysis of lignocellulosic biomass can be to reduce the enzyme loading, achieved by enhancing the efficiency of the process. To that end, the most studied approach is resorting to low-cost additives during the saccharification process [85]. Thus, it can also be tested the addition of BSA [78] or other inexpensive proteins, like soy protein [85], to the saccharification process. These work as surfactants, the general theory being that the surfactants bind to lignin, and therefore reduce the chance of binding between cellulases and lignin, as these bonds are unproductive and can also result in the enzyme's inactivation [85,86]. However, there is a study where it was shown that the surfactant PEG 4000 prevents cellulase deactivation in both biomass and pure cellulose, suggesting that the deactivation is induced by cellulose itself and not lignin [87]. Either way, in a 2014 study [78] the addition of BSA to the saccharification process resulted in a glucose yield increase from 54 to 68% when using free Cellic cTec2, and from 21 to 30% when using immobilized cTec2. Thus, it might be advantageous to study this option in the future.

Finally, for the optimization of the enzymatic saccharification of the lignocellulosic substrate, there is information that points out that the optimal pH range for a more stable and higher efficiency reaction is different than that for pure cellulose, used as standard. That study [43] was performed using both CelluClast 1.5L and Cellic cTec2, just like in this thesis. It recommends that for both solutions, when using lignocellulosic biomass instead of pure cellulose, higher pH conditions be used than the 4.8 to 5 pH, usually suggested by the manufacturers and used in almost all the available literature. More specifically, it recommends a pH between 5.2 to 5.7 when using CelluClast 1.5L, and a surprisingly high pH of 5.5 to 6.2 for Cellic cTec2. Since in this thesis the conditions for both enzymes were pH 5, it can be interesting to test if there is a noticeable increase in saccharification of lignocellulosic biomass with the increase of pH from 5 to 6.

# 9. Webgraphy


1. Global Footprint Network. *Earth Overshoot Day 2019.* [Online] [Cited: 15 Aug 2019.] https://www.overshootday.org/.

2. International Energy Agency. Data and statistics. *CO2 emissions.* [Online] [Cited: 25 Mar 2020.] https://www.iea.org/data-and-statistics?country=WORLD&fuel=CO2%20emissions&indicator=Total%20CO2%20emissions.

3. M. Garside. statista. *Fuel ethanol production worldwide in 2019, by country (in million gallons).* [Online] 26 Feb 2020. [Cited: 4 Apr 2020.] https://www.statista.com/statistics/281606/ethanol-production-in-selected-countries/.

4. FAO (Food and Agriculture Organization of the UN). FAOSTAT. *Crops, grapes, world.* [Online] 2018. [Cited: 20 Apr 2020.] http://www.fao.org/faostat/en/#data/QC/visualize.

5. ExPASy. EC 3.2.1.4. *Cellulase.* [Online] [Cited: 24 Apr 2020.] https://enzyme.expasy.org/EC/3.2.1.4.

6. —. EC 3.2.91. *Cellulose 1,4-beta-cellobiosidase (non-reducing end).* [Online] [Cited: 24 Apr 2020.] https://enzyme.expasy.org/EC/3.2.1.91.

7. —. EC 3.2.1.176. *Cellulose 1,4-beta-cellobiosidase (reducing end).* [Online] [Cited: 24 Apr 2020.] https://enzyme.expasy.org/EC/3.2.1.176.

8. —. EC 3.2.1.21. *Beta-glucosidase.* [Online] [Cited: 24 Apr 2020.] https://enzyme.expasy.org/EC/3.2.1.21.

9. —. EC 3.2.1.8. *Endo-1,4-beta-xylanase.* [Online] [Cited: 27 Jul 2020.] https://enzyme.expasy.org/EC/3.2.1.8.

10. —. EC 3.2.1.37. *Xylan 1,4-beta-xylosidase.* [Online] [Cited: 27 Jun 2020.] https://enzyme.expasy.org/EC/3.2.1.37.

11. (FAO), Food and Agriculture Organization of the UN. FAOSTAT. *Food Supply - Livestock and Fish Primary Equivalent, crustaceans, world, food supply quantity.* [Online] 2013. [Cited: 4 Aug 2020.] http://www.fao.org/faostat/en/?#data/CL.

12. ThermoFisher SCIENTIFIC. Dionex™ AminoTrap Columns. [Online] [Cited: 23 Oct 2020.] https://www.thermofisher.com/order/catalog/product/SP5578?SID=srch-srp-SP5578#/SP5578?SID=srch-srp-SP5578.

13. —. Dionex™ CarboPac™ PA10 IC Columns. [Online] [Cited: 23 Oct 2020.] https://www.thermofisher.com/order/catalog/product/057180#/057180.

14. BASi. Pulsed Amperometric Detection. [Online] [Cited: 23 Oct 2020.] https://www.basinc.com/manuals/LC_epsilon/Operation/PAD/pad.

15. Novozymes. Celluclast® 1.5 L. [Online] [Cited: 13 Sep 2019.] https://new.novozymes.com/food-beverages/juice-fruit-vegetables/vegetables/celluclast-1.5-l.

16. National Center for Biotechnology Education, University of Reading . Enzymes for education. *Carbohydrase mix (Viscozyme).* [Online] [Cited: 12 Feb 2020.] http://www.ncbe.reading.ac.uk/MATERIALS/Enzymes/viscozyme.html#:~:text=The%20optimal%20conditions%20for%20Viscozyme,for%20at%20least%20a%20year..

17. Sigma-Aldrich. Cellulase, enzyme blend. [Online] [Cited: 16 Jan 2020.] https://www.sigmaaldrich.com/catalog/product/sigma/sae0020?lang=pt&region=PT.

18. —. Cellulase from Trichoderma reesei. [Online] [Cited: 16 Jan 2020.] https://www.sigmaaldrich.com/catalog/product/sigma/c2730?lang=pt&region=PT.

19. —. Viscozyme® L. [Online] [Cited: 12 Feb 2020.] https://www.sigmaaldrich.com/catalog/product/sigma/v2010?lang=pt&region=PT.

# 10. Bibliography


[1] IPCC, Summary for Policymakers., in: Clim. Chang. 2013 Phys. Sci. Basis, 2013: pp. 11–12, 19.

[2] J.M. Hall-Spencer, B.P. Harvey, Ocean acidification impacts on coastal ecosystem services due to habitat degradation, Emerg. Top. Life Sci. 3 (2019) 197–206.

[3] M. Mutalipassi, V. Mazzella, V. Zupo, Ocean acidification influences plant-animal interactions: The effect of Cocconeis scutellum parva on the sex reversal of Hippolyte inermis, PLoS One. 14 (2019) 1–14.

[4] L. Al-Ghussain, Global warming: review on driving forces and mitigation, Environ. Prog. Sustain. Energy. 38 (2019) 13–21.

[5] European Commission, EU Climate Action Progress Report 2019, (2019).

[6] G. Coling, Energy, the Environment and Human Health., 2008.

[7] F. Venn, The oil crisis, Routledge, New York, 2013.

[8] J. Sheehan, V. Camobreco, J. Duffield, M. Graboski, H. Shapouri, Life Cycle Inventory of Biodiesel and Petroleum Diesel for Use in an Urban Bus, Nrel/Sr-580-24089. (1998) Medium: ED; Size: vp.

[9] R.E.H. Sims, Bioenergy - A renewable carbon sink, Renew. Energy. 22 (2001) 31–37.

[10] O. Rosales-Calderon, V. Arantes, A review on commercial-scale high-value products that can be produced alongside cellulosic ethanol, BioMed Central, 2019.

[11] A. Demirbas, The importance of bioethanol and biodiesel from biomass, Energy Sources, Part B Econ. Plan. Policy. 3 (2008) 177–185.

[12] M.N. Hossain, M.S.U.S. Bhuyan, A.H.M.A. Alam, Y.C. Seo, Optimization of biodiesel production from waste cooking oil using S–TiO2/SBA-15 heterogeneous acid catalyst, Catalysts. 9 (2019).

[13] P.R. Adler, S.J. Del Grosso, W.J. Parton, Life-cycle assessment of net greenhouse-gas flux for bioenergy cropping systems, Ecol. Appl. 17 (2007) 675–691.

[14] P. Roy, K. Tokuyasu, T. Orikasa, N. Nakamura, T. Shiina, A Review of Life Cycle Assessment (LCA) of Bioethanol from Lignocellulosic Biomass, Japan Agric. Res. Q. 46 (2012) 41–57.

[15] Netherlands Standardization Institute, Overview of specifications and regulations on ( bio ) fuels, Worldw. Fuels Stand. 31 (2006).

[16] P. Adewale, M.J. Dumont, M. Ngadi, Recent trends of biodiesel production from animal fat wastes and associated production techniques, Renew. Sustain. Energy Rev. 45 (2015) 574–588.

[17] C.Y. Yu, L.Y. Huang, I.C. Kuan, S.L. Lee, Optimized production of biodiesel from waste cooking oil by lipase immobilized on magnetic nanoparticles, Int. J. Mol. Sci. 14 (2013) 24074–24086.

[18] S. Puhan, N. Vedaraman, B. V. Rambrahamam, G. Nagarajan, Mahua (Madhuca indica) seed oil: A source of renewable energy in India, J. Sci. Ind. Res. (India). 64 (2005) 890–896.

[19] F. Anwar, U. Rashid, M. Ashraf, M. Nadeem, Okra (Hibiscus esculentus) seed oil for biodiesel production, Appl. Energy. 87 (2010) 779–785.

[20] E. Bertrand, L.P.S. Vandenberghe, C.R. Soccol, J.-C. Sigoillot, C. Faulds, Green Fuels Technology: First Generation Bioethanol, in: Green Energy Technol., 2016: pp. 175–212.

[21] K. Robak, M. Balcerek, Review of second generation bioethanol production from residual biomass, Food Technol. Biotechnol. 56 (2018) 174–187.

[22] S.A. Jambo, R. Abdulla, S.H. Mohd Azhar, H. Marbawi, J.A. Gansau, P. Ravindra, A review on third generation bioethanol feedstock, Renew. Sustain. Energy Rev. 65 (2016) 756–769.

[23] B.C. Saha, Hemicellulose bioconversion, J. Ind. Microbiol. Biotechnol. 30 (2003) 279–291.

[24] N. Qureshi, B.C. Saha, R.E. Hector, B. Dien, S. Hughes, S. Liu, L. Iten, M.J. Bowman, G. Sarath, M.A. Cotta, Production of butanol (a biofuel) from agricultural residues: Part II - Use of corn stover and switchgrass hydrolysates, in: Biomass and Bioenergy, 2010: pp. 566–571.

[25] N. Qureshi, B.C. Saha, M.A. Cotta, V. Singh, An economic evaluation of biological conversion of wheat straw to butanol: A biofuel, Energy Convers. Manag. 65 (2013) 456–462.

[26] M. Salazar-Ordóñez, P.P. Pérez-Hernández, J.M. Martín-Lozano, Sugar beet for bioethanol production: An approach based on environmental agricultural outputs, Energy Policy. 55 (2013) 662–668.

[27] A. Almodares, M.R. Hadi, Production of bioethanol from sweet sorghum: A review, African J. Agric. Res. 4 (2009) 772–780.

[28] A.P. de Souza, A. Grandis, D.C.C. Leite, M.S. Buckeridge, Sugarcane as a Bioenergy Source: History, Performance, and Perspectives for Second-Generation Bioethanol, Bioenergy Res. 7 (2014) 24–35.

[29] J.C. López-Linares, I. Romero, C. Cara, E. Ruiz, M. Moya, E. Castro, Bioethanol production from rapeseed straw at high solids loading with different process configurations, Fuel. 122 (2014) 112–118.

[30] A. Zabaniotou, O. Ioannidou, V. Skoulou, Rapeseed residues utilization for energy and 2nd generation biofuels, Fuel. 87 (2008) 1492–1502.

[31] P. Vaithanomsat, S. Chuichulcherm, W. Apiwatanapiwat, Bioethanol production from enzymatically saccharified sunflower stalks using steam explosion as pretreatment, World Acad. Sci. Eng. Technol. 37 (2009) 140–143.

[32] M. Ioelovich, Waste Paper as Promising Feedstock for Production of Biofuel, J. Sci. Res. Reports. 3 (2014) 905–916.

[33] M.Y. Menetrez, An overview of algae biofuel production and potential environmental impact, Environ. Sci. Technol. 46 (2012) 7073–7085.

[34] G.S. Rathna, R. Saranya, M. Kalaiselvam, Original Research Article Bioethanol from sawdust using cellulase hydrolysis of Aspergillus ochraceus and fermentation by Saccharomyces cerevisiae, Int. J. Curr. Microbiol. Appl. Sci. 3 (2014) 733–742.

[35] P. Reyes, R.T. Mendonça, M.G. Aguayo, J. Rodríguez, B. Vega, P. Fardim, Extração e caracterização de hemiceluloses de pinus radiata e sua viabilidade para a produção de bioetanol, Rev. Arvore. 37 (2013) 175–180.

[36] K. Anne, Development of pretreatment technology and enzymatic hydrolysis for biorefineries, 2014.

[37] S. Haghighi Mood, A. Hossein Golfeshan, M. Tabatabaei, G. Salehi Jouzani, G.H. Najafi, M. Gholami, M. Ardjmand, Lignocellulosic biomass to bioethanol, a comprehensive review with a focus on pretreatment, Renew. Sustain. Energy Rev. 27 (2013) 77–93.

[38] H. Guo, Y. Chang, D.J. Lee, Enzymatic saccharification of lignocellulosic biorefinery: Research focuses, Bioresour. Technol. 252 (2018) 198–215.

[39] J. Alftrén, T.J. Hobley, Immobilization of cellulase mixtures on magnetic particles for hydrolysis of lignocellulose and ease of recycling, Biomass and Bioenergy. 65 (2014) 72–78.

[40] A. Limayem, S.C. Ricke, Lignocellulosic biomass for bioethanol production: Current perspectives, potential issues and future prospects, Prog. Energy Combust. Sci. 38 (2012) 449–467.

[41] J.A. Thomson, Molecular biology of xylan degradation, FEMS Microbiol. Lett. 104 (1993) 65–82.

[42] F.M. Gírio, C. Fonseca, F. Carvalheiro, L.C. Duarte, S. Marques, R. Bogel-Łukasik, Hemicelluloses for fuel ethanol: A review, Bioresour. Technol. 101 (2010) 4775–4800.

[43] V. Mehnati-Najafabadi, A. Taheri-Kafrani, A.K. Bordbar, A. Eidi, Covalent immobilization of xylanase from Thermomyces lanuginosus on aminated superparamagnetic graphene oxide nanocomposite, J. Iran. Chem. Soc. 16 (2019) 21–31.

[44] H. Fraga, I.G. De Cortázar Atauri, A.C. Malheiro, J. Moutinho-Pereira, J.A. Santos, Viticulture in Portugal: A review of recent trends and climate change projections, Oeno One. 51 (2017) 61–69.

[45] K. Dwyer, F. Hosseinian, M. Rod, The Market Potential of Grape Waste Alternatives, J. Food Res. 3 (2014) 91.

[46] IOV, 2019 Statistical Report on World Vitiviniculture, Int. Organ. Vine Wine. (2019) 23.

[47] M.A. Bustamante, R. Moral, C. Paredes, A. Pérez-Espinosa, J. Moreno-Caselles, M.D. Pérez-Murcia, Agrochemical characterisation of the solid by-products and residues from the winery and distillery industry, Waste Manag. 28 (2008) 372–380.

[48] I.S. Arvanitoyannis, D. Ladas, A. Mavromatis, Wine waste treatment methodology, Int. J. Food Sci. Technol. 41 (2006) 1117–1151.

[49] B.M. Pedras, G. Regalin, I. Sá-Nogueira, P. Simões, A. Paiva, S. Barreiros, Fractionation of red wine grape pomace by subcritical water extraction/hydrolysis, J. Supercrit. Fluids. 160 (2020).

[50] Ó.J. Sánchez, C.A. Cardona, Trends in biotechnological production of fuel ethanol from different feedstocks, Bioresour. Technol. 99 (2008) 5270–5295.

[51] R. Liguori, V. Ventorino, O. Pepe, V. Faraco, Bioreactors for lignocellulose conversion into fermentable sugars for production of high added value products, Appl. Microbiol. Biotechnol. 100 (2016) 597–611.

[52] S.S. Toor, L. Rosendahl, A. Rudolf, Hydrothermal liquefaction of biomass: A review of subcritical water technologies, Energy. 36 (2011) 2328–2342.

[53] V.S. Ferreira-Leitão, M.C. Cammarota, E.C.G. Aguieiras, L.R.V. de Sá, R. Fernandez-Lafuente, D.M.G. Freire, The protagonism of biocatalysis in green chemistry and its environmental benefits, Catalysts. 7 (2017) 3, 5.

[54] H. Shokrkar, S. Ebrahimi, M. Zamani, A review of bioreactor technology used for enzymatic hydrolysis of cellulosic materials, Cellulose. 25 (2018) 6279–6304.

[55] M. Ask, K. Olofsson, T. Di Felice, L. Ruohonen, M. Penttilä, G. Lidén, L. Olsson, Challenges in enzymatic hydrolysis and fermentation of pretreated Arundo donax revealed by a comparison between SHF and SSF, Process Biochem. 47 (2012) 1452–1459.

[56] D. Dahnum, S.O. Tasum, E. Triwahyuni, M. Nurdin, H. Abimanyu, Comparison of SHF and SSF processes using enzyme and dry yeast for optimization of bioethanol production from empty fruit bunch, Energy Procedia. 68 (2015) 107–116.

[57] Y. Sudiyani, D. Dahnum, D. Burhani, A.M.H. Putri, Evaluation and comparison between simultaneous saccharification and fermentation and separated hydrolysis and fermentation process, Second Third Gener. Feed. Evol. Biofuels. (2019) 273–290.

[58] S. Sukhang, S. Choojit, T. Reungpeerakul, C. Sangwichien, Bioethanol production from oil palm empty fruit bunch with SSF and SHF processes using Kluyveromyces marxianus yeast, Cellulose. 27 (2020) 301–314.

[59] G. Liu, J. Zhang, J. Bao, Cost evaluation of cellulase enzyme for industrial-scale cellulosic ethanol production based on rigorous Aspen Plus modeling, Bioprocess Biosyst. Eng. 39 (2016) 133–140.

[60] D. Klein-Marcuschamer, P. Oleskowicz-Popiel, B.A. Simmons, H.W. Blanch, The challenge of

enzyme cost in the production of lignocellulosic biofuels, Biotechnol. Bioeng. 109 (2012) 1083–1087.

[61] X. Luo, J. Liu, P. Zheng, M. Li, Y. Zhou, L. Huang, L. Chen, L. Shuai, Promoting enzymatic hydrolysis of lignocellulosic biomass by inexpensive soy protein, Biotechnol. Biofuels. 12 (2019) 1–13.

[62] J. Song, H. Fan, J. Ma, B. Han, Conversion of glucose and cellulose into value-added products in water and ionic liquids, Green Chem. 15 (2013) 2619–2635.

[63] A.K. Chandel, G. Chandrasekhar, M.B. Silva, S. Silvério Da Silva, The realm of cellulases in biorefinery development, Crit. Rev. Biotechnol. 32 (2012) 187–202.

[64] J.S. Van Dyk, B.I. Pletschke, A review of lignocellulose bioconversion using enzymatic hydrolysis and synergistic cooperation between enzymes-Factors affecting enzymes, conversion and synergy, Biotechnol. Adv. 30 (2012) 1458–1480.

[65] X. Li, S.H. Chang, R. Liu, Industrial applications of cellulases and hemicellulases, Fungal Cellulolytic Enzym. Microb. Prod. Appl. (2018) 267–282.

[66] F. Zhang, B. Bunterngsook, J.-X. Li, X.-Q. Zhao, V. Champreda, C.-G. Liu, F.-W. Bai, Regulation and production of lignocellulolytic enzymes from Trichoderma reesei for biofuels production, 1st ed., Elsevier Inc., 2019.

[67] R. Wohlgemuth, Biocatalysis-key to sustainable industrial chemistry, Curr. Opin. Biotechnol. 21 (2010) 713–724.

[68] M. Vert, Y. Doi, K.H. Hellwich, M. Hess, P. Hodge, P. Kubisa, M. Rinaudo, F. Schué, Terminology for biorelated polymers and applications (IUPAC recommendations 2012), Pure Appl. Chem. 84 (2012) 377–410.

[69] R.A. Meryam Sardar, Enzyme Immobilization: An Overview on Nanoparticles as Immobilization Matrix, Biochem. Anal. Biochem. 04 (2015) 1–8.

[70] B. Krajewska, Application of chitin- and chitosan-based materials for enzyme immobilizations: A review, Enzyme Microb. Technol. 35 (2004) 126–139.

[71] T. Eriksson, J. Börjesson, F. Tjerneld, Mechanism of surfactant effect in enzymatic hydrolysis of lignocellulose, Enzyme Microb. Technol. 31 (2002) 353–364.

[72] J. Li, S. Li, C. Fan, Z. Yan, The mechanism of poly(ethylene glycol) 4000 effect on enzymatic hydrolysis of lignocellulose, Colloids Surfaces B Biointerfaces. 89 (2012) 203–210.

[73] S. Datta, L.R. Christena, Y.R.S. Rajaram, Enzyme immobilization: an overview on techniques and support materials, 3 Biotech. 3 (2013) 1–9.

[74] I.R.M. Tébéka, A.G.L. Silva, D.F.S. Petti, Hydrolytic activity of free and immobilized cellulase, Langmuir. 25 (2009) 1582–1587.

[75] T. Tosa, T. Mori, N. Fuse, I. Chibata, Studies on continuous enzyme reactions. I. Screening of carriers for preparation of water-insoluble aminoacylase., Enzymologia. 31 (1966) 214–224.

[76] E.G. Griffin, J.M. Nelson, The Influence of certain substances on the activity of invertase, J. Am. Chem. Soc. 38 (1916) 722–730.

[77] J.M. Nelson, E.G. Griffin, Adsorption of Invertase, J. Am. Chem. Soc. 38 (1916) 1109–1115.

[78] B. Brena, P. González-pombo, F. Batista-viera, Immobilization of Enzymes : A Literature Survey, in: Immobil. Enzym. Cells Third Ed. Methods Mol. Biol., 3rd ed., 2013: pp. 15–31.

[79] P. Kafarski, Rainbow code of biotechnology, Chemik. 66 (2012) 814–816.

[80] M. Coradi, M. Zanetti, A. Valério, D. de Oliveira, A. da Silva, S. Souza, A. Souza, Production of antimicrobial textiles by cotton fabric functionalization and pectinolytic enzyme immobilization, Mater. Chem. Phys. 208 (2018) 28–34.

[81] M.F. Khana, D. Kundua, C. Hazrab, S. Patra, A strategic approach of enzyme engineering by attribute ranking and enzyme immobilization on zinc oxide nanoparticles to attain thermostability in mesophilic Bacillus subtilis lipase for detergent formulation, Int. J. Biol. Macromol. 134 (2019) 66–82.

[82] S. Bhavaniramya, R. Vanajothi, S. Vishnupriya, K. Premkumar, M.S. Al-Aboody, R. Vijayakumar, D. Baskaran, Enzyme Immobilization on Nanomaterials for Biosensor and Biocatalyst in Food and Biomedical Industry, Curr. Pharm. Des. 25 (2019) 2661–2676.

[83] S. Adhikari, N. Pramanik, Application of Immobilized Enzymes in the Food Industry, in: Enzym. Food Biotechnol. Prod. Appl. Futur. Prospect., 2019: pp. 711–721.

[84] O.M. Darwesh, I.A. Matter, M.F. Eida, Development of peroxidase enzyme immobilized magnetic nanoparticles for bioremediation of textile wastewater dye, J. Environ. Chem. Eng. 7 (2018).

[85] B. Ranjan, S. Pillai, K. Permaul, S. Singh, Simultaneous removal of heavy metals and cyanate in a wastewater sample using immobilized cyanate hydratase on magnetic-multiwall carbon nanotubes, J. Hazard. Mater. 363 (2019) 73–80.

[86] M. Rai, A.P. Ingle, R. Pandit, P. Paralikar, J.K. Biswas, S.S. da Silva, Emerging role of nanobiocatalysts in hydrolysis of lignocellulosic biomass leading to sustainable bioethanol production, Catal. Rev. - Sci. Eng. 61 (2019) 1–26.

[87] B. Brena, P. González-Pombo, F. Batista-Viera, Immobilization of enzymes: A literature survey, 2nd ed., 2013.

[88] N.R. Mohamad, N.H.C. Marzuki, N.A. Buang, F. Huyop, R.A. Wahab, An overview of technologies for immobilization of enzymes and surface analysis techniques for immobilized enzymes, Biotechnol. Biotechnol. Equip. 29 (2015) 205–220.

[89] C. Spahn, S. Minteer, Enzyme Immobilization in Biotechnology, Recent Patents Eng. 2 (2008) 195–200.

[90] M.N. Gupta, M. Kaloti, M. Kapoor, K. Solanki, Nanomaterials as matrices for enzyme immobilization, Artif. Cells, Blood Substitutes, Biotechnol. 39 (2011) 98–109.

[91] S.L. Hirsh, M.M.M. Bilek, N.J. Nosworthy, A. Kondyurin, C.G. Dos Remedios, D.R. McKenzie, A Comparison of covalent immobilization and physical adsorption of a cellulase enzyme mixture, Langmuir. 26 (2010) 14380–14388.

[92] C. Lee, A.-N. Au-Duong, Enzyme Immobilization on Nanoparticles : Recent applications, in: Emerg. Areas Bioeng., 2018: pp. 67–80.

[93] A.C. Rodrigues, A.F. Leitão, S. Moreira, C. Felby, M. Gama, Recycling of cellulases in lignocellulosic hydrolysates using alkaline elution, Bioresour. Technol. 110 (2012) 526–533.

[94] F.A. Mostafa, A.A.A. El Aty, M.E. Hassan, G.E.A. Awad, Immobilization of xylanase on modified grafted alginate polyethyleneimine bead based on impact of sodium cation effect, Int. J. Biol. Macromol. 140 (2019) 1284–1295.

[95] H.R. Sørensen, S. Pedersen, A. Viksø-Nielsen, A.S. Meyer, Efficiencies of designed enzyme combinations in releasing arabinose and xylose from wheat arabinoxylan in an industrial ethanol fermentation residue, Enzyme Microb. Technol. 36 (2005) 773–784.

[96] M. Perwez, R. Ahmad, M. Sardar, A reusable multipurpose magnetic nanobiocatalyst for industrial applications, Int. J. Biol. Macromol. 103 (2017) 16–24.

[97] A.B. Muley, A.S. Thorat, R.S. Singhal, K. Harinath Babu, A tri-enzyme co-immobilized magnetic complex: Process details, kinetics, thermodynamics and applications, Int. J. Biol. Macromol. 118 (2018) 1781–1795.

[98] X. Yang, Y. Chen, S. Yao, J. Qian, H. Guo, X. Cai, Preparation of immobilized lipase on magnetic nanoparticles dialdehyde starch, Carbohydr. Polym. 218 (2019) 324–332.

[99] J. Garcia, Y. Zhang, H. Taylor, O. Cespedes, M.E. Webb, D. Zhou, Multilayer enzyme-coupled magnetic nanoparticles as efficient, reusable biocatalysts and biosensors, Nanoscale. 3 (2011) 3721–3730.

[100] A.C. Rodrigues, C. Felby, M. Gama, Cellulase stability, adsorption/desorption profiles and recycling during successive cycles of hydrolysis and fermentation of wheat straw, Bioresour. Technol. 156 (2014) 163–169.

[101] S.P. Schwaminger, P. Fraga-García, F. Selbach, F.G. Hein, E.C. Fuß, R. Surya, H.C. Roth, S.A. Blank-Shim, F.E. Wagner, S. Heissler, S. Berensmeier, Bio-nano interactions: cellulase on iron oxide nanoparticle surfaces, Adsorption. 23 (2017) 281–292.

[102] K. Khoshnevisan, A.K. Bordbar, D. Zare, D. Davoodi, M. Noruzi, M. Barkhi, M. Tabatabaei, Immobilization of cellulase enzyme on superparamagnetic nanoparticles and determination of its activity and stability, Chem. Eng. J. 171 (2011) 669–673.

[103] O. Rosales-Calderon, H.L. Trajano, S.J.B. Duff, Stability of commercial glucanase and β-glucosidase preparations under hydrolysis conditions, PeerJ. 2014 (2014) 3, 4.

[104] M.P. Klein, M.R. Nunes, R.C. Rodrigues, E. V. Benvenutti, T.M.H. Costa, P.F. Hertz, J.L. Ninow, Effect of the support size on the properties of β-galactosidase immobilized on chitosan: Advantages and disadvantages of macro and nanoparticles, Biomacromolecules. 13 (2012) 2456–2464.

[105] A. Kumari, P. Kaila, P. Tiwari, V. Singh, S. Kaul, N. Singhal, P. Guptasarma, Multiple thermostable enzyme hydrolases on magnetic nanoparticles: An immobilized enzyme-mediated approach to saccharification through simultaneous xylanase, cellulase and amylolytic glucanotransferase action, Int. J. Biol. Macromol. 120 (2018) 1650–1658.

[106] K. Liburdi, I. Benucci, F. Palumbo, M. Esti, Lysozyme immobilized on chitosan beads: Kinetic characterization and antimicrobial activity in white wines, Food Control. 63 (2016) 46–52.

[107] E. Biró, A.S. Németh, C. Sisak, T. Feczkó, J. Gyenis, Preparation of chitosan particles suitable for enzyme immobilization., J. Biochem. Biophys. Methods. 70 (2008) 1240–1246.

[108] M.R. Ladole, A.B. Muley, I.D. Patil, M.I. Talib, R. Parate, Immobilization of tropizyme-P on amino-functionalized magnetic nanoparticles for fruit juice clarification, J. Biochem. Technol. 5 (2015) 838–845.

[109] U. V. Sojitra, S.S. Nadar, V.K. Rathod, A magnetic tri-enzyme nanobiocatalyst for fruit juice clarification, Food Chem. 213 (2016) 296–305.

[110] J. Jia, W. Zhang, Z. Yang, X. Yang, N. Wang, X. Yu, Novel Magnetic Cross-Linked Cellulase Aggregates with a Potential Application in Lignocellulosic Biomass Bioconversion, Molecules. (2017).

[111] S. Talekar, A.F. Patti, R. Vijayraghavan, A. Arora, Recyclable enzymatic recovery of pectin and punicalagin rich phenolics from waste pomegranate peels using magnetic nanobiocatalyst, Food Hydrocoll. 89 (2019) 468–480.

[112] R.S. Singh, R.P. Singh, J.F. Kennedy, Immobilization of yeast inulinase on chitosan beads for the hydrolysis of inulin in a batch system, Int. J. Biol. Macromol. 95 (2017) 87–93.

[113] S.M. de Oliveira, S. Moreno-Perez, C.R.F. Terrasan, M. Romero-Fernández, M.F. Vieira, J.M. Guisan, J. Rocha-Martin, Covalent immobilization-stabilization of β-1,4-endoxylanases from Trichoderma reesei: Production of xylooligosaccharides, Process Biochem. 64 (2018) 170–176.

[114] A.S.G. Lorenzoni, L.F. Aydos, M.P. Klein, M.A.Z. Ayub, R.C. Rodrigues, P.F. Hertz, Continuous production of fructooligosaccharides and invert sugar by chitosan immobilized enzymes: Comparison between in fluidized and packed bed reactors, J. Mol. Catal. B Enzym. 111 (2015) 51–55.

[115] H. Chen, L. Liu, S. Lv, X. Liu, M. Wang, A. Song, X. Jia, Immobilization of aspergillus niger

xylanase on chitosan using dialdehyde starch as a coupling agent, Appl. Biochem. Biotechnol. 162 (2010) 24–32.

[116] E. Jackson, S. Correa, L. Betancor, Cellulose-Based Nanosupports for Enzyme Immobilization, 2019.

[117] A.M. El-Nahas, T.A. Salaheldin, T. Zaki, H.H. El-Maghrabi, A.M. Marie, S.M. Morsy, N.K. Allam, Functionalized cellulose-magnetite nanocomposite catalysts for efficient biodiesel production, Chem. Eng. J. 322 (2017) 167–180.

[118] P.R. Coulet, D.C. Gautheron, Enzymes immobilized on collagen membranes: A tool for fundamental research and enzyme engineering, J. Chromatogr. A. 215 (1981) 65–72.

[119] S. Fierro, M. del Pilar Sánchez-Saavedra, C. Copalcúa, Nitrate and phosphate removal by chitosan immobilized Scenedesmus, Bioresour. Technol. 99 (2008) 1274–1279.

[120] C. Ispas, I. Sokolov, S. Andreescu, Enzyme-functionalized mesoporous silica for bioanalytical applications, Anal. Bioanal. Chem. 393 (2009) 543–554.

[121] R.H. Taylor, S.M. Fournier, B.L. Simons, H. Kaplan, M.A. Hefford, Covalent protein immobilization on glass surfaces: Application to alkaline phosphatase, J. Biotechnol. 118 (2005) 265–269.

[122] F. Assa, H. Jafarizadeh-malmiri, H. Ajamein, N. Anarjan, H. Vaghari, Z. Sayyar, A. Berenjian, A biotechnological perspective on the application of iron oxide nanoparticles, Nano Res. 9 (2016) 2203–2225.

[123] M. Vert, Y. Doi, K.H. Hellwich, M. Hess, P. Hodge, P. Kubisa, M. Rinaudo, F. Schué, Terminology for biorelated polymers and applications (IUPAC recommendations 2012), Pure Appl. Chem. 84 (2012) 377–410.

[124] K. Khoshnevisan, E. Poorakbar, H. Baharifar, M. Barkhi, Recent Advances of Cellulase Immobilization onto Magnetic Nanoparticles: An Update Review, Magnetochemistry. 5 (2019) 36.

[125] A.H. Lu, E.L. Salabas, F. Schüth, Magnetic nanoparticles: Synthesis, protection, functionalization, and application, Angew. Chemie - Int. Ed. 46 (2007) 1222–1244.

[126] K. McNamara, S.A.M. Tofail, Nanoparticles in biomedical applications, Adv. Phys. X. 2 (2017) 54–88.

[127] A. Díaz-Hernández, J. Gracida, B.E. García-Almendárez, C. Regalado, R. Núñez, A. Amaro-Reyes, Characterization of Magnetic Nanoparticles Coated with Chitosan: A Potential Approach for Enzyme Immobilization, J. Nanomater. 2018 (2018) 1,2,10.

[128] E. Katz, Magnetic nanoparticles, Wiley-VCH, 2009.

[129] P. I. P. Soares, P. Isabel, P. Soares, Chitosan-based magnetic nanoparticles for osteosarcoma theranostic, Faculdade de Ciências e Tecnologias da Universidade Nova de Lisboa, 2015.

[130] S. Villa, P. Riani, F. Locardi, F. Canepa, Functionalization of Fe3O4 NPs by silanization: Use of amine (APTES) and thiol (MPTMS) silanes and their physical characterization, Materials (Basel). 9 (2016).

[131] L.N. Song, N. Gu, Y. Zhang, A moderate method for preparation DMSA coated Fe3O4 nanoparticles, IOP Conf. Ser. Mater. Sci. Eng. 164 (2017).

[132] A. Ruiz, P.C. Morais, R. Bentes de Azevedo, Z.G.M. Lacava, A. Villanueva, M. del Puerto Morales, Magnetic nanoparticles coated with dimercaptosuccinic acid: development, characterization, and application in biomedicine, J. Nanoparticle Res. 16 (2014).

[133] R.A. Sperling, W.J. Parak, Surface modification, functionalization and bioconjugation of colloidal Inorganic nanoparticles, Philos. Trans. R. Soc. A Math. Phys. Eng. Sci. 368 (2010) 1333–1383.

[134] S.I.C.J. Palma, M. Marciello, A. Carvalho, S. Veintemillas-Verdaguer, M. del P. Morales, A.C.A. Roque, Effects of phase transfer ligands on monodisperse iron oxide magnetic nanoparticles, J. Colloid Interface Sci. 437 (2015) 147–155.

[135] C. Chaparro, Application of hyperthermia for cancer treatment: Synthesis and characterization of magnetic nanoparticles and their internalization on tumor cell lines, FCT/UNL, Dissertation of Master Program in Biotechnology, 2017.

[136] Y. Liu, Y. Li, X.M. Li, T. He, Kinetics of (3-aminopropyl)triethoxylsilane (aptes) silanization of superparamagnetic iron oxide nanoparticles, Langmuir. 29 (2013) 15275–15282.

[137] Thermo Fisher, Crosslinking technology: Reactivity chemistries, applications and structure references, 2012.

[138] Saima, M. Kuddus, Roohi, I.Z. Ahmad, Isolation of novel chitinolytic bacteria and production optimization of extracellular chitinase, J. Genet. Eng. Biotechnol. 11 (2013) 39–46.

[139] I. Hamed, F. Özogul, J.M. Regenstein, Industrial applications of crustacean by-products (chitin, chitosan, and chitooligosaccharides): A review, Trends Food Sci. Technol. 48 (2016) 40–50.

[140] M. Rinaudo, Chitin and chitosan: Properties and applications, Prog. Polym. Sci. 31 (2006) 603–632.

[141] J. Patrício, Immobilization of enzymes on polymeric microparticles, FCT/UNL, Dissertation of Master Program in Material Engineering, 2018.

[142] M.L. Verma, S. Kumar, A. Das, J.S. Randhawa, Enzyme Immobilization on Chitin and Chitosan-Based Supports for Biotechnological Applications, in: Sustain. Agric. Rev. 35, 2019: pp. 147–173.

[143] Y. Xu, M. Bajaj, R. Schneider, S.L. Grage, A.S. Ulrich, J. Winter, C. Gallert, Transformation of the matrix structure of shrimp shells during bacterial deproteination and demineralization, Microb. Cell Fact. 12 (2013) 1–12.

[144] N. Islam, I. Dmour, M.O. Taha, Degradability of chitosan micro/nanoparticles for pulmonary drug delivery, Heliyon. 5 (2019) e01684.

[145] R.C.F. Cheung, T.B. Ng, J.H. Wong, W.Y. Chan, Chitosan: An update on potential biomedical and pharmaceutical applications, Mar. Drugs. 13 (2015) 5156–5186.

[146] O. Hassan, T. Chang, Chitosan for Eco-friendly Control of Plant Disease, Asian J. Plant Pathol. 11 (2017) 53–70.

[147] M. Aider, Chitosan application for active bio-based films production and potential in the food industry: Review, LWT - Food Sci. Technol. 43 (2010) 837–842.

[148] R. Yang, H. Li, M. Huang, H. Yang, A. Li, A review on chitosan-based flocculants and their applications in water treatment, Water Res. 95 (2016) 59–89.

[149] R.A.A. Muzzarelli, G. Barontini, R. Rocchetti, Immobilized enzymes on chitosan columns: α-Chymotrypsin and acid phosphatase, Biotechnol. Bioeng. 18 (1976) 1445–1454.

[150] R.A.A. Muzzarelli, Immobilization of enzymes on chitin and chitosan, Enzym. Microb. Technol. 2 (1980) 177–184.

[151] A.R. Gentili, M.A. Cubitto, M. Ferrero, M.S. Rodriguéz, Bioremediation of crude oil polluted seawater by a hydrocarbon-degrading bacterial strain immobilized on chitin and chitosan flakes, Int. Biodeterior. Biodegrad. 57 (2006) 222–228.

[152] X. Mao, G. Guo, J. Huang, Z. Du, Z. Huang, L. Ma, P. Li, L. Gu, A novel method to prepare chitosan powder and its application in cellulase immobilization, J. Chem. Technol. Biotechnol. 81 (2006) 189–195.

[153] S.D. Gür, N. İdil, N. Aksöz, Optimization of Enzyme Co-Immobilization with Sodium Alginate and Glutaraldehyde-Activated Chitosan Beads, Appl. Biochem. Biotechnol. (2017) 1–15.

[154] J. Wu, M. Luan, J. Zhao, Trypsin immobilization by direct adsorption on metal ion chelated macroporous chitosan-silica gel beads, Int. J. Biol. Macromol. 39 (2006) 185–191.

[155] C.E. Orrego, N. Salgado, J.S. Valencia, G.I. Giraldo, O.H. Giraldo, C.A. Cardona, Novel chitosan membranes as support for lipases immobilization: Characterization aspects, Carbohydr. Polym. 79 (2010) 9–16.

[156] X.J. Huang, D. Ge, Z.K. Xu, Preparation and characterization of stable chitosan nanofibrous membrane for lipase immobilization, Eur. Polym. J. 43 (2007) 3710–3718.

[157] J.R. Lakkakula, T. Matshaya, R.W.M. Krause, Cationic cyclodextrin/alginate chitosan nanoflowers as 5-fluorouracil drug delivery system, Mater. Sci. Eng. C. 70 (2017) 169–177.

[158] T.C. Lin, F.H. Lin, J.C. Lin, In vitro feasibility study of the use of a magnetic electrospun chitosan nanofiber composite for hyperthermia treatment of tumor cells, Acta Biomater. 8 (2012) 2704–2711.

[159] M. Laser, D. Schulman, S.G. Allen, J. Lichwa, M.J. Antal, L.R. Lynd, A comparison of liquid hot water and steam pretreatments of sugar cane bagasse for bioconversion to ethanol, Bioresour. Technol. 81 (2002) 33–44.

[160] O.H. Lowry, N.J. Rosebrought, A.L. Farr, R.J. Randall, Protein measurement with the folin phenol reagent, J. Biol. Chem. 193 (1951) 265–275.

[161] M.M. Bradford, A Rapid and Sensitive Method for the Quantitation of Microgram Quantities of Protein Utilizing the Principle of Protein-Dye Binding, Anal. Biochem. 72 (1976) 248–254.

[162] V. Martina, K. Vojtech, A Comparison of Biuret, Lowry and Bradford Methods for Measuring the Egg's Protein, MendelNet. (2015) 394–398.

[163] J.H. Waterborg, The Lowry Method for Protein Quantitation, in: Protein Protoc. Handb., 3rd ed., Humana Press, 2009: pp. 7–9.

[164] S.J. Compton, C.G. Jones, Mechanism of dye response and interference in the Bradford protein assay, Anal. Biochem. 151 (1985) 369–374.

[165] N.J. Kruger, The Bradford Method For Protein Quantification, in: Protein Protoc. Handb., 3rd ed., 2009: pp. 17–24.

[166] M. Dubois, K.A. Gilles, J.K. Hamilton, P.A. Rebers, F. Smith, Colorimetric Method for Determination of Sugars and Related Substances, Anal. Chem. 28 (1956) 350–356.

[167] S. Fanali, P.R. Haddad, C.F. Poole, P. Schoenmakers, D. Lloyd, Liquid Chromatography: Fundamentals and Instrumentation, 2nd ed., Elsevier Inc., 2013.

[168] S. Fanali, P.R. Haddad, C. Poole, M.-L. Riekkola, Liquid Chromatography: Applications, 2nd ed., Elsevier Inc., 2017.

[169] S.S. Nielsen, Phenol-Sulfuric Acid Method for Total Carbohydrates, in: Food Anal. Lab. Man., 2010: pp. 47–53.

[170] B. Pedras, Valorization of grape pomace through hot compressed water extraction / hydrolysis, FCT/UNL, Dissertation of Master Program in Biotechnology, 2015.

[171] Thermo Fisher, DIONEX, Product manual for Dionex CarboPac™ MA1, PA1, PA10 and PA100 columns 031824-08, 2009.

[172] T.K. Ghose, Measurement of cellulase activities, Pure Appl. Chem. 59 (1987) 257–268.

[173] H.J. Strobel, Biofuels: Methods (Culturing Anaerobes), 581 (2010) 247–261.

[174] B. Adney, J. Baker, Measurement of cellulase activities, Laboratory Analytical Procedure. National Renewable Energy Laboratory., Nrel/Tp-510-42628. (2008) 8.

[175] M. Selig, N. Weiss, Y. Ji, Enzymatic Saccharification of Lignocellulosic Biomass Laboratory Analytical Procedure (LAP) Issue Date: 3/21/2008, (2008).

[176] P.I.P. Soares, A.M.R. Alves, L.C.J. Pereira, J.T. Coutinho, I.M.M. Ferreira, C.M.M. Novo, J.P.M.R. Borges, Effects of surfactants on the magnetic properties of iron oxide colloids, J. Colloid Interface Sci. 419 (2014) 46–51.

[177] W.B. Fortune, M.G. Mellon, Determination of Iron with o-Phenanthroline: A Spectrophotometric Study, Ind. Eng. Chem. - Anal. Ed. 10 (1938) 60–64.

[178] R. Matos, Desenvolvimento de membranas magnéticas para tratamento de cancro, FCT/UNL, ation of Master Program in Biomedical Engineering, 2017.

[179] B.C. Smith, Fundamentals of Fourier Transform Infrared Spectroscopy, CRC Press, 1995.

[180] PerkinElmer, FT-IR Spectroscopy Spectroscopy Attenuated Total Reflectance ( ATR ), 2005.

[181] J.F. Richardson, J.H. Harker, J.R. Backhurst, Leaching, in: Chem. Eng., 5th ed., 2002: pp. 502–541.

[182] L. Fernandez-Lopez, S.G. Pedrero, N. Lopez-Carrobles, B.C. Gorines, J.J. Virgen-Ortíz, R. Fernandez-Lafuente, Effect of protein load on stability of immobilized enzymes, Enzyme Microb. Technol. 98 (2017) 18–25.

[183] T. Arakawa, S.N. Timasheff, Stabilization of Protein Structure by Sugars, Biochemistry. 21 (1982) 6536–6544.

[184] Novozymes, Cellic® CTec2 and HTec2 -Enzymes for hydrolysis of lignocellulosic materials, (2010) 1–9.

[185] D. Nabi Saheb, J.P. Jog, Natural fiber polymer composites: A review, Adv. Polym. Technol. 18 (1999) 351–363.

[186] G. Siqueira, V. Arantes, J.N. Saddler, A. Ferraz, A.M.F. Milagres, Limitation of cellulose accessibility and unproductive binding of cellulases by pretreated sugarcane bagasse lignin, Biotechnol. Biofuels. 10 (2017).

[187] X. Li, Y. He, L. Zhang, Z. Xu, H. Ben, M.J. Gaffrey, Y. Yang, S. Yang, J.S. Yuan, W.J. Qian, B. Yang, Discovery of potential pathways for biological conversion of poplar wood into lipids by co-fermentation of Rhodococci strains, Biotechnol. Biofuels. 12 (2019) 1–16.

[188] W.C. Li, J.Q. Zhu, X. Zhao, L. Qin, T. Xu, X. Zhou, X. Li, B.Z. Li, Y.J. Yuan, Improving co-fermentation of glucose and xylose by adaptive evolution of engineering xylose-fermenting Saccharomyces cerevisiae and different fermentation strategies, Renew. Energy. 139 (2019) 1176–1183.

[189] T.H.F. Costa, V.G.H. Eijsink, S.J. Horn, The use of lytic polysaccharide monooxygenases in anaerobic digestion of lignocellulosic materials, Biotechnol. Biofuels. 12 (2019) 1–14.

[190] C.-H. Shen, Quantification and Analysis of Proteins, Diagnostic Mol. Biol. (2019) 187–214.

[191] Novozyme, Celluclast 1.5L Product Data Sheet Product Data Sheet Uses, (2011) 6–7.

[192] A.C. Rodrigues, M.Ø. Haven, J. Lindedam, C. Felby, M. Gama, Celluclast and Cellic® CTec2: Saccharification/fermentation of wheat straw, solid-liquid partition and potential of enzyme recycling by alkaline washing, Enzyme Microb. Technol. 79–80 (2015) 70–77.

[193] C.T. Tsai, A.S. Meyer, Enzymatic cellulose hydrolysis: Enzyme reusability and visualization of β-glucosidase immobilized in calcium alginate, Molecules. 19 (2014) 19390–19406.

[194] Q. Zhang, J. Bao, Industrial cellulase performance in the simultaneous saccharification and co-fermentation (SSCF) of corn stover for high-titer ethanol production, Bioresour. Bioprocess. 4 (2017).

[195] T.Q. Lan, H. Lou, J.Y. Zhu, Enzymatic Saccharification of Lignocelluloses Should be Conducted at Elevated pH 5.2-6.2, Bioenergy Res. 6 (2013) 476–485.

[196] X. Zhao, G.K. Moates, A. Elliston, D.R. Wilson, M.J. Coleman, K.W. Waldron, Simultaneous

saccharification and fermentation of steam exploded duckweed: Improvement of the ethanol yield by increasing yeast titre, Bioresour. Technol. 194 (2015) 263–269.

[197] M. Herbaut, A. Zoghlami, G. Paës, Dynamical assessment of fluorescent probes mobility in poplar cell walls reveals nanopores govern saccharification, Biotechnol. Biofuels. 11 (2018) 1–13.

[198] A. Romaní, H.A. Ruiz, F.B. Pereira, L. Domingues, J.A. Teixeira, Effect of hemicellulose liquid phase on the enzymatic hydrolysis of autohydrolyzed Eucalyptus globulus wood, Biomass Convers. Biorefinery. 4 (2014) 77–86.

[199] C. Fang, J.E. Schmidt, I. Cybulska, G.P. Brudecki, C.G. Frankær, M.H. Thomsen, Hydrothermal pretreatment of date palm (Phoenix dactylifera L.) leaflets and rachis to enhance enzymatic digestibility and bioethanol potential, Biomed Res. Int. (2015).

[200] C. Martín, G.J. De Moraes Rocha, J.R.A. Dos Santos, M.C. De Albuquerque Wanderley, E.R. Gouveia, Enzyme loading dependence of cellulose hydrolysis of sugarcane bagasse, Quim. Nova. 35 (2012) 1927–1930.

[201] A. González Quiroga, A. Bula Silvera, R. Vasquez Padilla, A.C. Da Costa, R. Maciel Filho, Continuous and semicontinuous reaction systems for high-solids enzymatic hydrolysis of lignocellulosics, Brazilian J. Chem. Eng. 32 (2015) 805–819.

[202] H.R. Sørensen, A.S. Meyer, S. Pedersen, Enzymatic hydrolysis of water-soluble wheat arabinoxylan. 1. Synergy between α-L-arabinofuranosidases, endo-1,4-β-xylanases, and β-xylosidase activities, Biotechnol. Bioeng. 81 (2003) 726–731.

[203] B.T. Kusema, G. Hilmann, P. Mäki-Arvela, S. Willför, B. Holmbom, T. Salmi, D.Y. Murzin, Selective hydrolysis of arabinogalactan into arabinose and galactose over heterogeneous catalysts, Catal. Letters. 141 (2011) 408–412.

[204] J. Coates, Encyclopedia of Analytical Chemistry -IInterpretation of Infrared Spectra, A Practical Approach, Encycl. Anal. Chem. (2004) 1–23.

[205] P.Y. Bruice, Beauchamp Spectroscopy Tables 1, Org. Chem. 2620 (2011) A-16, A17.

[206] J.M. Guisan, L. Betancor, Glutaraldehyde : A Very Simple Immobilization Protocol, in: Immobil. Enzym. Cells Methods Protoc. Methods Mol. Biol., Springer Nature, 2020: pp. 119–127.

[207] N. Mufti, T. Atma, A. Fuad, E. Sutadji, Synthesis and characterization of black, red and yellow nanoparticles pigments from the iron sand, AIP Conf. Proc. 1617 (2014) 165–169.

[208] J.T. Keiser, C.W. Brown, R.H. Heidersbach, Oxidation of Fe3O4 on iron and steel surfaces, Corrosion. 38 (1982) 357–360.

[209] K.E. Rasmussen, J. Albrechtsen, Glutaraldehyde. The influence of pH, temperature, and buffering on the polymerization rate, Histochemistry. 38 (1974) 19–26.

[210] A.S.G. Lorenzoni, L.F. Aydos, M.P. Klein, R.C. Rodrigues, P.F. Hertz, Fructooligosaccharides synthesis by highly stable immobilized β-fructofuranosidase from Aspergillus aculeatus, Carbohydr. Polym. 103 (2014) 193–197.

[211] J. Sánchez-Ramírez, J.L. Martínez-Hernández, P. Segura-Ceniceros, G. López, H. Saade, M.A. Medina-Morales, R. Ramos-González, C.N. Aguilar, A. Ilyina, Cellulases immobilization on chitosan-coated magnetic nanoparticles: application for Agave Atrovirens lignocellulosic biomass hydrolysis, Bioprocess Biosyst. Eng. 40 (2017) 9–22.

# 11. Annexes

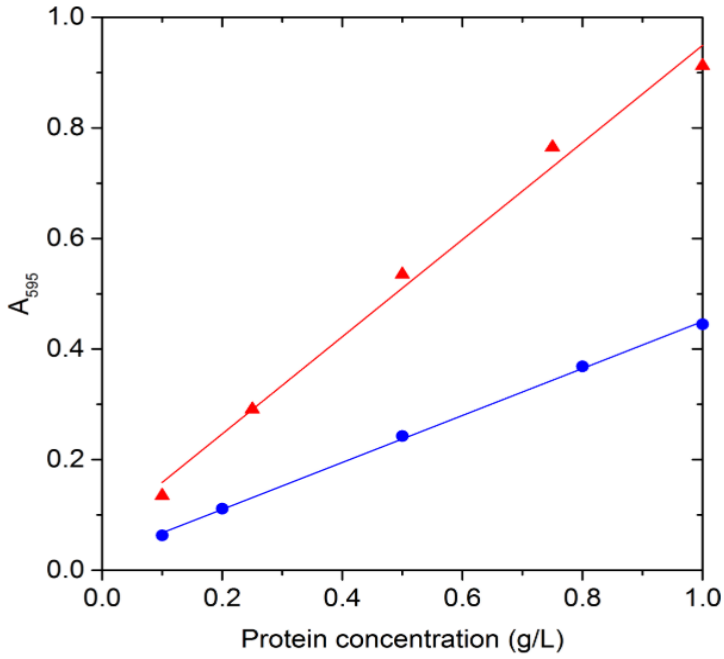


**Figure 1 Protein calibration curves.** Protein calibration curves (solid lines) for P-cellulase and P-$\beta$-glucosidase (▲); and Bovine Serum Albumin (BSA) (●).

Annex 1: Protein calibration curves of BSA and other standard proteins using Bradford assay. The ratio between the absorbance of BSA and other proteins are congruent with the results obtained in this thesis, where using BSA as standard for the Bradford assay, the results were roughly half the ones obtained by the Lowry method. Taken from [103].

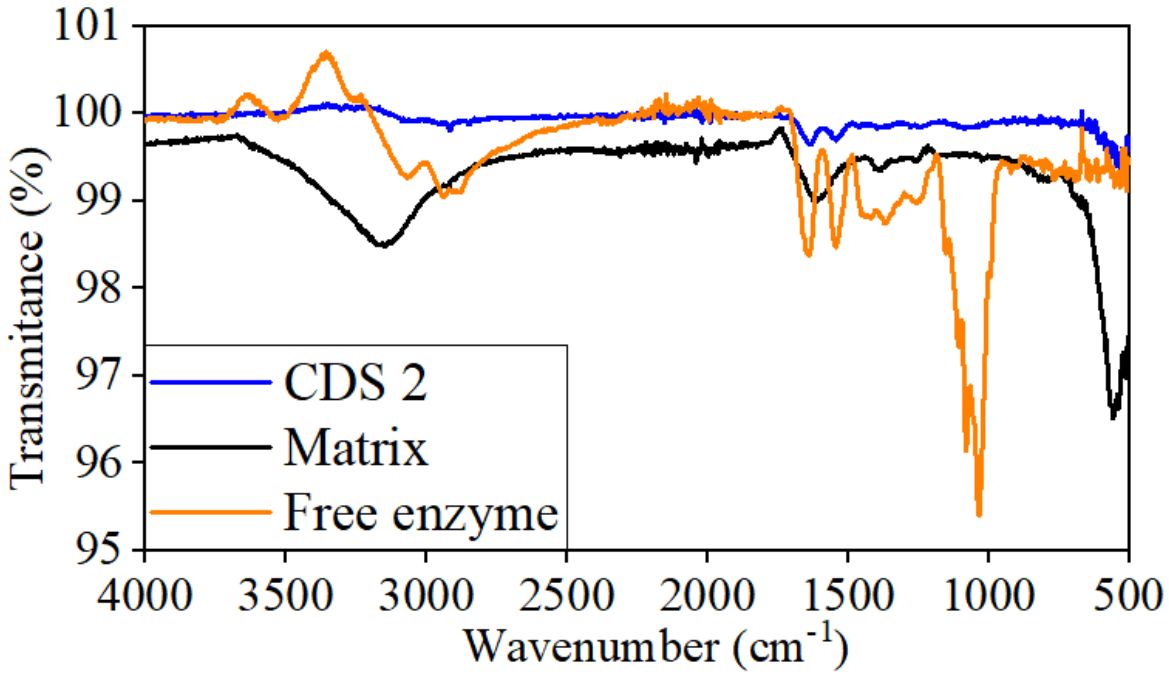


Annex 2: FTIR spectrum for the confirmation of immobilization CDS 2 by comparison of the profiles of the SPIONs matrix (in black), Cellic cTec 2 enzymatic solution (in orange), as well as the complex (in dark blue). Data points represent the average of 2 replicate experiments.

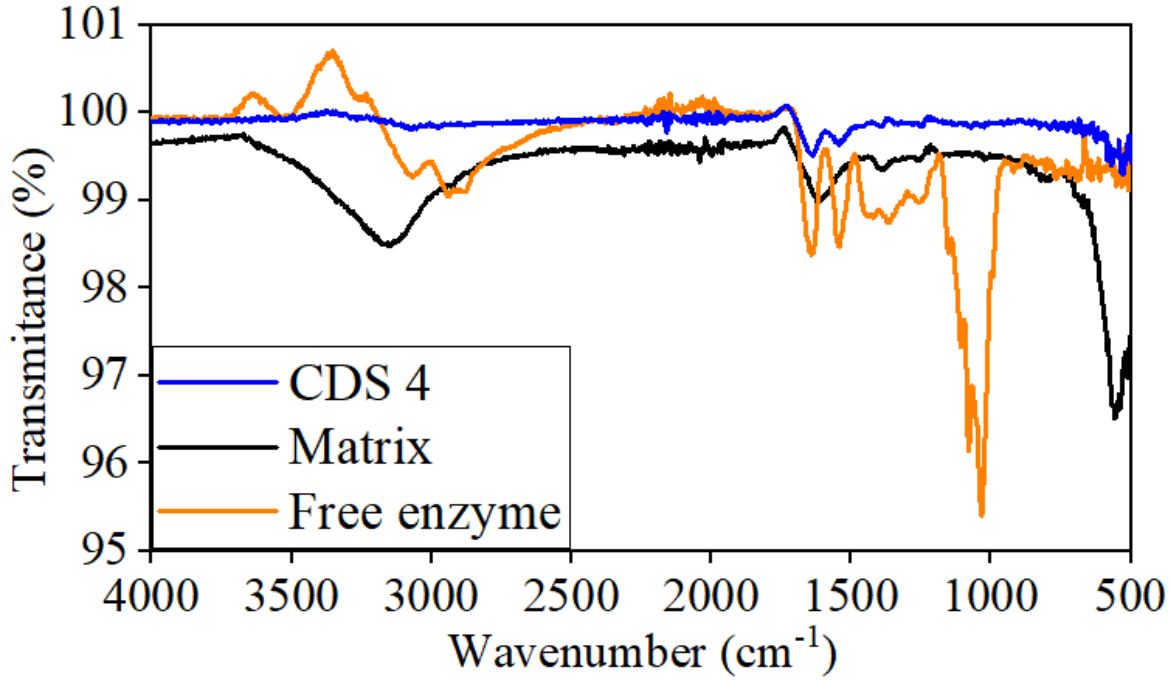


Annex 3: FTIR spectrum for the confirmation of immobilization CDS 4 by comparison of the profiles of the SPIONs matrix (in black), Cellic cTec 2 enzymatic solution (in orange), as well as the complex (in dark blue). Data points represent the average of 2 replicate experiments.

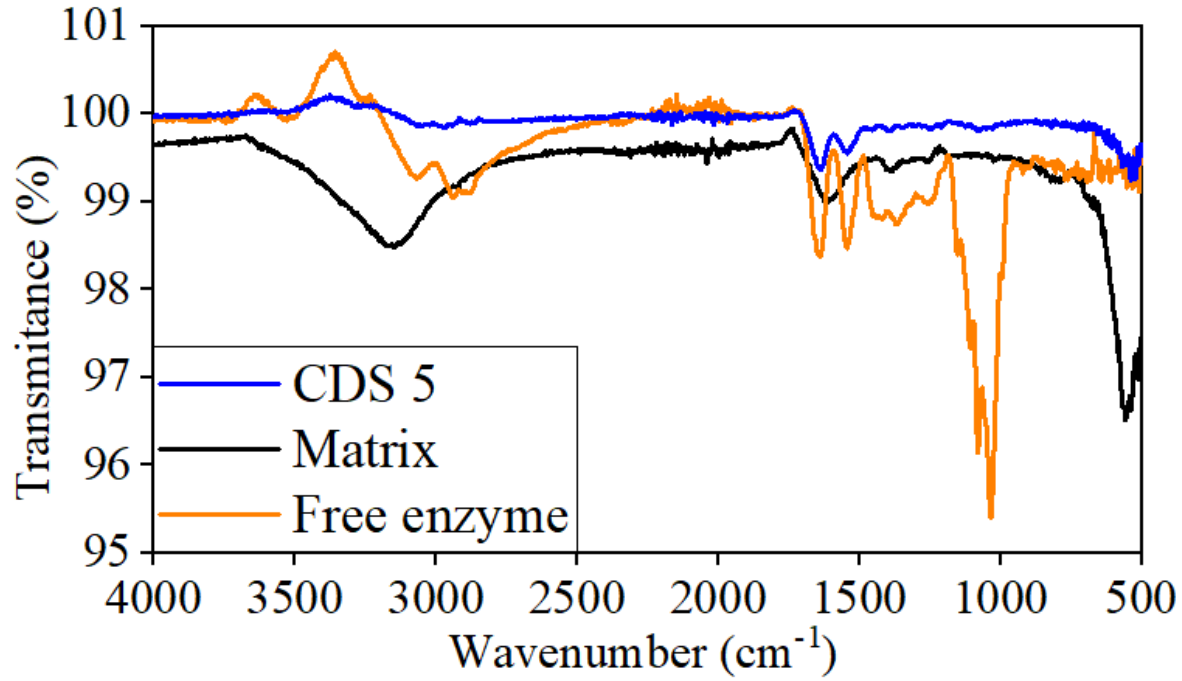


Annex 4: FTIR spectrum for the confirmation of immobilization CDS 5 by comparison of the profiles of the SPIONs matrix (in black), Cellic cTec 2 enzymatic solution (in orange), as well as the complex (in dark blue). Data points represent the average of 2 replicate experiments.

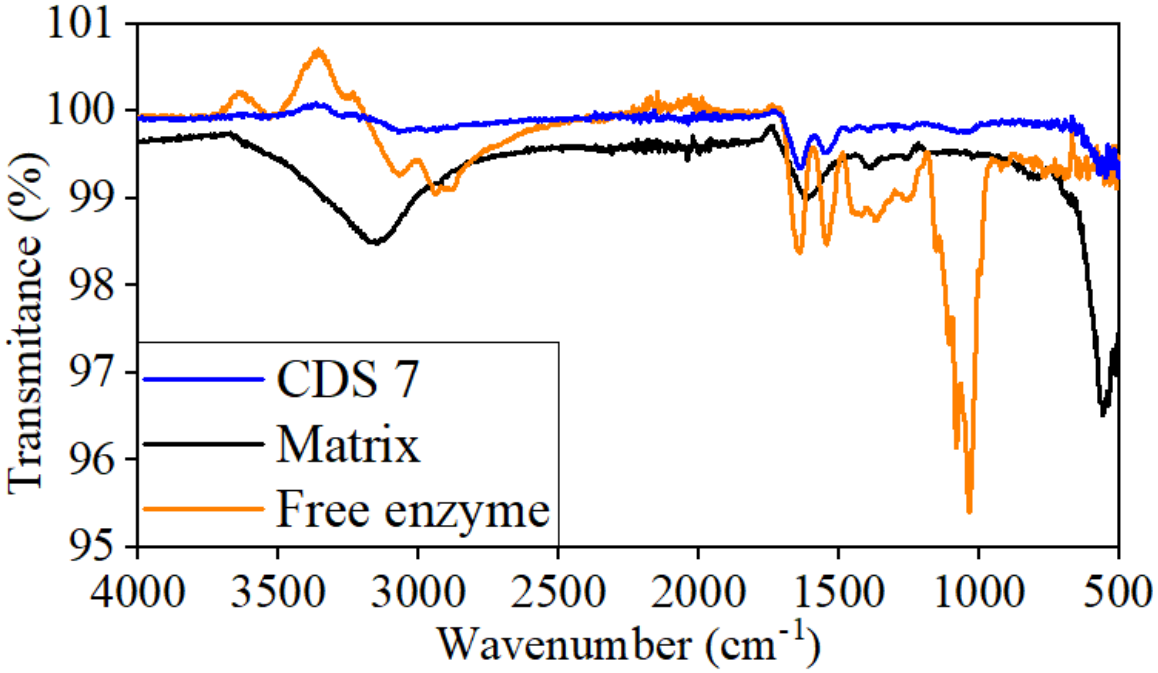


Annex 5: FTIR spectrum for the confirmation of immobilization CDS 7 by comparison of the profiles of the SPIONs matrix (in black), Cellic cTec 2 enzymatic solution (in orange), as well as the complex (in dark blue). Data points represent the average of 2 replicate experiments.